

**Titre:** Surface Finish Control of Inconel 625 Components Produced by Additive Manufacturing Using Combined Chemical-Abrasive Flow Polishing  
**Title:**

**Auteur:** Neda Mohammadian  
**Author:**

**Date:** 2017

**Type:** Mémoire ou thèse / Dissertation or Thesis

**Référence:** Mohammadian, N. (2017). Surface Finish Control of Inconel 625 Components Produced by Additive Manufacturing Using Combined Chemical-Abrasive Flow Polishing [Master's thesis, École Polytechnique de Montréal]. PolyPublie.  
**Citation:** <https://publications.polymtl.ca/2815/>

 **Document en libre accès dans PolyPublie**  
Open Access document in PolyPublie

**URL de PolyPublie:** <https://publications.polymtl.ca/2815/>  
**PolyPublie URL:**

**Directeurs de recherche:** Sylvain Turenne, & Vladimir Brailovski  
**Advisors:**

**Programme:** Génie mécanique  
**Program:**

UNIVERSITÉ DE MONTRÉAL

SURFACE FINISH CONTROL OF INCONEL 625 COMPONENTS PRODUCED BY  
ADDITIVE MANUFACTURING USING COMBINED CHEMICAL-ABRASIVE FLOW  
POLISHING

NEDA MOHAMMADIAN

DÉPARTEMENT DE GÉNIE MÉCANIQUE  
ÉCOLE POLYTECHNIQUE DE MONTRÉAL

MÉMOIRE PRÉSENTÉ EN VUE DE L'OBTENTION  
DU DIPLÔME DE MAÎTRISE ÈS SCIENCES APPLIQUÉES

(GÉNIE MÉCANIQUE)

SEPTEMBRE 2017

UNIVERSITÉ DE MONTRÉAL

ÉCOLE POLYTECHNIQUE DE MONTRÉAL

Ce mémoire intitulé:

SURFACE FINISH CONTROL OF INCONEL 625 COMPONENTS PRODUCED BY  
ADDITIVE MANUFACTURING USING COMBINED CHEMICAL-ABRASIVE FLOW  
POLISHING

présenté par: MOHAMMADIAN Neda

en vue de l'obtention du diplôme de: Maîtrise ès sciences appliquées

a été dûment accepté par le jury d'examen constitué de:

Mme BROCHU Myriam, Ph. D., présidente

M. TURENNE Sylvain, Ph. D., membre et directeur de recherche

M. BRAILOVSKI Vladimir, Ph. D., membre et codirecteur de recherche

M. BALAZINSKI Marek, Docteur ès sciences, membre

## **DEDICATION**

*I would like to dedicate this thesis to my husband, Esmail and my little son, Adrien.*

## ACKNOWLEDGEMENTS

I would like to express my profound gratitude, and sincere gratitude to my advisor, Professor Sylvain Turenne, and my co-director, Professor Vladimir Brailovski for the excellent opportunity they have given me to study at Polytechnique Montréal and work at the “Laboratoire de recherche sur les Alliages à Mémoire et les Systèmes Intelligents (LAMSI) of École de Technologie Supérieure (ÉTS)”. Without their thrust, guidance, patience and continuous supports, my research would not have been successful. Undoubtedly, they were the most influential person during my M.Sc. and the best teachers of my student life. It was a great honor to work with you.

My immense appreciation extends to Professor Marek Balazinski and Professor Myriam Brochu serving as members of jury of my M.Sc. defense committee and for providing valuable comments.

I appreciate Consortium de Recherche et d’Innovation en Aérospatiale au Québec (CRIAQ) for their supports.

I would also like to thank ÉTS laboratory technicians for their excellent cooperation.

I am grateful to my colleagues at LAMSI laboratory, especially Alena Kreitchberg and Victor Urlea for all their helps.

My warmest thanks and appreciation to my parents for their unwavering supports, kind words and love. Also, my endless thanks to my brother for his support and kindness. Thank you for everything.

And finally, heartfelt thanks to my beloved husband, Esmaeil, who has been a constant source of support and encouragement during the challenges of graduate school and life. I am truly thankful for having you in my life.

## RÉSUMÉ

Les secteurs manufacturiers à l'échelle mondiale, particulièrement dans les domaines de l'aérospatial et de l'automobile, expriment de plus en plus le besoin de produire des composants de géométrie complexe en utilisant des approches de fabrication additive plutôt que d'emprunter des voies de fabrication plus traditionnelles. Ainsi, les techniques de fabrication additive de fusion sélective par laser ou faisceau d'électron permettent de réduire le temps de fabrication et la quantité de matière pour produire les pièces tout en améliorant la performance des matériaux. Dans le procédé de fusion sélective par laser, un faisceau laser de haute puissance est utilisé pour fondre localement une poudre métallique pour fabriquer une pièce couche par couche. Cette méthode offre l'avantage de produire des composants à partir de matériaux durs et à haut point de fusion.

Bien que les techniques de fabrication additives permettent d'obtenir des caractéristiques uniques du point de vue de la géométrie des pièces, il demeure une problématique au niveau du fini de surface des composants, particulièrement pour les surfaces internes de pièces utilisées pour contenir des écoulements de fluide. La présence de particules partiellement fondues soudées à la surface peut causer une pollution indésirable dans le fluide de même que la rugosité de surface peut limiter l'écoulement du fluide. Ainsi, un des sujets les plus critiques en recherche qui amène une pénalité importante pour les procédés de fabrication additive concerne les opérations secondaires de finition de surface. Peu de résultats de recherche ont été publiés sur les procédés secondaires de polissage de surfaces internes dans les pièces de géométrie complexe. Ceci devient plus important considérant la variété de matériaux utilisés en fabrication additive. Les quelques résultats publiés reliés aux techniques de polissage chimique, électrolytique et mécanique montrent bien les limites de la fabrication additive.

Les principaux objectifs des travaux de recherche sont de concevoir, fabriquer et valider une méthode de polissage basée sur la combinaison de produits chimiques et de particules abrasives pour des surfaces internes de pièces aéronautiques en IN-625 produites par fabrication additive. Pour atteindre ce but, on envisage d'étudier : a) l'écoulement de produits chimiques, b) l'écoulement d'abrasifs et c) l'écoulement combiné de produits chimiques et d'abrasifs. Les effets de l'orientation de la surface par rapport à la direction de croissance de la pièce ainsi que celui de la vitesse du fluide de polissage seront considérés dans l'étude expérimentale de la

qualité du fini de surface découlant des trois techniques de polissage. Les résultats expérimentaux montrent la faisabilité d'adopter une approche combinée de polissage par écoulement de produits chimiques et d'abrasifs pour obtenir une meilleure efficacité de polissage. Par cette approche, les particules partiellement fondues en surface sont éliminées et la rugosité est sensiblement réduite.

## ABSTRACT

World manufacturing sectors, in particular aerospace and automotive industries, wish to produce highly complex and customized components by adopting additive manufacturing (AM) of products compared to the conventional fabrication methods. This has brought attention to the AM techniques, most commonly selective laser melting (SLM) and electron beam melting (EBM), that have been proven to reduce time to market, decrease buy-to-fly ratio and improve parts performance. In the SLM process, a high-power density laser selectively melts and fuses powders within and between layers to produce a component. Several advantages are offered by SLM such as processing hard materials and production of materials with high melting points.

Regardless of excellent features of SLM additive manufacturing technique, the processing conditions lead to some surface problems in the case of internal surfaces of parts designed for fluid flows. This involves appearance of semi-welded particles attached to the surface, causing pollution in the fluid system, and relatively high surface roughness and texture, compromising the fluid flow. Therefore, one of the critical research issues and excessive cost factors penalizing AM approaches is post-processing surface finish. There is a lack of knowledge on the post-AM surface finish techniques that are appropriate for improving the internal surface quality of complex parts. This becomes more complicated when it comes to the wide range of materials produced by AM techniques. According to the review of the literature, some chemical, electrochemical and mechanical techniques have been investigated that deal with the polishing limitations of SLM-built parts.

The main objectives of this study were to design, manufacture and validate a post-SLM surface finish technique, used for internal surface polishing of tubular IN-625 parts designed for aerospace industry, employing a combination of chemical and abrasive flow actions. For this purpose, comprehensive experimental studies included: a) chemical flow polishing, b) abrasive flow polishing and c) chemical-abrasive flow polishing. The effect of SLM build orientation and fluid velocity on the surface finish quality for the three polishing techniques was studied. The obtained results showed the feasibility of using the combined chemical-abrasive polishing to reach better polishing efficiency. Indeed, the semi-welded powder particles attached to the surface were removed and surface roughness and texture notably improved.



## TABLE OF CONTENTS

DEDICATION .....	III
ACKNOWLEDGEMENTS .....	IV
ABSTRACT .....	VII
TABLE OF CONTENTS .....	VIII
LIST OF TABLES .....	XI
LIST OF FIGURES.....	XII
LIST OF SYMBOLS AND ABBREVIATIONS.....	XVI
CHAPTER 1 INTRODUCTION.....	1
CHAPTER 2 LITERATURE REVIEW.....	5
2.1 Introduction.....	5
2.2 Chemical flow polishing .....	5
2.2.1 Chemical polishing process.....	5
2.2.2 Chemical reaction.....	7
2.2.3 Dynamic action in chemical polishing .....	8
2.2.4 Polishing solutions .....	10
2.3 Abrasive flow polishing .....	11
2.3.1 Mechanical polishing process using abrasive flow .....	11
2.3.2 Research on abrasive flow finishing techniques .....	11
2.3.3 Process parameters control for abrasive flow finishing performance .....	14
2.4 Chemical-abrasive flow polishing.....	17
CHAPTER 3 EXPERIMENTAL METHODS AND TECHNIQUES .....	24
3.1 Introduction .....	24
3.2 Experimental setup.....	24

3.2.1	Pump and sensor.....	24
3.2.2	Wet materials.....	27
3.2.3	Safety plan.....	28
3.2.4	Cost.....	30
3.3	Experimental plan .....	31
3.3.1	Identifying experimental objectives .....	31
3.3.2	Optimizing the polishing fluid .....	31
3.3.3	Conducting the three polishing processes .....	33
3.3.4	Conducting the experimental study.....	35
CHAPTER 4 ARTICLE 1: SURFACE FINISH CONTROL OF ADDITIVELY- MANUFACTURED INCONEL 625 COMPONENTS USING COMBINED CHEMICAL- ABRASIVE FLOW POLISHING .....		38
4.1	Abstract .....	38
4.2	Introduction .....	39
4.3	Methodology .....	41
4.3.1	Experimental setup.....	41
4.3.2	Experimental conditions.....	42
4.3.3	Surface characterization before and after polishing.....	46
4.4	Results .....	48
4.4.1	Static versus flow chemical polishing.....	48
4.4.2	Comparison of chemical, abrasive and chemical-abrasive flow polishing processes	50
4.5	Discussion .....	56
4.5.1	Chemical flow polishing .....	56
4.5.2	Abrasive flow polishing .....	57
4.5.3	Combined chemical-abrasive flow polishing.....	58

4.6	Conclusions .....	59
4.7	Acknowledgements .....	60
CHAPTER 5 GENERAL DISCUSSION.....		61
5.1	Introduction .....	61
5.2	Original scientific hypothesis.....	61
5.3	Discussion on some methodological aspects and results .....	63
5.4	Scaling up the chemical-abrasive polishing process .....	69
CHAPTER 6 CONCLUSION AND RECOMMENDATIONS.....		71
BIBLIOGRAPHY .....		74

## LIST OF TABLES

Table 3.1: Wet materials for the polishing setup parts resistant to high concentrated HF and HNO <sub>3</sub> at room temperature .....	28
Table 3.2: Thesis project equipment and materials cost .....	30
Table 3.3: Results of roughness reduction for the abrasive flow polishing using three abrasive particle sizes for the determined process conditions .....	32
Table 3.4: Experimental plan for the number of specimens used for each type of tests .....	34
Table 3.5: Experimental plan for investigating the correlation between various parameters obtained by the studied polishing processes .....	36
Table 3.6: Specifications of Surface roughness tester SJ-410, Mitutoyo .....	36
Table 3.7: LEXT OLS4100 laser confocal microscope .....	37

## LIST OF FIGURES

Figure 1.1: The process of selective laser melting (SLM) (Mumtaz & Hopkinson, 2010) .....	2
Figure 2.1: SEM micrographs a Ti-6Al-4V strut with an open porous structure (a) as-built, (b) after chemical polishing, and (c) after the chemical-electrochemical polishing (Pyka et al., 2012).....	6
Figure 2.2: The mass loss percentage of the specimens polished using ultrasonic cleaner and magnetic stirrer (Łyczkowska et al., 2014).....	10
Figure 2.3: Schematic illustration of the working principle of the abrasive flow machining technique (Bremerstein et al., 2015) .....	12
Figure 2.4: $R_a$ and $R_z$ surface roughness, obtained by profilometry, of inner wall of the 500- $\mu$ m stainless steel 304 bores polished by abrasive flow polishing. (Yin et al., 2004).....	14
Figure 2.5: Input parameters in AFM process (Bremerstein et al., 2015).....	15
Figure 2.6: Surface roughness as a function of number of slurry passes for various abrasive concentrations in abrasive flow polishing process of tool steel (JIS:SKD11) (Kurobe et al., 2002).....	16
Figure 2-7: Surface roughness as a function of number of slurry pass for different abrasive particle sizes in abrasive flow polishing process of tool steel (JIS:SKD11) (Kurobe et al., 2002).....	16
Figure 2.8: Expected mechanisms for material removal of the CMP process (Lee et al., 2016)...	19
Figure 2.9: Three trends of MRR in accordance with abrasive sizes in CMP process (Lee et al., 2016).....	20
Figure 2.10: Three trends of MRR in accordance with abrasive concentrations in CMP process (Lee et al., 2016) .....	21
Figure 2.11: Schematic diagram of the slurry erosion wear test (Ramesh et al., 2014).....	22
Figure 2.12: Influence of slurry concentration, speed and particle size on slurry erosive wear (Ramesh et al., 2014).....	22

Figure 3.1: Effect of various pumps on large particle concentrations in the slurry for CMP process (Litchy & Schoeb, 2005).....	26
Figure 3.2: Levitronix PTM, pump and mixer .....	26
Figure 3.3: Flow sensor design (LFS Levitronix) .....	27
Figure 3.4: Polishing setup dimensions.....	29
Figure 3.5: (a) Safe installation of the pump and sensor devices far from the setup, and (b) air cooling module for the pump .....	30
Figure 3.6: Experimental plan flowchart.....	31
Figure 3.7: (a) Edge-shaped specimen with build orientations of 15° and 135°, and (b) plate-shaped specimen with build orientation of 135° on the rougher face.....	34
Figure 3.8: (a) Polishing specimen assembly, (b) chemical abrasive fluid flow inside the polished specimen, (c) edge shape specimen on the SLM building platform .....	35
Figure 3.9: Surface roughness tester SJ-410, Mitutoyo .....	36
Figure 3.10: LEXT OLS4100 laser confocal microscope .....	37
Figure 4.1: (a) Schematic and (b) real illustration of the chemical abrasive polishing setup .....	42
Figure 4.2: (a) Polishing specimen assembly, (b) chemical abrasive fluid flow inside the polished specimen, (c) edge shape specimen on the SLM building platform .....	43
Figure 4.3: Surface roughness as a function of the surface orientation, as measured on as-built IN625 specimens (adapted from Urlea and Brailovski, 2017).....	44
Figure 4.4: Roughness results of static chemical polishing for the four chemical solutions. The tests were performed for 8 hours at room temperature .....	45
Figure 4.5: Roughness measurement direction of the stylus profilometer for the edge-shaped specimen. Non-polished surface with build orientation of 15° .....	46
Figure 4.6: Planar view of the edge-shaped specimen captured by a confocal microscope for polishing depth measurements as a function of velocity.....	47

Figure 4.7: Roughness improvement for static chemical polishing and chemical flow polishing processes at build orientations of 15° and 135°. Polishing time for the two processes was 1 hour.....	48
Figure 4.8: 3D topography confocal microscope surface images at two build orientations of 15° and 135° for the as-built, static chemical polished and chemical flow polished surfaces. Polishing time for the two processes was 1 hour .....	49
Figure 4.9: Roughness improvement using the three polishing processes at build orientations of 15° and 135°. Polishing time for the three processes was 1 hour .....	50
Figure 4.10: Required polishing time for the 135° build orientation surface using different polishing techniques to achieve similar surface roughness.....	51
Figure 4.11: $R_a$ and $R_z$ roughness versus polishing time through the three polishing techniques for the two build orientations of (a, b) 15° and (c, d) 135° .....	52
Figure 4.12: 3D surface roughness profilometry for 15° build orientation before and after polishing using three different polishing techniques for each increment of polishing time ..	53
Figure 4.13: 3D surface roughness profilometry for 135° build orientation before and after polishing using three different polishing techniques for each polishing time increment.....	54
Figure 4.14: The logarithmic graphs show the polishing depth versus fluid velocity of the edge-shaped specimen using (a) chemical flow polishing, (b) abrasive flow polishing and (c) chemical-abrasive flow polishing (polishing time 1 hour, build orientation 135°). The scheme (d) represents the material removal pattern on the inclined surfaces of the edge-shaped specimen for the selected velocity range .....	55
Figure 4.15: Logarithmic graphs of (a) and (b) present the polishing depth versus the velocity for build orientations of 15° and 135°, respectively. The results were obtained after applying chemical-abrasive flow polishing for 1, 2 and 3 hours .....	56
Figure 5.1: Striped texture exists on the as built surface and persists after chemical-abrasive flow polishing for 1 hour on the build orientation of 15°, although the semi-welded particles are completely removed after chemical-abrasive flow polishing .....	64

Figure 5.2: Influence of particle impact angle on wear rate of non-heat treated St 37 (ductile material steel) (Kosa & Göksenli, 2015).....65



## LIST OF SYMBOLS AND ABBREVIATIONS

$A$	Cross sectional area through which the flow passes
AFM	Abrasive Flow Machining
$Al_2O_3$	Aluminium Oxide
AM	Additive Manufacturing
$B$	Preston's coefficient
$c$	Concentration of the species in the bulk of the solution
CAGR	Compound Annual Growth Ratio
$CeO_2$	Cerium (IV) Oxide
CFAAFM	Centrifugal Force Assisted Abrasive Flow Machining
$Cl_2$	Dichlorine
CMP	Chemical Mechanical Polishing
$Cr_2O_3$	Chromium (III) Oxide
$D$	Diffusion coefficient of the reacting species in the solution
$d$	Polishing depth
DBGAFF	Drill Bit Guided Abrasive Flow Finishing
$dn/dt$	Dissolution rate
EBM	Electron Beam Melting
$ECA_2FM$	Electrochemical Assisted Abrasive Flow Machining
$Fe_2O_3$	Ferric Oxide
$H_2O_2$	Hydrogen Peroxide
$H_2SiF_6$	Hexafluorosilicic acid
HDPE	High-Density Polyethylene
HF	Hydrofluoric acid

$\text{HNO}_2$	Nitrous acid
$\text{HNO}_3$	Nitric acid
IN-625	Nickel alloy (Inconel 625)
IN-718	Nickel alloy (Inconel 718)
$K$	Empirical constant in polishing depth equation
LPBF	Laser Powder-Bed Fusion
$m$	Empirical constant in polishing depth equation
$M$	Surface atom in dissolution process
MAFM	Magnetic Abrasive Flow Machining
MMR	Material Removal Rate
$n$	Empirical constant in polishing depth equation
NaCl	Sodium Chloride
NOCl	Nitrosyl Chloride
$P$	Wafer Pressure
PFA	Perfluoroalkoxy,
PTFE	Polytetrafluoroethylene,
PTM	Pump Tank Mixer
PVC	Polyvinyl Chloride,
PVDF	Polyvinylidene Fluoride,
$Q$	Flow rate
$R_a$	Arithmetical average roughness value
R-AFF	Rotational Abrasive Flow Finishing
$R_z$	Average roughness depth
$S$	Surface area of the specimen

Si	Silicon
Si <sub>3</sub> N <sub>4</sub>	Silicon Nitride
SiC	Silicon Carbide
SiO <sub>2</sub>	Silicon Dioxide
SKD11	Tool steel
SLM	Selective Laser Melting
ST-37	Steel
<i>t</i>	Polishing time
Ti-6Al-4V	Titanium alloy
Ti-6Al-7Nb	Titanium alloy
<i>v</i>	Flow velocity
<i>V</i>	Relative velocity between the wafer and polishing pad
<i>x</i>	Distance on the x-axis of edge-shaped specimen where the velocity is measured
<i>X</i>	Oxidizing agent in dissolution process
<i>z</i>	Average particle size
ZrO <sub>2</sub>	Zirconium Dioxide
$\delta$	Thickness of the reactant depleted layer neighboring the surface
$\lambda_c$	Distance the probe will travel for a single measurement
$\lambda_s$	Width of the smallest feature that will be considered

## CHAPTER 1 INTRODUCTION

Inconel 625 is a nickel-based alloy containing mainly additive elements of carbon, chromium, molybdenum and niobium. This alloy possesses outstanding oxidation and corrosion resistance in industrial environment (Shankar et al., 2001). Excellent high temperature corrosion and stress resistance are the critical properties responsible for the reliability of this alloy in aircraft engine parts (Dinda et al., 2009).

Aerospace and automotive industries are increasingly interested in additive manufacturing (AM) of materials to fabricate fully functional parts from metal powders. This includes production of lightweight and highly complex nickel-based alloy parts. The process of AM refers to the fabrication of parts by depositing material layer by layer. There is a high geometric freedom in production of parts using a computer-aided design model (Petrovic et al., 2011). The commercial technological progress of AM for three decades comes into the higher accuracy, mechanical property improvements, increasing applications, and the cost reduction of facilities and AM-processed parts (Gibson, et al., 2015).

Mumtaz & Hopkinson (2010) described that laser powder-bed fusion (LPBF), known also selective laser melting (SLM), is a particular additive manufacturing technology, in which laser beam consolidate the metal to generate the parts. The use of this technology has the potential to reduce time to market, decrease buy-to-fly ratio and improve parts performance. Figure 1.1 shows the SLM process. The laser melts powdered metal, then, the powder bed moves downward after completing a layer. The next cross section of the part is built by adding a new layer of the metal powder by the powder depositor.

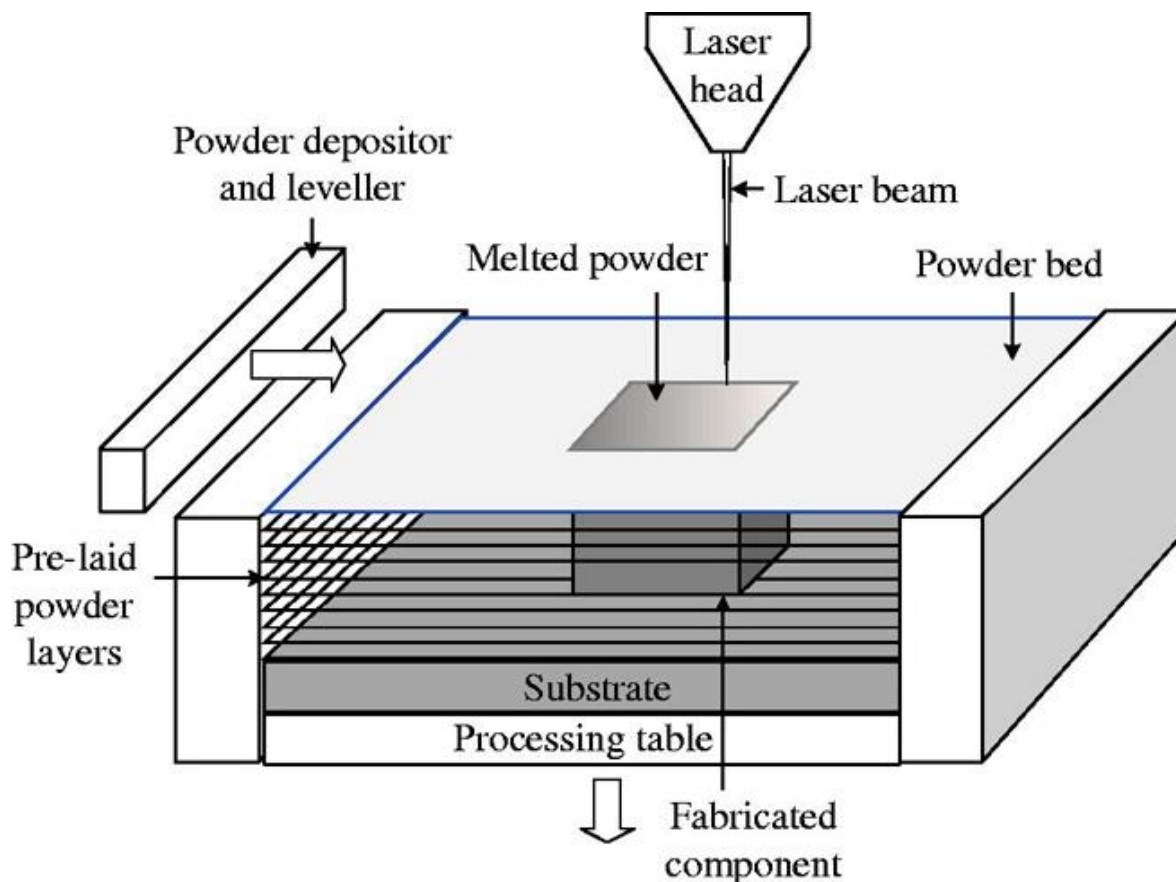


Figure 1.1: The process of selective laser melting (SLM) (Mumtaz & Hopkinson, 2010)

SLM is a promising technique to be used for any purpose of production development such as design concept and low volume part production (Yadroitsev & Smurov, 2010). SLM-built Inconel 625 is a promising alloy that is used to fabricate high-performance components in aeronautics, chemical and petrochemical industries. Kreitzberg et al. (2017) showed that the overall mechanical strengths and elongation to failure of the SLM-built Inconel 625 equal or proceed to those of the annealed wrought alloy at room temperature. However, its elongation to failure at elevated temperature (760 °C) is lower for the SLM-built specimens comparing to the annealed wrought ones. The mechanical properties of the Inconel 625 parts produced by SLM process can be improved by post-SLM HIP treatment. SLM process has a significant limitation due to relatively poor surface finish (Król & Tański, 2016). The surface roughness is critical for some parts functional properties like mechanical and frictional properties in order to avoid surface initiated cracking and thus premature failure (Pyka et al., 2013). Therefore, surface roughness reduction of SLM-built parts using post-processing techniques is a critical research

issue. Due to the complexity of the SLM-built parts and broad range of materials fabricated by this process, severe limitations exist for selecting the appropriate polishing technique. For example, chemical and electrochemical polishing techniques are limited by the chemical solutions and electrolyte, which are usually applicable for specific materials. For a new alloy, several tests are required to find the proper polishing medium. As for mechanical techniques, conventional mechanical polishing cannot be applied to finish the internal cavities of the complex parts.

Considering the challenges regarding the post-SLM surface finishing techniques, the research question of the current work is: could a combination of chemical and abrasive flow techniques advantageously be applied for efficient improvement of internal surface finish of AM IN-625 components?

The objective of this study is to show the feasibility and performance of the chemical-abrasive flow polishing process for surface finish control of the interior part of IN-625 SLM-built tubular samples. This investigation includes comparative studies on removal of semi-welded particles from the surface and surface roughness reduction using the three polishing techniques of chemical flow polishing, abrasive flow polishing and combined chemical-abrasive flow polishing.

Related to the scientific hypothesis of this work, it is needed to verify that there is a synergy effect in combining chemical and abrasive flow polishing techniques. The experimental procedure will be aimed to verify that the combined polishing technique lead to a more efficient removal of semi-welded particles from the surface and surface roughness reduction compared to the two other techniques applied separately.

To the knowledge of the master degree student, the chemical-mechanical polishing technique proposed in the present research work is the first of its kind based on pumping acidic chemicals as chemical polishing agent and abrasives as mechanical polishing agent through the interior surfaces of objects that could be viable for industrial practice.

The present thesis consists of six chapters, which starts with an introduction chapter, followed by the five other ones:

**Chapter 2** presents a comprehensive literature review on three categories of surface finishing techniques: chemical flow polishing, abrasive flow polishing, and chemical-abrasive flow polishing. The existing research studies for the three polishing techniques and their limitations regarding the thesis objectives are addressed comparatively.

**Chapter 3** presents the experimental methods and techniques. This chapter is devoted to the experimental setup including a brief overview of selection of setup parts, wet materials, safety plan and costs as well as the experimental plan for this study. The detail information on the experimental setup design, tests conditions and parameters used in the work are presented in chapter 4.

**Chapter 4** presents the article entitled « Surface finish control of additively-manufactured Inconel 625 components using combined chemical-abrasive flow polishing » that was submitted in the Journal of materials processing technology. The comprehensive experimental studies on evaluating and comparing the surface finish quality of the tubular samples obtained by the three polishing techniques are explained. The synergy effect stemmed from combining chemical and abrasive flow actions are discussed through investigating the obtained results.

**Chapter 5** presents the general discussion. This chapter provides insight into the studied problem of research and the presented solution by linking the objectives of the study, the results of the polishing tests, and comparative discussion on the obtained results.

**Chapter 6** presents the conclusions and recommendations.

## CHAPTER 2 LITERATURE REVIEW

### 2.1 Introduction

This literature review aims at studying different post processing surface finish techniques applicable for components with complex internal structures, that are manufactured by powder-based additive technologies like Selective Laser Melting (SLM). These internal surfaces are difficult to access by many technological tools. With this objective in mind, three polishing techniques have been studied, in which the flow of the polishing fluid through the interior surfaces of the parts are used: chemical flow polishing, abrasive flow polishing, and combination of chemical and abrasive flow polishing techniques.

### 2.2 Chemical flow polishing

#### 2.2.1 Chemical polishing process

For removing semi-welded particles from the SLM built surfaces and obtaining desired surface roughness, chemical and electrochemical methods are commonly used.

The surface is chemically polished by immersion in an appropriate corrosive solution where the corrosion process is controlled. Chemical polishing is intended to remove materials from the metallic surface and reduce surface roughness with parallel dissolution of passivation layers. The passivation layer is created on the surface as an effect of polishing solution and galvanic couples. Surface finish quality relates to the ratio of the passive layer formation and dissolution of this upper layer rates. The chemical polishing is provided by a ratio equal to one. Metal oxidation happens at a ratio greater than one and metal etching occurs for the less than one ratios. (ASM-Vol.9, 2004)

It is possible to increase the polishing rate by combining chemical polishing with electrochemical polishing, or with applying dynamic action to chemical polishing process such as using ultrasound vibration, magnetic agitation or fluid flow. Pyka et al. (2012) showed that using a combination of chemical polishing and electrochemical polishing reduced the surface roughness of Ti-6Al-4V SLM-parts significantly. Firstly, semi-welded particles are removed by chemical polishing. Then, the surface roughness reduction is obtained by electrochemical polishing. Figure



2.1 shows the SEM micrographs of a typical strut, which is a visual confirmation for the effectiveness of the chemical-electrochemical treatment.

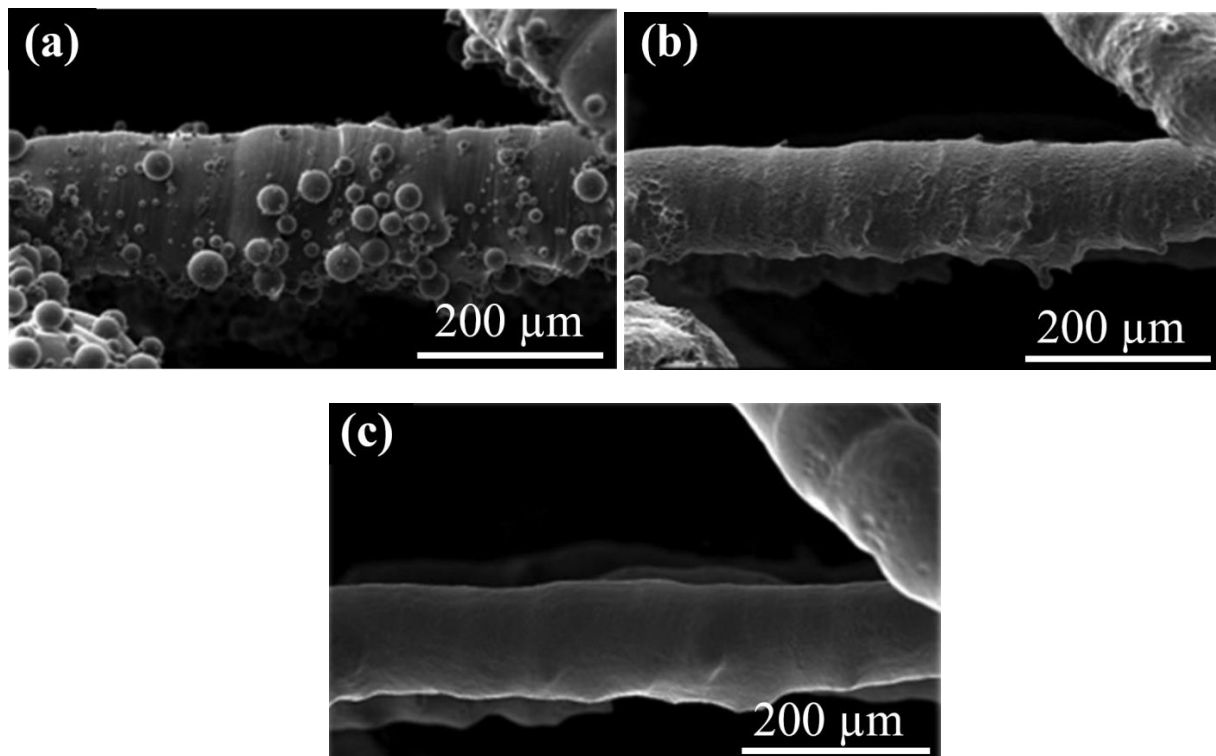


Figure 2.1: SEM micrographs a Ti-6Al-4V strut with an open porous structure (a) as-built, (b) after chemical polishing, and (c) after the chemical-electrochemical polishing (Pyka et al., 2012)

This surface treatment allows achieving a homogeneous and controllable surface topography. However, electropolishing requires the use of conformal electrodes, which complicates the finishing of narrow channels and cavities (Urlea & Brailovski, 2017). Besides, it is difficult to electropolish multiphase alloys due to the different polishing rates of the phases. Surface finish quality depends on whether one phase is strongly cathodic or anodic comparing to the other phases. Preferential dissolution can occur for the matrix if the second or third phases are cathodic relatively, causing the others not to be attached. In addition, the interface between two phases can be dissolved preferentially (Donachie, 2000).

Eliminating the limitations of combined chemical and electrochemical technique, chemical polishing with a dynamic action allows finishing of inaccessible areas and multiphase alloys. It also increases the polishing rate by increasing material removal rate (ASM-Vol.9, 2004).

Different medium delivery techniques used for chemical polishing are comparatively discussed in Section 2.2.3.

## 2.2.2 Chemical reaction

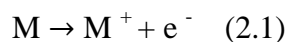
Chemical polishing is utilized for surface treatment of metallic components fabricated by conventional or additive manufacturing (AM) techniques. In this process, the resulting passive layer of the polished metal has higher dissolving rate in the peaks compared to the pits because of water-deficiency of the diffusive layer in the pits (Łyczkowska et al., 2014).

Usually, when a surface is chemically polished, the initial surface reaction is oxidization-reduction process. In general, chemical polishing bathes contain two agents (Tuck, 1975):

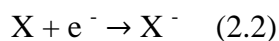
- An oxidizing agent: the oxidizing agent of the polishing solution, such as nitric acid or hydrogen peroxide, oxidizes the surface material. The oxidizer takes the place of the electric current applied in electropolishing process. Usually, the oxidization product is not soluble in the polishing solution and thus, remains on the surface.
- A complexing agent: it reacts with the oxidized material to make a soluble complex, which can pass into the solution. For example, the most commonly used complexing agent in chemical polishing of titanium is hydrofluoric acid.

Furthermore, water is often used to dilute the chemical solution. A high proportion of chemicals are in the form of concentrated aqueous solutions.

The oxidization-reduction processes can be considered as a combination of cathodic and anodic reactions. In the first stage, the anode reaction takes place, where the surface of solid is dissolved in an oxidizing solution. The surface atom,  $M$ , becomes positive ion by losing an electron (the reaction simplified by assuming  $M$  to be singly charged).



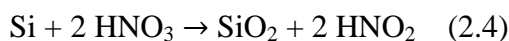
In the liquid, the oxidizing agent,  $X$ , diffuses to the surface and gains the electron, which is called the cathode reaction.



Anode and cathode areas can act alternatively. These areas are finely distributed over the solid surface. The overall reaction is obtained by combining Equation 2.1 and 2.2:



The atom,  $M$ , can be removed from the surface if the reaction product,  $MX$ , is soluble in the polishing solution. Otherwise, a complexing agent should be added into the chemical solution to form a soluble compound. For some materials having good corrosion resistance, the reaction product is dense and adherent to the metal, giving a protective layer against the corrosive solution. Taking the chemical polishing of silicon in a solution of nitric acid (oxidizing agent), hydrofluoric acid (complexing agent) and water (diluent) as an example, the overall dissolution process is obtained by adding cathodic and anodic equations:



Then, HF produces a soluble product by reacting with  $\text{SiO}_2$ :



In some chemical polishing processes, the chemical reactions are more complicated. For instance, the solution constituents can react with each other. Goldstein (1960) studied this action for an aqua regia etchant used for chemical polishing of a semiconductor, where the reaction between the acids of  $\text{HNO}_3$  and  $\text{HCl}$  forms chlorine:



### 2.2.3 Dynamic action in chemical polishing

To understand the correlation between the dynamic action and the dissolution rate in chemical polishing, the dissolution process mechanism must be studied. Chemical reactions involved in chemical polishing (dissolution) process have been discussed in Section 2.2.2. (Tuck, 1975). The dissolution process mechanism could be described as a) reaction-controlled, b) autocatalytic, or c) diffusion-controlled. However, more than one dissolution processes can take place at the surface of material because sometimes several chemical reactions are involved in the process. Hence, the rate-limiting process for dissolution is the slowest mechanism.

Dokoumetzidis et al. (2008) explained that the dissolution in a reaction-controlled process is supposed to be a reaction on the polished surface, which takes place between undissolved species

and molecules of the dissolution medium. Therefore, the rate of dissolution is controlled by the reaction at solid-liquid interface. In other words, the concentration of the undissolved species controls the dissolution rate. Here, the solubility is referred to the concentration of the undissolved species after reaction equilibrium. Therefore, the dissolution rate is not affected by the dynamic action in a reaction-controlled process.

In a different manner, the dissolution rate of the autocatalytic reaction reduces by applying dynamic action as described by (Tuck, 1975). In the autocatalytic reaction, the concentration of the catalyst products controls the dissolution process, i.e. as the reactions at the solid-liquid interface proceed, they provide their own starting materials to continue the dissolution. Besides, an induction time is needed before getting to the steady-state rate of dissolution. Hence, introducing a dynamic action to the process may help removal of the catalyst products from the surface, and slow down the reaction.

When the rate-limiting process for dissolution is diffusion of reacting species to the surface, the concentration of the species close to the surface is assumed to be about zero because they are consumed continuously when reaching the surface. The thickness of reactant-depleted layer neighboring the surface reduces by applying dynamic action because the rate of approaching of the species to the surface is increases. As a result, the dissolution rate increases by introducing dynamic action to the chemical polishing for a diffusion-limited process (Tuck, 1975).

The effect of dynamic action on dissolution rate can be proved by studying the work done by (Łyczkowska et al., 2014). They investigated the effect of two different medium delivery methods, ultrasound vibration and magnetic agitation, on the mass loss of scaffolds made of Ti-6Al-7Nb alloy by additive manufacturing. The loss of mass was a result of removing partially bound powder particles from surface and reducing the diameters of the parts. As shown in Figure 2.2, the percentage of mass loss was larger for the specimens polished using the ultrasound cleaner than those polished in the magnetic stirrer. Indeed, the dissolution rate increases by agitating the solution in a diffusion-controlled process, as a result of supplying fresh reactant to the surface, as described by (Vossen & Kern, 1978).

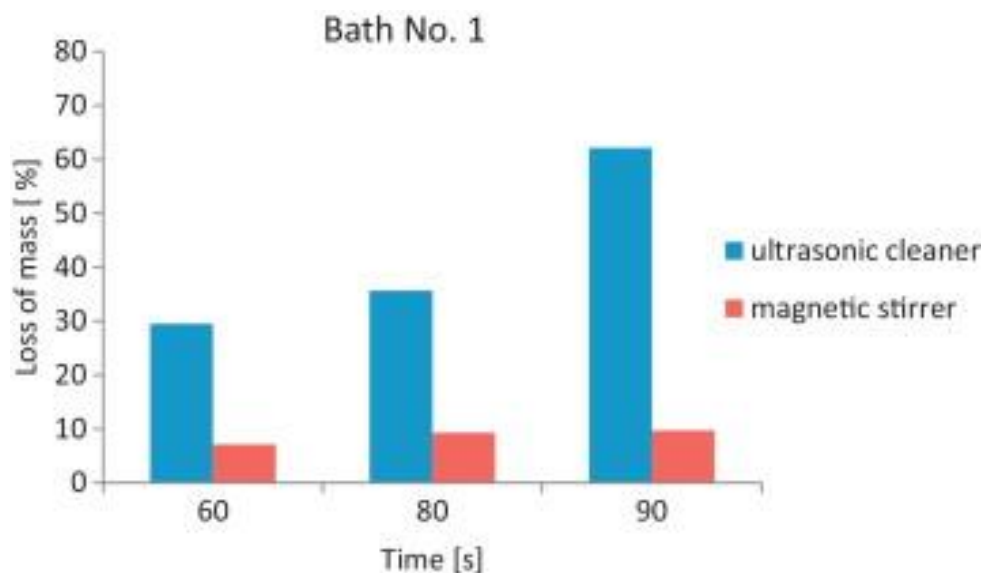


Figure 2.2: The mass loss percentage of the specimens polished using ultrasonic cleaner and magnetic stirrer (Łyczkowska et al., 2014)

#### 2.2.4 Polishing solutions

A few systematic studies have been done in the literature giving detailed information on chemical polishing systems. This involves comprehensive investigations on chemical reactions occurring in the solution medium and on the surface of solid. There seems to be a lot of work for collecting all required data for a specific polishing system such as testing different compositions of the polishing solution, observing the effect of dynamic action, varying the temperature of the test and noting the effect of adding abrasives to the process. In addition, appropriate chemical bathes are often obtained during a trial. Thus, chemical polishing can be defined something of an art until more scientific information is collected in this area (Tuck, 1975).

The list of chemical polishing solutions for various materials are listed by ASM-Vol.9 (2004) and Kutzelnigg (1960).

Finally, an important factor for preparing an experimental plan for handling and management of chemicals in the tests is determining the associated hazards and risks. A book by National Research Council (US) (2011) delivers a practical guide for evaluating the risks and hazards with these chemical activities in the laboratory.

## **2.3 Abrasive flow polishing**

### **2.3.1 Mechanical polishing process using abrasive flow**

Mechanical polishing techniques use abrasives to reduce surface roughness of material by applying a controlled material removal on the surface. Mechanical polishing materials involve polishing wheels, abrasive stones, abrasive pastes, rubber polishers (Gonçalves et al., 2008) and abrasive fluids. Techniques using abrasive fluids for polishing material such as abrasive flow machining (AFM) (Rhoades, 1991), abrasive-waterjet machining (Relekar, Kalase, & Dubal) and abrasive flow polishing (Yin et al., 2004) are suitable for interior surface finishing of components. These processes are characterized by introducing a flow of abrasive fluid through the internal cavity of the work-piece, which are difficult to access by most of the finishing techniques. As an example, complex metal parts of additive manufacturing process show an inappropriate surface roughness for service requirements. AFM presents efficiency and accuracy for complex structure components.

The polishing mechanism of abrasive finishing processes is the interaction between abrasive particle and work-piece involving one or more of material deformation modes, such as cutting, ploughing and sliding. The cutting is referred to material removal process, ploughing is related to material displacement process and sliding is considered as a surface modification process (Yadav et al., 2011).

The force of abrasive particles, exerted by the fluid, produces abrasive action, which gently hones the raised surface features and edges. The abrasive finishing action can be compared to lapping or grinding operation as the abrasive medium smooths the internal surfaces of the work-piece (Yin et al., 2004).

The characteristics and applications of abrasive flow machining and abrasive flow polishing to finishing metal parts produced by additive manufacturing techniques are discussed in Section 2.3.2.

### **2.3.2 Research on abrasive flow finishing techniques**

*Abrasive Flow Machining (AFM)*

AFM is a new effective machining process that is used where interior surface finishing is required. The complex internal passages are difficult to reach by many conventional finishing techniques. AFM, as an advanced process, finishes the rough surfaces using a flow of very viscous, pressurized, semi-solid media through the work-piece. Polymeric carrier and abrasive particles such as  $\text{Al}_2\text{O}_3$ , SiC and diamond are the constituents of the abrasive medium (Gupta & Chahal, 2015).

In AFM process, the work-piece is clamped and sealed between two opposing cylinders. The viscous abrasive medium is extruded back and forth into the work-piece by hydraulic pistons placed inside the cylinders (Bremerstein et al., 2015). Rhoades (1991) presented a detailed study on the process principles of AFM machining. Spur et al. (1997) also explained this advanced machining technique in general including the semisolid abrasive medium that is employed in the process. The concentration of abrasive particles in the polymeric carrier medium is up to 40 vol.%. The working principle of abrasive flow machining is shown in Figure 2.3.

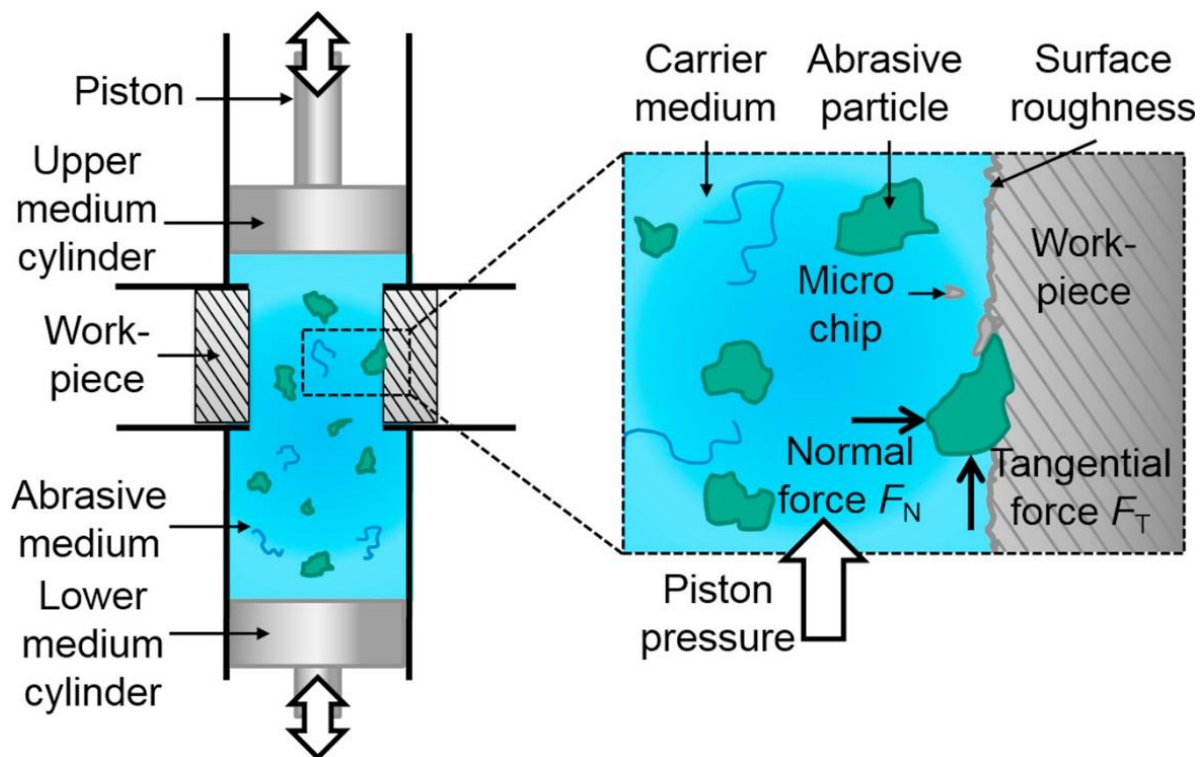


Figure 2.3: Schematic illustration of the working principle of the abrasive flow machining technique (Bremerstein et al., 2015)

AFM has generally a low material removal rate, and it is labor intensive process. This limitation make the process complicated to be used for large stock-removal operations (Benedict, 1987). To improve the accuracy and efficiency of finishing operation of AFM, many modified processes such as Magnetic Abrasive Flow Machining (MAFM), Drill Bit Guided Abrasive Flow Finishing (DBGAFF), Centrifugal Force Assisted Abrasive Flow Machining (CFAAFM), Rotational Abrasive Flow Finishing (R-AFF), Spiral Polishing Method and Electrochemical Assisted Abrasive Flow Machining (ECA<sub>2</sub>FM) have been developed (Gupta & Chahal, 2015; Yadav et al., 2011).

To overcome the restriction of low material removal rate, ECA<sub>2</sub>FM can be used, which offers a better surface finish quality and higher material removal rate as compare to AFM process. ECA<sub>2</sub>FM is the hybrid process of electrochemical machining and abrasive flow machining consisting of a salts-abrasive laden media passes into the cathode rod and the anode work-piece with the source of DC power. This process is a good example of a modified process combining electrochemical polishing and abrasive finishing technique, which results in more machining along with high surface finish quality in comparison to abrasive finishing technique taken individually (Gupta & Chahal, 2015).

AFM is capable of meeting the finishing requirements of different sectors of industrial applications such as aerospace, automotive, electronics, medical, precision dies and molds (Yadav et al., 2011).

### *High speed slurry flow finishing*

Kurobe et al. (1998) developed the high-speed slurry flow finishing method that is used for high precision polishing of inner walls of stainless steel capillaries with fine holes and long size. The polishing action is performed by flowing of the high-speed slurry through the capillary. Yin et al. (2004) showed the feasibility of applying high-speed abrasive flow polishing for the surface roughness reduction of metal and ceramic micro-bores. The material removal mechanism is mainly abrasion. Abrasive polishing medium grinds the surface irregularities, leaving a uniform and smooth surface.

The inner wall polishing of inaccessible areas is very complicated to be performed by many ordinary polishing technologies. For instance, the electrolytic polishing and the honing have the limitation of means of polishing tools, while the magnetic polishing and chemical polishing need



to control the polishing media quality like magnetic fluid and chemical solution (Yasunaga, 1994). On the other hand, the high-speed slurry flow finishing employs the abrasive fluid as a polishing tool, where the fluid tool can conform to the shape of the work-piece hole (Kurobe et al., 2002). Yin et al. (2004) found that the surface roughness reduction increases with increasing the number of slurry passes and surface texture is eliminated within several polishing passes with abrasive flow polishing. The graphs of surface roughness measurements for the inner wall of the 500- $\mu\text{m}$  stainless steel 304 bores obtained after abrasive flow polishing are shown in Figure 2.4.

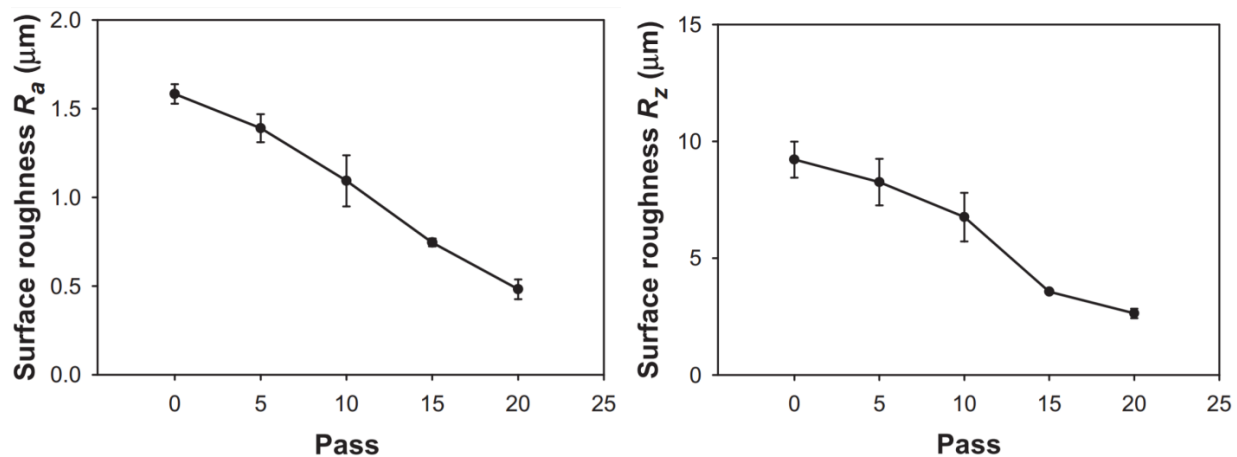


Figure 2.4:  $R_a$  and  $R_z$  surface roughness, obtained by profilometry, of inner wall of the 500- $\mu\text{m}$  stainless steel 304 bores polished by abrasive flow polishing. (Yin et al., 2004)

Despite many improvements in abrasive flow finishing techniques, there is space for more research in this area.

### 2.3.3 Process parameters control for abrasive flow finishing performance

Abrasive flow finishing process covers a huge range of finishing operations, where complexity of parts is a limitation for utilizing many ordinary finishing methods. Here, controlling the parameters of the process is very critical to achieve a uniform surface, predictable and repeatable results. For understanding the effect of process parameters on the surface finishing results, some related researches are reviewed in this section.

In AFM process, many input parameters can affect the surface finish quality and material removal rate. This makes it complicated to predict the process output parameters. Bremerstein et al. (2015) listed the input parameters of AFM into three groups of machines, work-pieces and work-piece fixtures, and abrasive medium, which are presented in Figure 2.5.

Machine	Workpiece / workpiece fixture	Abrasive medium
<ul style="list-style-type: none"> <li>• Medium pressure / flow velocity</li> <li>• Number of cycles</li> <li>• Volume of medium</li> <li>• Temperature</li> </ul>	<ul style="list-style-type: none"> <li>• Initial surface quality</li> <li>• Workpiece material and geometry</li> <li>• Design of workpiece fixture</li> </ul>	<ul style="list-style-type: none"> <li>• Size and shape of abrasive particles</li> <li>• Abrasive concentration</li> <li>• Abrasive type</li> <li>• Composition of carrier medium</li> <li>• Viscosity</li> </ul>

Figure 2.5: Input parameters in AFM process (Bremerstein et al., 2015)

Rajasha et al. (2010) stated that the rheological behavior of the abrasive medium dominates the results of AFM. Moreover, (Kar et al., 2009) stated that the percentage ingredients of the abrasive medium along with the number of cycles control the rheological behavior of the medium; hence, it is the basic input parameter. Considering the abrasive medium as the basic input parameter, Wang et al. (2007) conduct simulation and experiments to study the properties of abrasive gels in AFM. They found that a higher viscosity lead to more material removal rate due to the generation of larger shear force. Sankar et al. (2011) explained that more material removal rate is obtained by higher medium viscosity and larger particle size. However, this has a negative effect on the surface finish quality.

For abrasive flow polishing, Kurobe et al. (1998) showed that the abrasive concentration in the medium, particle size and slurry flow pass directly affect the surface finish quality of inner wall of a die hole (Figure 2.6 and 2.7). They reported that the surface roughness and polishing time decreases by increasing the number of slurry flow pass. Later, they showed that the hardness of die materials affects the surface roughness reduction. Therefore, the selection of polishing conditions like particle size and abrasive concentration is dependent on the polished material (Kurobe et al., 2002).

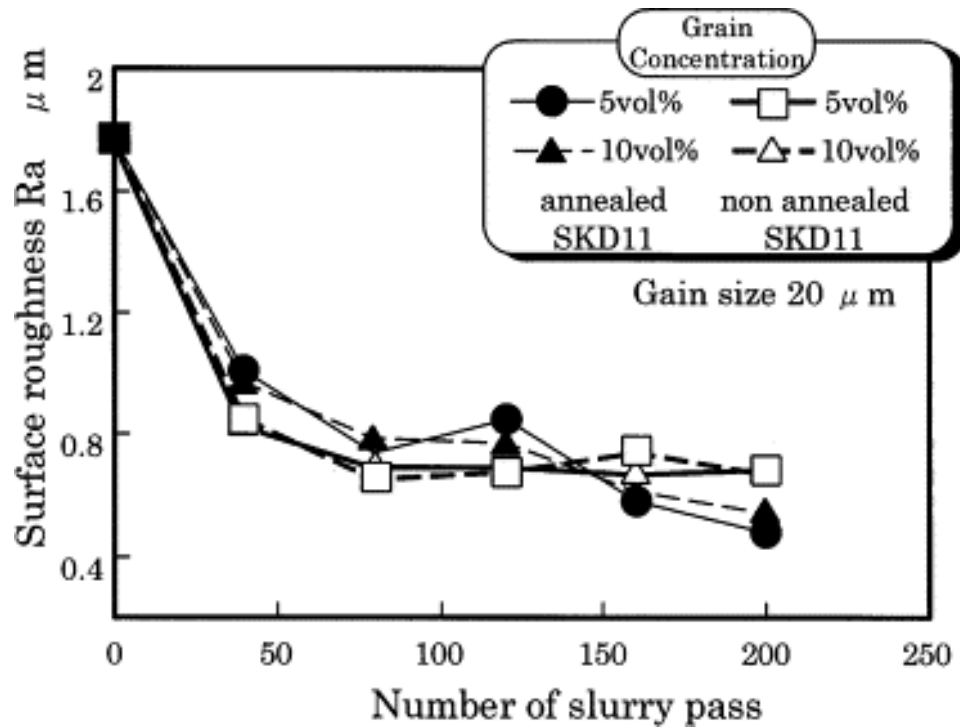


Figure 2.6: Surface roughness as a function of number of slurry passes for various abrasive concentrations in abrasive flow polishing process of tool steel (JIS:SKD11) (Kurobe et al., 2002)

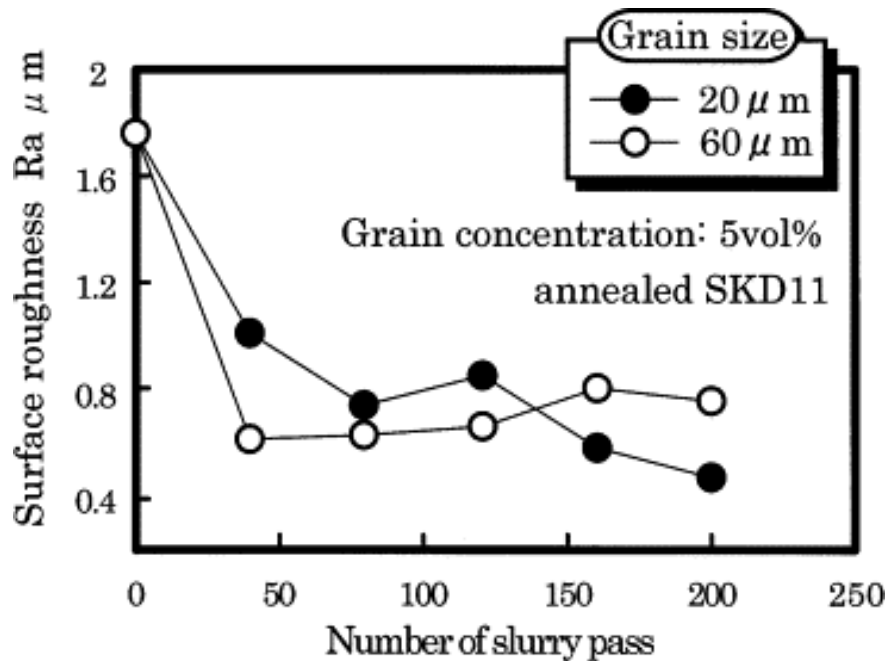


Figure 2-7: Surface roughness as a function of number of slurry pass for different abrasive particle sizes in abrasive flow polishing process of tool steel (JIS:SKD11) (Kurobe et al., 2002)

## 2.4 Chemical-abrasive flow polishing

Combining the chemical flow polishing and abrasive flow finishing techniques might be an economic way of polishing surface integrities of AM components, which can be addressed in two concepts.

Firstly, there are some limitations for using chemical flow polishing and abrasive flow polishing individually:

- Machining near net shape parts to the final dimensions is applicable for the parts with relatively simple geometry. This strategy was studied by Thakur & Gangopadhyay (2016) for nickel-based superalloys and Rawal et al. (2013) for AM spacecraft components of Ti-6Al-4V. For the parts with internal design complexities, techniques equipped with hard polishing tools are inadequate.
- In abrasive flow machining, there is a limitation for polishing of large channels due to the high viscosity of the abrasive medium, (Rhoades, 1991).
- As with chemical polishing, most of the solutions are applicable for specific alloys; no general chemical solution exists. For a new alloy, some tests should be performed to obtain the appropriate solution. For example, to the best knowledge of the authors' knowledge, there is no proper chemical solution for Ni-Cr-Mo alloys. The high content of chromium and molybdenum in the composition of this family of alloys explain its exceptional chemical resistance to both oxidizing and reducing environments, (Crook, 2005).
- Despite the efficiency of using electrochemical polishing for polishing AM components, the use of conformal electrodes complicates the polishing of narrow channels and cavities, (Urlea & Brailovski, 2017).

Secondly, using combined and modified techniques can overcome some of the limitations of chemical polishing and abrasive flow finishing methods, improving efficiency and accuracy of the finishing operation. ECA<sub>2</sub>FM process (explained in Section 2.3.2.) is an example of a modified technique, which results in higher material removal rate and surface quality than the AFM process (Gupta & Chahal, 2015).

Using a combination of chemical and mechanical actions is an effective approach, however it is very complicated to understand and predict the results. The mechanisms of chemical reaction and mechanical material removal have been studied through two combined techniques of chemical mechanical polishing (CMP) and slurry erosion wear tests, which are presented in the following section.

### *Chemical Mechanical Polishing (CMP)*

The CMP process is a combination of mechanical grinding and etching methods. In CMP, the surface is polished utilizing a chemical-abrasive slurry formulation and a mechanical action introduced by a downforce pressure of a pad simultaneously. Lee et al. (2016) reviewed the CMP process for surface polishing of Ti-6Al-4V alloy. They explained that investigating the chemical composition of the polishing slurry and the property of the target material is the key to clarify the chemical reaction mechanism of the CMP. Nevertheless, the basic factor for predicting the results of CMP is determining the mechanism of mechanical material removal. Different process parameters and consumables affect the complex mechanical action of the CMP. In respect to obtaining an optimum result for CMP, they stated that there must be a balance between the chemical reaction and the mechanical force. Insufficient removal occurs by excessive chemical action and an abundance of scratches arise on the surface after strong mechanical force. The expected mechanisms of material removal are presented in Figure 2.8.

To explain the role of chemical reaction in CMP, Si et al. (2011) described that the mechanical abrasion generated from sliding and rolling of the abrasive particles is easier on the oxidized or hydrated layer of the surface. The passive layer is produced continuously by a chemical reaction between the surface and the chemical slurry.

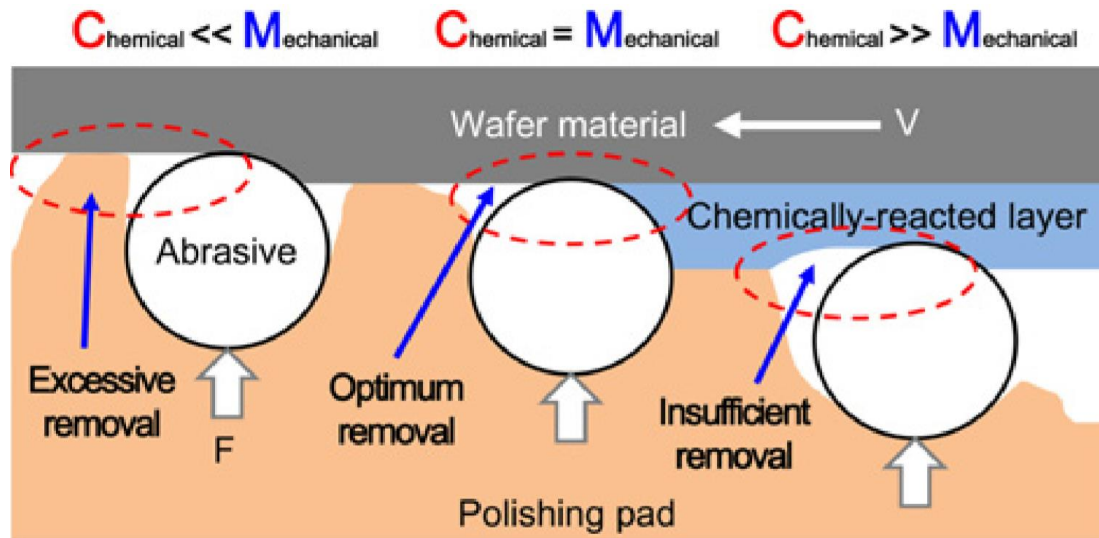


Figure 2.8: Expected mechanisms for material removal of the CMP process (Lee et al., 2016)

The same as abrasive flow finishing, the process parameters and consumables like relative velocity, abrasive size, shape and concentration strongly influences the results of CMP process. Therefore, it is worth summarizing the mechanical characteristics of these process variables.

According to the Preston's equation (Preston, 1927), the basic model of wafer-scale material removal rate ( $MRR$ ) is obtained as a function of wafer pressure ( $P$ ) and relative velocity between the wafer and polishing pad ( $V$ ):

$$MRR = B P V \quad (2.7)$$

where the Preston's coefficient ( $B$ ) explains other process parameters of CMP.

As presented in Equation 2.7, the relative velocity affects  $MRR$ , its distribution and uniformity. The  $MRR$  increases with the velocity (Hocheng et al., 2000).

Lee et al. (2016) described some qualifications for the CMP abrasive particles:

- There must be no agglomeration of abrasives in CMP slurry and the particles should be suspended.
- The abrasives should not be dissolved in the chemical solution.
- Their hardness must be greater than or equal to the surface material hardness.
- The size, shape and concentration of the particles should be optimized to obtain controllable results. There is a complex relationship between these three factors.

They explained that although a non-spherical shape of abrasive causes higher  $MRR$ , the use of spherical abrasive eliminated scratches on the surface. Three trends can be observed for the variation of  $MRR$  in a relation with the size and concentration of abrasives, which are shown in Figure 2.9 and 2.10. Lee et al. (2016) stated that obtaining conflicting trends for the  $MRR$  in the two presented figures is the result of complex relationship between abrasive size distribution, abrasive size and abrasive concentration. According to the model developed by Luo & Dornfeld (2003) for material removal mechanism in CMP process, two points should be considered in the influence of the abrasive size distribution on the material removal:

- I. The size of the active abrasives: Larger abrasives result in higher  $MRR$  compared to the smaller ones, because of their larger indentation volume.
- II. The number of active abrasives: The larger number of active abrasives increases the  $MRR$ . On the other hand, the real contact area between the material surface and polishing pad limits the number of active abrasives.

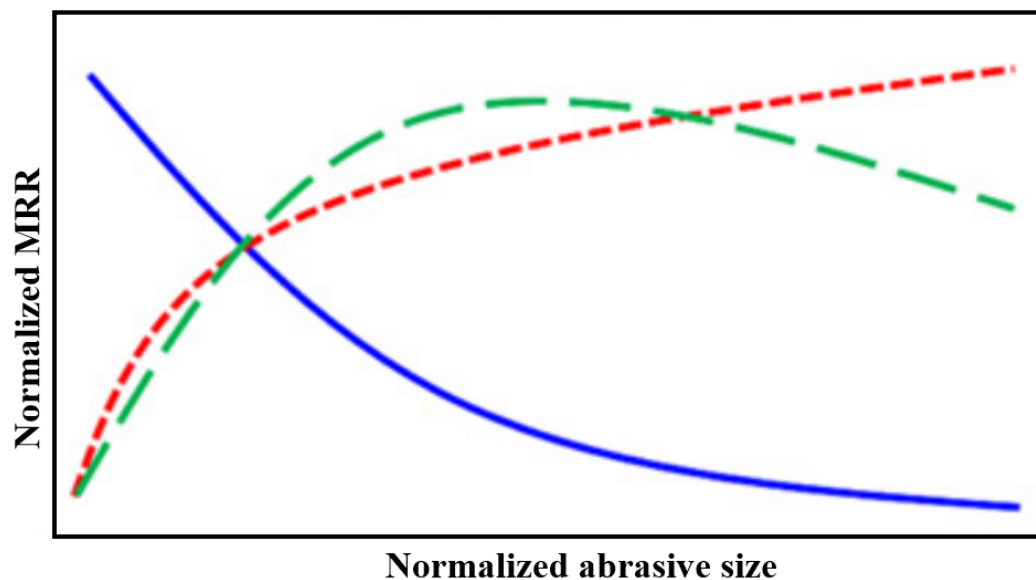


Figure 2.9: Three trends of MRR in accordance with abrasive sizes in CMP process (Lee et al., 2016)

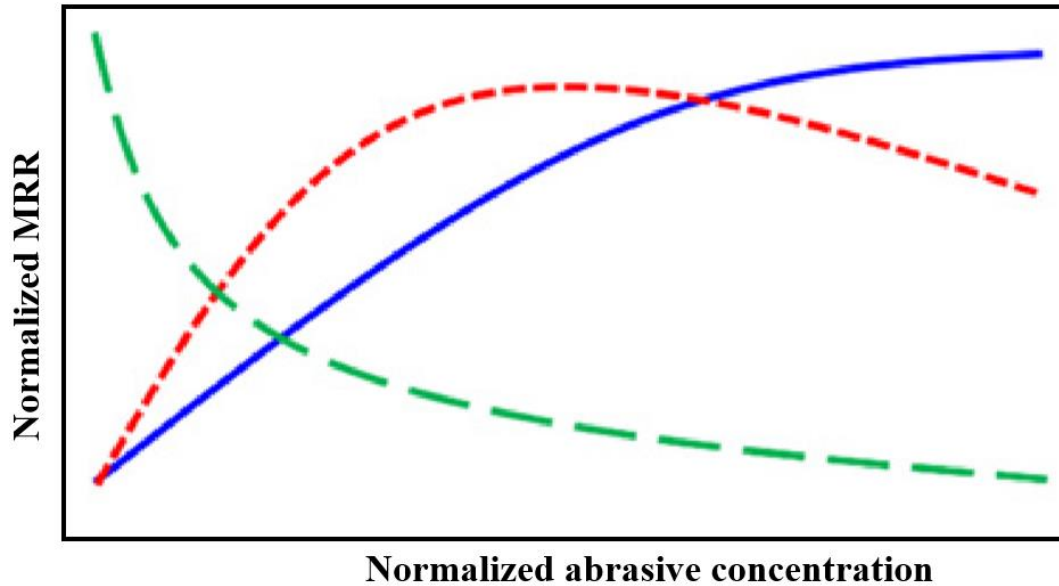


Figure 2.10: Three trends of MRR in accordance with abrasive concentrations in CMP process  
(Lee et al., 2016)

### *Slurry erosion wear test*

Slurry erosion wear test is a technique that is utilized to simulate slurry erosion wear in laboratory conditions. The test consists of a combination of chemical solution and abrasive particles jet-flow action. It is conducted to study the influence of different parameters such as flow speed, abrasive size and concentration of the slurry on erosion wear of the investigated surface material (Ramesh et al., 2011). Figure 2.11 illustrates an example of schematic representation of the slurry erosion wear tester, designed by Ramesh et al. (2014). They investigated slurry erosive wear behavior of inconel-718 coatings on copper. The specimen is fixed on the spindle, which is fully immersed in the slurry containing 3.5% NaCl solution and erodent silica sand particles. The size and concentration of abrasives, and the slurry rotational speed were the test variables. The slurry erosion wear was determined by calculating the weight loss of the coated specimen after the test. The wear results as a function of test variable are presented in Figure 2.12.



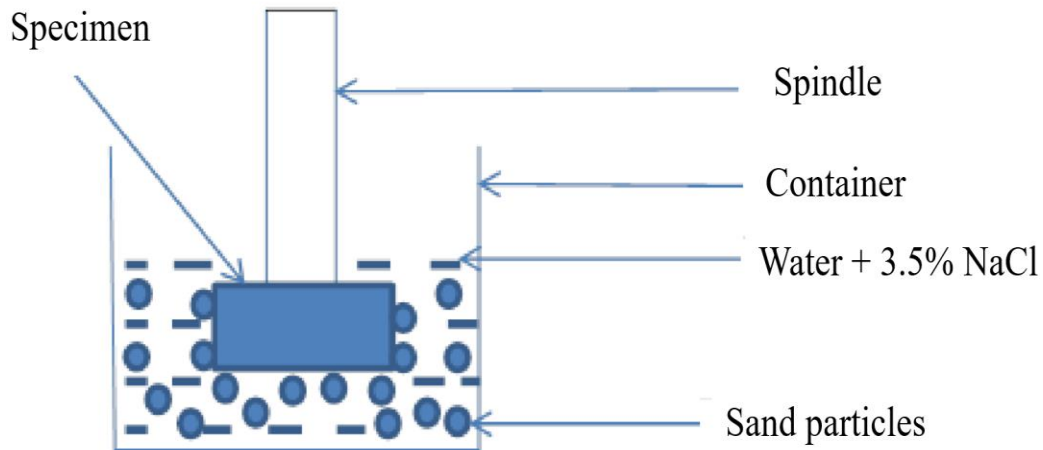


Figure 2.11: Schematic diagram of the slurry erosion wear test (Ramesh et al., 2014)

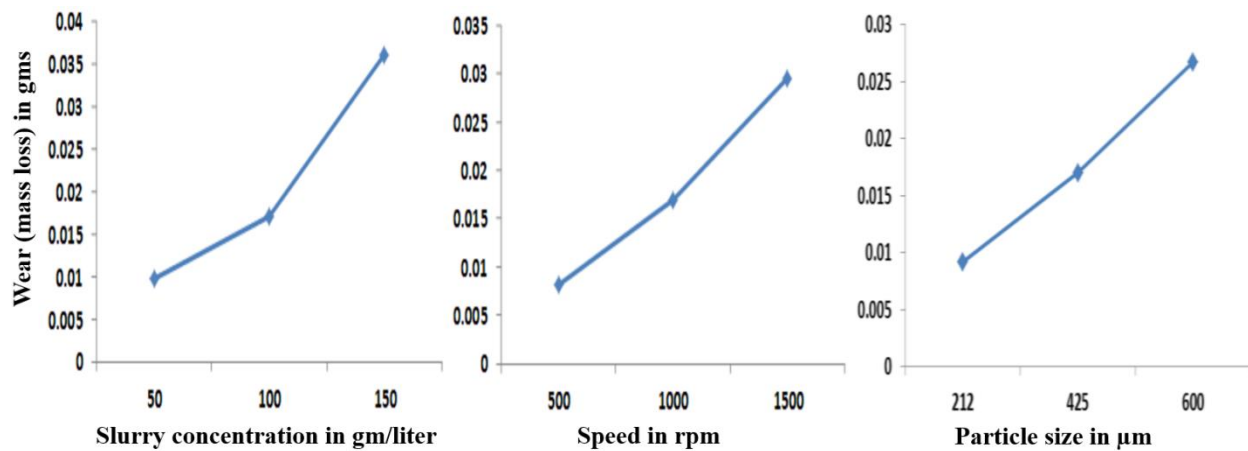


Figure 2.12: Influence of slurry concentration, speed and particle size on slurry erosive wear (Ramesh et al., 2014)

Research showed that the *MRR* increases by increasing the abrasive particle concentration (Ojala et al., 2015; Zuet al., 1990). Ramesh et al. (2014) described that more impingements are subjected to the surface by increasing the abrasive concentration in the slurry, which results in increment of mass loss. They also found that the *MRR* decreases with increasing the surface hardness, strength and corrosion resistance of the surface material. Lynn et al. (1991) studied the effect of particle size in slurry erosion rate of steel specimens in 1.2 wt.% SiC suspension in oil. They explained that decreasing the particle size leads to decrement of erosion rate because of the combined effect of two factors:

- I. The proportion of abrasive particles impacting the surface decreases due to the decrement of collision efficiency of particles with decreasing particle size.
- II. The impact velocity also decreases, which reflects decreasing of particle inertia for the smaller particles. Therefore, smaller particles are more easily deflected by the flow of the fluid near the surface to follow fluid streamlines, which decreases the impact angle of the particles to about  $0^\circ$ . In fact, by descending or ascending from intermediate impact angles, less material is removed from the ductile surface.

They also noted that for particle sizes greater than  $100\ \mu\text{m}$ , the erosion rate is in accordance with the kinetic energy of impacting particles for the dilute suspensions of the test. However, for smaller particles sizes, the dominant mechanism of material removal changes.

To conclude, in respect to the necessity of employing a mechanical force, CMP polishing is inappropriate for polishing complex components with inaccessible areas. Furthermore, studying erosion wear test is aimed for investigating the wear behavior of a material against chemical abrasive slurry, not for polishing the surface. However, studying the research in these areas helps to understand the mechanisms of material removal and the synergetic effect chemical and abrasive actions.

## CHAPTER 3      EXPERIMENTAL METHODS AND TECHNIQUES

### 3.1 Introduction

The main purpose of this experimental study was to investigate the synergetic effect of chemical and abrasive flow polishing techniques with the aim of finishing the interior part of IN-625 surfaces fabricated by SLM process. For this purpose, three polishing techniques were investigated. Removal of semi-welded particles and surface roughness reduction were used to determine the performance of each polishing technique. The main parameters of the experiment were the surface roughness ( $R_a$  and  $R_z$ ), the polishing depth, the surface texture and topography, fluid velocity, polishing time and build orientation. The methodology used to conduct for the current study is presented in Section 4.2. In this chapter, the complementary information regarding the experimental setup and the experimental plan is explained.

### 3.2 Experimental setup

A chemical-abrasive flow polishing setup in the laboratory was developed to apply a corrosive and erosive flow of acids and abrasive particles into the interior surface of hollow cylindrical specimen. The detailed information of the setup design and operation is presented in Section 4.3.1. The polishing fluid flow is generated and controlled by a centrifugal pump and the flow rate is measured by an ultrasonic flow sensor. In this section, the selection criteria and specifications of the pump and the sensor as well as the utilized wet materials of the setup are provided. Later, the safety procedure and cost of chemical tests and manufacturing the polishing setup are explained.

#### 3.2.1 Pump and sensor

Improper handling methods of slurry and fluid delivery can cause damage in abrasive particles. The size distribution of the particles changes and agglomeration occurs in the system. This may significantly alter the slurry characteristics including viscosity, density and solid concentration (Johl et al., 2005). Nicholes et al. (2003) showed that agglomeration and production of large particles in CMP slurry results in surface defects such as micro-scratches.

Studies have been done on the effect of slurry delivery technique on the metrology parameters of the slurry for CMP polishing systems (Johl et al., 2005; Litchy & Schoeb, 2005). Some of these studies have compared the performance of different pump and vacuum-pressure dispensing methods for slurry distribution in CMP process (Singh & Johl, 2001). The results of these investigations were helpful for the selection of the appropriate fluid delivery technology in our polishing setup. Litchy & Schoeb (2005) studied the effect of utilizing three pump types of bellows, diaphragm and centrifugal, on large particle concentration in the slurry without applying filtration to the system. They obtained significantly different results for the ratio of the measured concentration to the initial particle concentration as a function of turnovers for the three types of pumps. In the bellows and diaphragm pump systems, the large particle concentration for particles  $\geq 0.56 \mu\text{m}$  increased by turnovers, due essentially to particle agglomeration. However, it remained constant for the centrifugal pump. They observed similar results of concentration changes for large particle sizes. Johl et al. (2005) reported no change for the large particle concentration until 100 turnovers and 40% decrement after 1000 turnovers using magnetically levitated (maglev) centrifugal pump. They explained that the advantage of maglev pumps in slurry handling is related to the use of a moderate shear level to the slurry, which results in crushing the loose agglomerates.

Based on the studied research, centrifugal pump was selected to be used for the chemical-abrasive polishing setup. The centrifugal pump tank mixer (PTM-1, Levitronix, max. flow rate of 17 L/min) was used for the polishing system. There is no mechanical wear in the mixing system of the pump, thus no particle coming from worn pump components occurs. The speed of the flow is electronically controlled by the pump impeller speed.

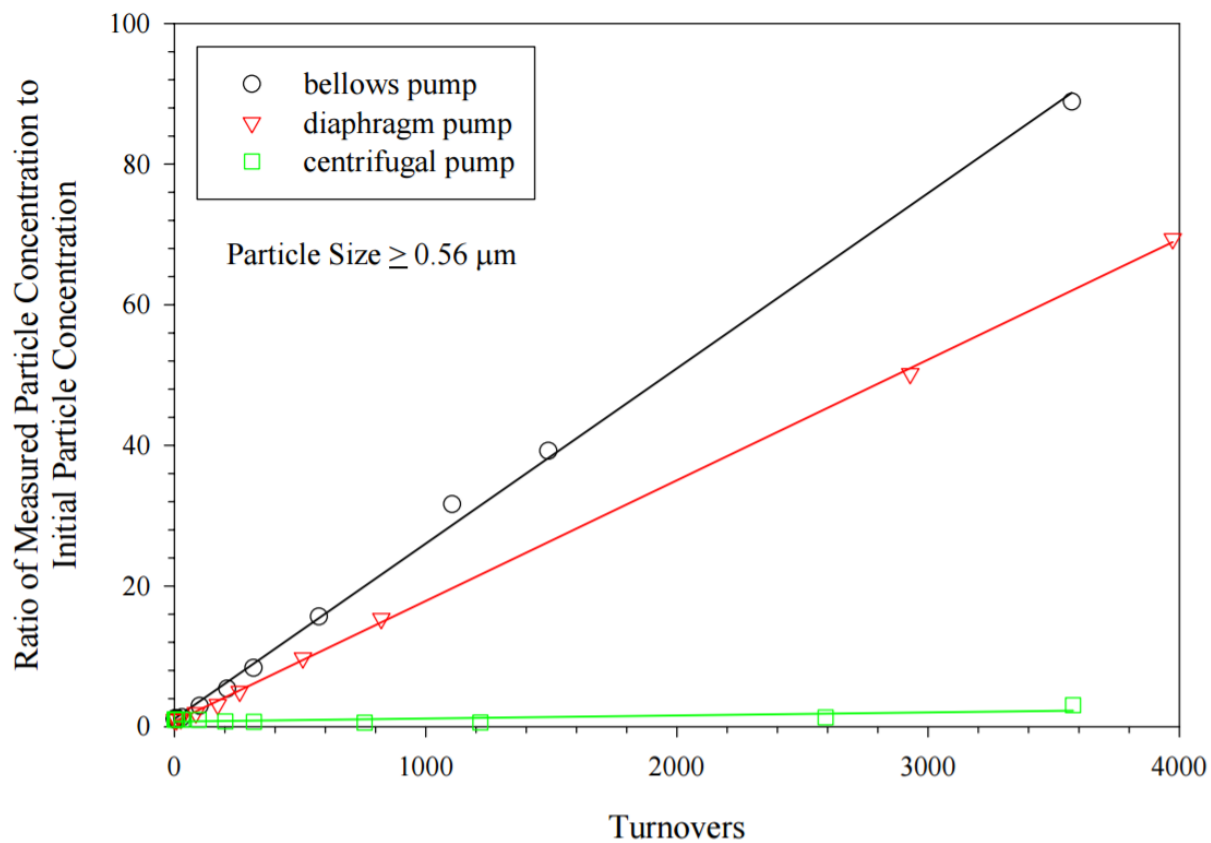


Figure 3.1: Effect of various pumps on large particle concentrations in the slurry for CMP process (Litchy & Schoeb, 2005)

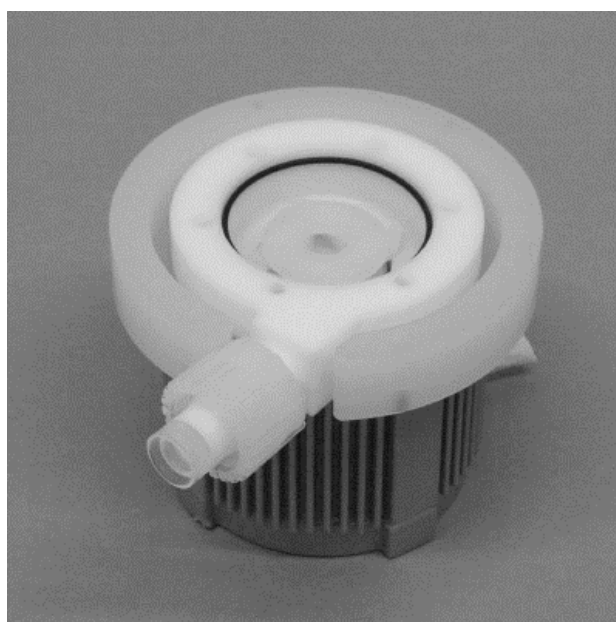


Figure 3.2: Levitronix PTM, pump and mixer ([www.levitronix.com](http://www.levitronix.com))

An ultrasound sensor (LFS-20, Levitronix) was used to provide a flow range measurement of 0-20 L/min. The sensor avoids contamination due to its non-invasive measurement. Also, it has high accuracy and no particle generation because there is no moving part in the sensor. The flow control is in combination with the Levitronix PTM pump tank mixer.

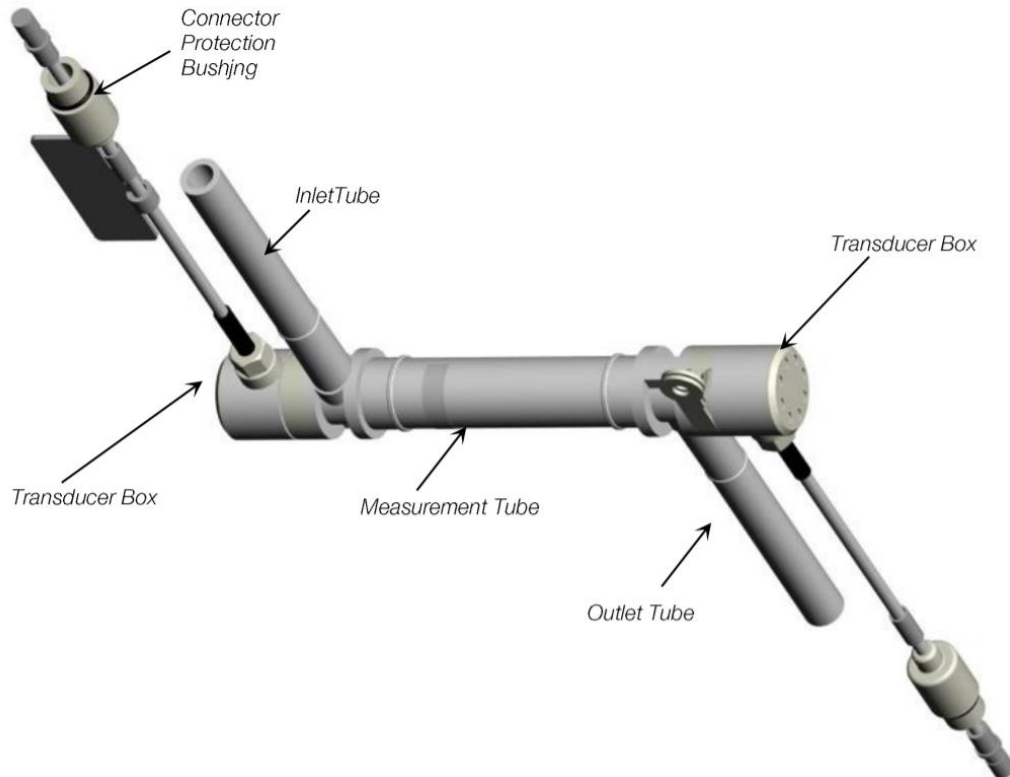


Figure 3.3: Flow sensor design (LFS Levitronix) ([www.levitronix.com](http://www.levitronix.com))

### 3.2.2 Wet materials

Static chemical polishing tests were performed to select the proper chemical solution for the chemical-abrasive polishing process, which are presented in Section 4.3.2. The selected chemical solution was 40 vol.% of concentrated hydrofluoric acid (HF), 40 vol.% of concentrated nitric acid (HNO<sub>3</sub>) and 20 vol.% of distilled water. The criteria for selection of the wet materials of the setup was good chemical resistance to the acidic-based chemical solution of the fluid in the room temperature. The list of used materials for different parts of the setup are presented in Table 3.1.

Table 3.1: Wet materials for the polishing setup parts resistant to high concentrated HF and HNO<sub>3</sub> at room temperature ([www.sevierlab.vet.cornell.edu](http://www.sevierlab.vet.cornell.edu), [www.plasticsintl.com](http://www.plasticsintl.com), [www.parrinst.com](http://www.parrinst.com))

Setup part	Wet material	Supplier
Pump	PFA / PTFE / Perfluoroelastomer / PVDF	<a href="http://www.levitronix.com">www.levitronix.com</a>
Sensor	PFA	
Tanks	PVDF	<a href="http://www.polyfab.com">www.polyfab.com</a>
Sealing O-rings	Perfluoroelastomer	<a href="http://www.gbs.ca">www.gbs.ca</a>
Tubing	PVC	<a href="http://www.mcmaster.com">www.mcmaster.com</a>
Pipe	PVDF	
Depletion tank	HDPE	
Valve	PVC	
Fittings	PVDF / PVC	

PFA: Perfluoroalkoxy, PTFE: Polytetrafluoroethylene, PVDF: Polyvinylidene fluoride, PVC: Polyvinyl chloride, HDPE: High-density polyethylene

### 3.2.3 Safety plan

It is necessary to create tailored safety plan for working with hazardous materials and processes in a laboratory. For this project, the safety operating procedure before conducting the experiments are listed below:

- The training course, Atelier de formation en santé-sécurité, was taken to learn safety instructions of working in a laboratory.
- For handling and management of chemical experiments, the risks of chemical activities were studied using the information provided in a book by National Research Council (US) (2011).

- The chemical reactions of the acidic-based solution and abrasives were tested through static tests. Also, corrosion resistance of the wet materials of the setup was checked by immersing the parts in the selected chemical solution, 40 vol.% of concentrated hydrofluoric acid (HF), 40 vol.% of concentrated nitric acid (HNO<sub>3</sub>) and 20 vol.% of distilled water, for 48 hours at room temperature.
- Protective clothing including chemical resistant gloves (Barrier 2-100, [www.ansellcanada.ca](http://www.ansellcanada.ca)), chemical waste disposal containers (HDPE, [www.mcmaster.com](http://www.mcmaster.com)), lab coat (Polypropylene, SEC853, [www.zenithsafety.com](http://www.zenithsafety.com)) and first aid box were prepared.
- The size of the polishing setup parts for ordering were considered in a way that the set up can be easily mounted under the fume hood, model VBA-48, using a designed and built movable holder. The final set up dimensions was 80 × 30 × 80 cm<sup>3</sup>, which is shown in Figure 3.4.
- The pump and sensor system devices including power supply and converters were installed out of the fume hood for safety purposes, as shown in Figure 3.5(a). To keep the devices cool, they were installed in vertical direction and a fan was used for cooling the pump converter. Also, an air cooling module is being used for cooling the pump motor, as shown in Figure 3.5(b).

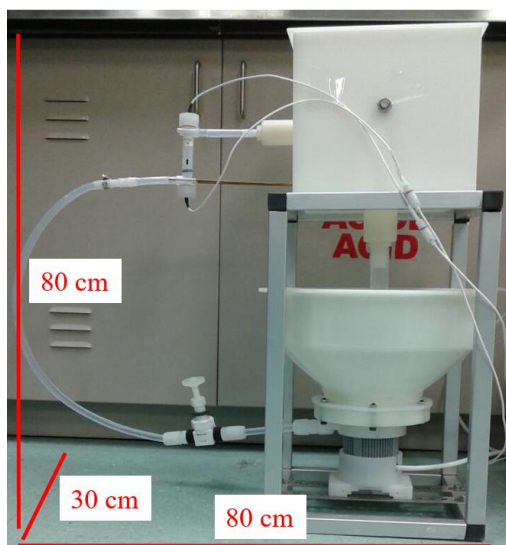


Figure 3.4: Polishing setup dimensions



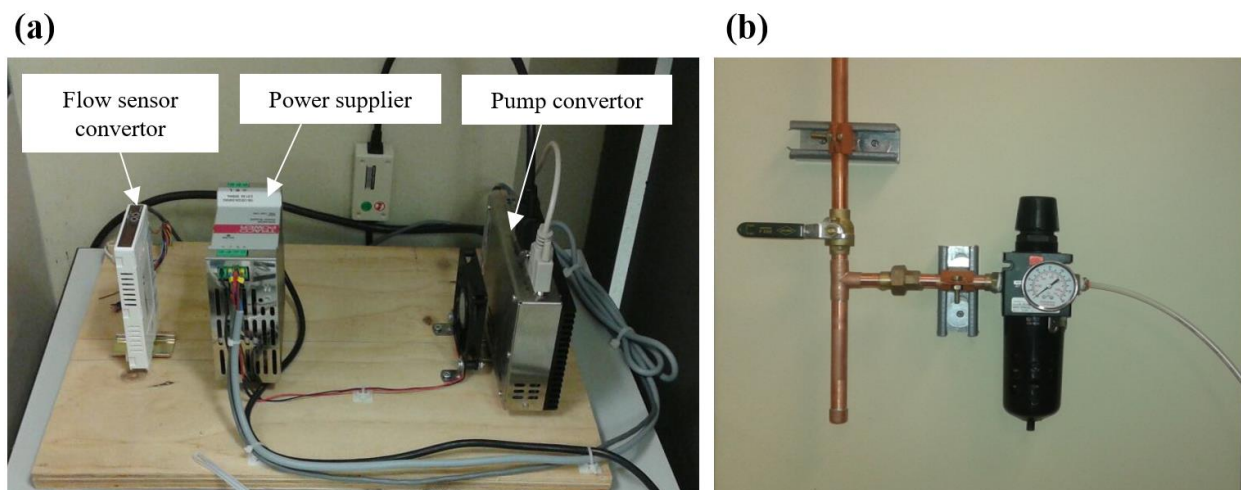


Figure 3.5: (a) Safe installation of the pump and sensor devices far from the setup, and (b) air cooling module for the pump

### 3.2.4 Cost

The details of the equipment cost for the project of this thesis are presented in Table 3.2.

Table 3.2: Thesis project equipment and materials cost

Equipment and material		Cost (\$)
<b>Setup</b>	Pump & flow sensor	12 200
	Polishing tanks	5 800
	<i>Miscellaneous</i> parts	1 200
	computer	1 000
<b>Fluid</b>	Acids: HF + HNO <sub>3</sub>	700
	Al <sub>2</sub> O <sub>3</sub> abrasives	100
<b>Total before tax (CAD)</b>		<b>21 000</b>

### 3.3 Experimental plan

The experimental strategy is the first stage of each experimental investigation, and it is necessary to define for any experimental study to conduct it properly. For this purpose, experimental plan, the process setup, materials and methods of analysis are studied thoroughly. The flowchart of experimental plan is presented in Figure 3.6 and explained in the following sections.

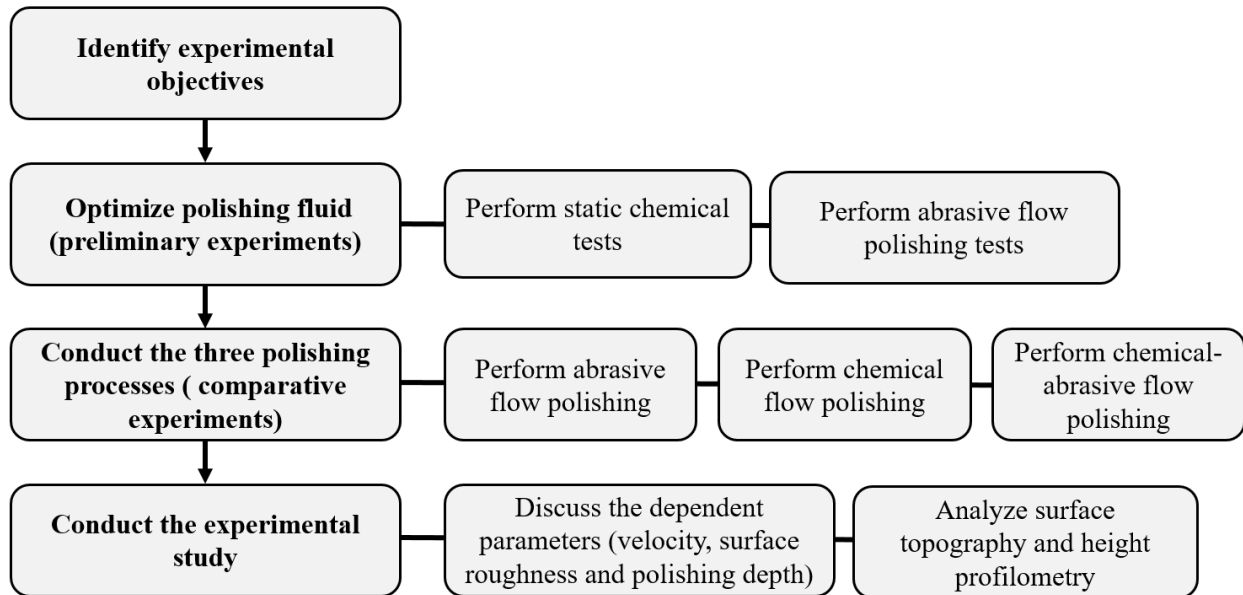


Figure 3.6: Experimental plan flowchart

#### 3.3.1 Identifying experimental objectives

The first step of the experimental plan was defining the experimental objectives, scientific hypothesis and process parameters. The objectives and hypothesis of the studied work are presented in Chapter 1(Introduction). The process variables of the experiments are as follows: The input parameters are pump speed, temperature, flow pressure, flow rate, velocity of the fluid, fluid materials (chemicals and abrasive particles), composition and concentration of chemical solution, and abrasive size and concentration. Dependent characteristics are, polishing depth ( $\mu\text{m}$ ) and surface roughness values for  $R_a$  and  $R_z$  ( $\mu\text{m}$ ).

#### 3.3.2 Optimizing the polishing fluid

The second step was optimizing the chemical and abrasive agents of the polishing fluid through preliminary static chemical polishing and abrasive flow polishing tests respectively.

The details of static chemical tests, aiming at the selection of chemical polishing solution for IN-625, are explained in Section 4.3.2.

The abrasive flow polishing tests were also performed to identify the abrasive material, size and appropriate concentration of the abrasive agent. In this study, aluminum oxide abrasive particles were selected as abrasive material because of the particle shape and hardness of alumina. Silva et al. (2011) stated that sharp edge particles show more abrasivity compared to round abrasive abrasives. In addition, the material removal volume increases with hardness of the abrasive particles in the abrasion process. Alumina particles have sharp edges and a hardness of about 2000 Vickers ([www.kramerindustriesonline.com](http://www.kramerindustriesonline.com)).

Three abrasive particle sizes were tested and the results are presented in Table 3.3. The concentration of abrasive particles in the water (polishing media) was 6 wt.%, the volume of water was 5 liters, the flow rate was kept constant at 10 L/min with a pumping pressure of about 32.2 psi, and the polishing time was 1 hour. The average particle size of 420  $\mu\text{m}$  was selected for the polishing process. As for abrasive concentration, the material removal rate increases by increment of abrasive concentration, which has been discussed in Section 2.3.3. The polishing setup can mix and pump a maximum concentration of 6 wt.% for  $\text{Al}_2\text{O}_3$  grits. Thus, the abrasive concentration was kept at the constant of 6 wt.%.

Table 3.3: Results of roughness reduction for the abrasive flow polishing using three abrasive particle sizes for the determined process conditions

<b>Average particle size</b>	<b>Application</b>	<b>Roughness reduction results</b>
1 $\mu\text{m}$	Chemical mechanical polishing, (Lee et al., 2016)	No roughness reduction
20 $\mu\text{m}$	Abrasive flow polishing, (Yin et al., 2004)	No roughness reduction
420 $\mu\text{m}$	Slurry erosion wear test, (Ramesh et al., 2014a)	1 $\mu\text{m}$ reduction in $R_a$ value for the two build orientations of 15° and 135°

### 3.3.3 Conducting the three polishing processes

The third step of the experimental plan was conducting a comparative experiment including the three polishing techniques: chemical, abrasive and combined chemical-abrasive flow polishing techniques. Later, the polishing results were compared to investigate the synergy effect of combining chemical and abrasive actions in polishing process. The experimental conditions for performing the three polishing techniques are explained in Section 4.3.2.

The number of IN-625 specimens used for the experiments are shown in Table 3.4. In this table, the preliminary tests refer to the static chemical and abrasive flow polishing tests, performed to select and optimize the chemical and abrasive agents of the polishing fluid respectively. The comparative tests refer to static chemical, chemical flow, abrasive flow and chemical-abrasive flow polishing experiments, in which the results of the tests were compared with each other to clarify the effect of dynamic flow action in chemical polishing and the synergy effect of combining chemical and abrasive flow polishing techniques. As presented in Figure 3.7, two shapes of specimens were utilized for the tests. The preliminary and comparative tests were performed using the edge-shaped specimen, shown in Figure 3.7(a). The plate-shaped specimen, Figure 3.7(b), were cut to 8 pieces to repeat the preliminary static chemical polishing tests. The results of chemical polishing for each of the four solutions repeated two times.

To clarify the plan for the design of specimens and its objectives, the information on the edge-shaped specimen is presented briefly in the following paragraph. However, the complete overview of the polishing specimens is presented in Section 4.3.2.

The edge-shaped IN-625 specimens were SLM-printed using a powder-bed M290 EOS SLM system (Germany). As presented in Section 4.3.2, the edge-shaped specimen is placed inside a cylindrical sleeve and locked with a ring. The polishing fluid flows through the cylindrical part, polishing the two surfaces of the specimen with build orientations of  $15^\circ$  (low roughness) and  $135^\circ$  (high roughness), described by (Urlea & Brailovski, 2017). The angle between the specimen and the central axis of the cylindrical holder is  $30^\circ$  to obtain maximum erosion wear rate, explained by (Kosa & Göksenli, 2015).

Table 3.4: Experimental plan for the number of specimens used for each type of tests

Test		Purpose	N° specimens
Preliminary tests	Static chemical polishing	Select an acidic solution for the chemical agent (four solutions were tested)	<b>4 edge shaped spec.</b> - evaluating 15° and 135° build orientations, <b>8 plate-shaped spec.</b> for repetition tests - evaluating 135° build orientation.
	Abrasive flow polishing	Select an abrasive particle size for the abrasive agent (3 particle sizes were tested)	<b>3 edge-shaped spec.</b> - 1 hour polishing, evaluating 15° and 135° build orientations.
Comparative tests	Static chemical polishing	Study the effect of dynamic action in chemical polishing	<b>1 edge-shaped spec.</b> for each polishing technique- 1, 2 and 3 hours polishing, evaluating 15° and 135° build orientations.
	Chemical flow polishing	Study the synergy effect stemmed from combining chemical and abrasive flow polishing	
	Abrasive flow polishing		
	Chemical-abrasive flow polishing		

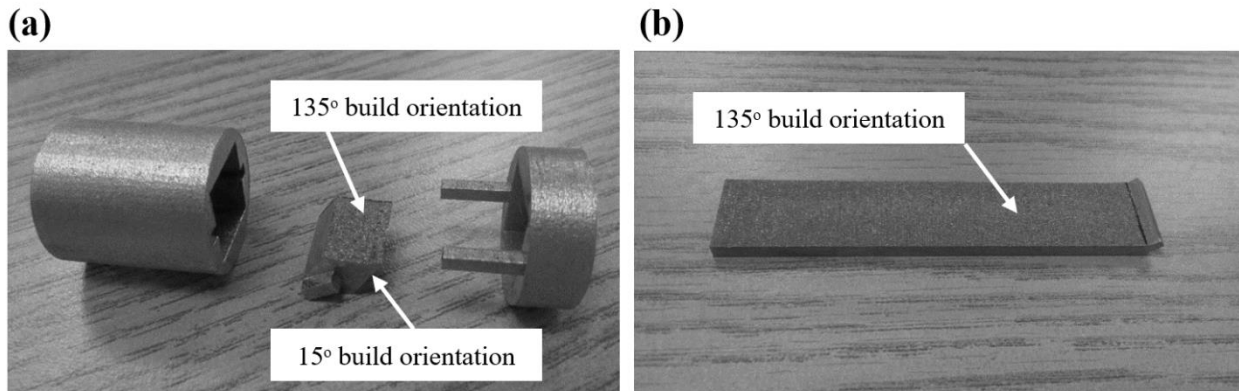


Figure 3.7: (a) Edge-shaped specimen with build orientations of 15° and 135°, and (b) plate-shaped specimen with build orientation of 135° on the rougher face

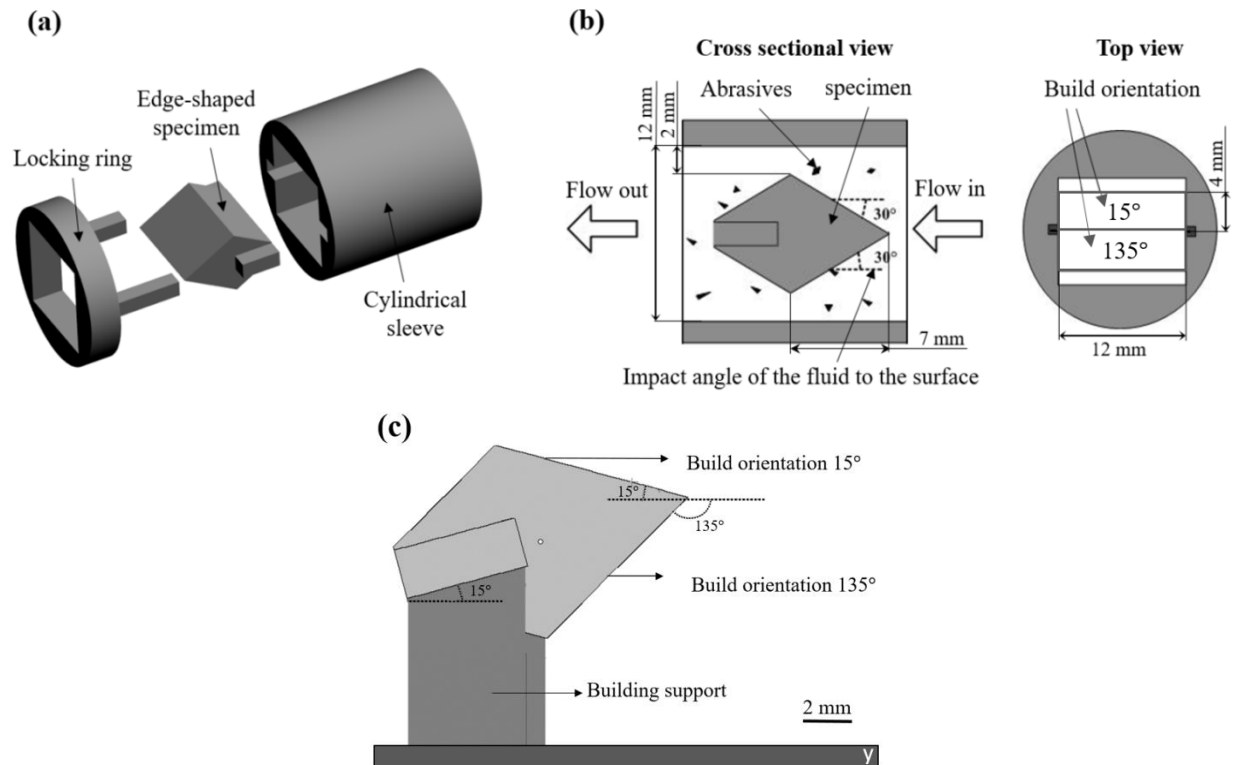


Figure 3.8: (a) Polishing specimen assembly, (b) chemical abrasive fluid flow inside the polished specimen, (c) edge shape specimen on the SLM building platform

### 3.3.4 Conducting the experimental study

The final step of the experimental plan was studying the correlation between various parameters obtained by the three studied polishing techniques, which is presented in Table 3.5.

The surface roughness measurements were performed by a surface roughness tester (SJ-410, Mitutoyo), Figure 3.9. The specifications of this device are presented in Table 3.6. The optical characterization including the polishing depth, the height profilometry, and the surface texture and topography was characterized by a confocal microscope (OLS 4100, OLYMPUS) as shown in Figure 3.10. The detailed information of the roughness measurements and optical characteristics are described in Section 4.3.3.

Table 3.5: Experimental plan for investigating the correlation between various parameters obtained by the studied polishing processes

Surface measurements and analysis	Correlated parameters to be studied	Utilized device
$R_a$ and $R_z$ surface finish	Polishing technique, polishing time, build orientation	surface roughness tester (SJ-410, Mitutoyo)
Polishing depth	Polishing technique, fluid velocity, build orientation	confocal microscope (OLS 4100, OLYMPUS)
Height profilometry	Polishing technique, polishing time, build orientation	
Topography	Polishing technique, build orientation	

Table 3.6: Specifications of Surface roughness tester SJ-410, Mitutoyo ([www.mitutoyo.com](http://www.mitutoyo.com))

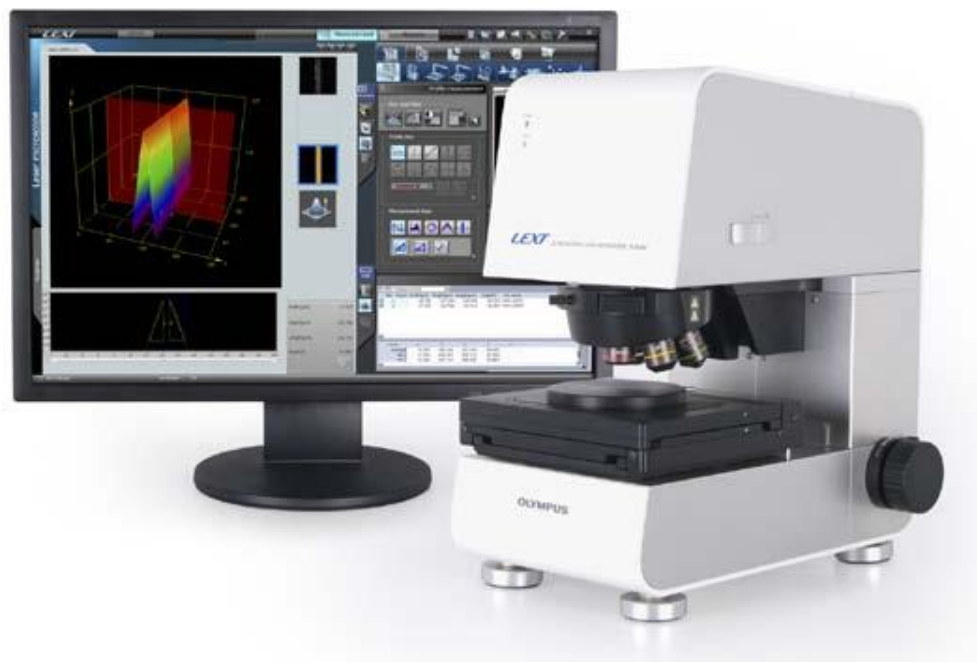
Specification	
Measuring Force	4 mN or 0.75 mN
Measuring range / Resolution	8 $\mu\text{m}$ /0.000125 $\mu\text{m}$
Traverse length(s)	0.3 $\mu\text{m}$ /25 mm or 0.5 $\mu\text{m}$ /50 mm
Filters	2CR, PC75, Gaussian filter



Figure 3.9: Surface roughness tester SJ-410, Mitutoyo ([www.mitutoyo.com](http://www.mitutoyo.com))

Table 3.7: LEXT OLS4100 laser confocal microscope ([www.olympus-ims.com](http://www.olympus-ims.com))

Specification	
Dual optical paths	laser and white light
Zoom ratio	8 ×
Maximum magnification	17 280 ×
Height measurements	10 nm

Figure 3.10: LEXT OLS4100 laser confocal microscope ([www.olympus-ims.com](http://www.olympus-ims.com))



## CHAPTER 4      ARTICLE 1: SURFACE FINISH CONTROL OF ADDITIVELY-MANUFACTURED INCONEL 625 COMPONENTS USING COMBINED CHEMICAL-ABRASIVE FLOW POLISHING

Neda Mohammadian, Sylvain Turenne, Vladimir Brailovski

This article has been accepted in the Journal of Materials Processing Technology in October 12<sup>th</sup>, 2017 and will be published in volume 252, pages 728-738 on February 2018.

### 4.1 Abstract

Little is understood about how to improve the interior surface quality of complex parts produced using additive manufacturing techniques, such as selective laser melting (SLM) and electron beam melting (EBM). Two surface-related problems can be highlighted in this context: the presence of semi-welded particles and a significant surface roughness and texture. Semi-welded particles could cause pollution in the fluid system of an engine part, while a significant surface roughness and texture could compromise fluid flow. This study aimed to design, manufacture and validate an innovative finishing technique combining chemical and abrasive flow polishing of interior surfaces of tubular IN625 components designed for the aerospace industry. The synergistic effect stemming from a combined use of the chemical and abrasive flows was investigated by studying: a) the flow of abrasive particles suspended in water, b) the flow of a chemical solution without abrasives, and c) the flow of abrasive particles suspended in a chemical solution. Considering the complexity of additively-manufactured components, the effect of the SLM build orientation on the internal surface finish was also characterized. The roughness and three-dimensional topography of the polished surface of IN625 parts for two SLM building orientations were assessed using the profilometry and confocal laser scanning microscopy techniques. The results obtained show that by employing the combined chemical-abrasive flow polishing technique, semi-welded particles on the interior surfaces of IN625 components can be completely removed and the surface roughness and texture, significantly improved.

**Keywords:** Additive manufacturing; Combined chemical-abrasive flow polishing; Surface roughness; Surface finishing; 3D surface topography characterization; Polishing processes.

## 4.2 Introduction

Inconel 625 (IN-625) is a nickel-based superalloy containing, as main alloying elements, chromium, molybdenum and niobium. Shankar et al. (2001) demonstrated that this alloy possesses outstanding oxidation and corrosion resistance in an industrial environment. In addition, Dinda et al. (2009) showed the excellent high temperature stress and corrosion resistance of this alloy, making it an excellent candidate for aircraft engine components.

Petrovic et al. (2011) reviewed that additive manufacturing (AM) of materials, including nickel-based alloys, is being considered by many industries, including the aerospace and automotive industries, where lightweight and highly complex parts are required. According to the report of (Wohlers, 2016), the compound annual growth ratio (CAGR) of the AM market services and products grew by 25.9% from \$4.102 to \$5.165 billion USD in 2015, while the combined growth percentage for the previous three years was 31.5%.

Arisoy et al. (2016) described laser powder bed fusion (LPBF), known also as selective laser melting (SLM), compared to many conventional manufacturing techniques, such as cast or wrought alloy processing, offers new possibilities of microstructure and mechanical properties control. These advantages can be gained through the new directional solidification approaches and different laser scan strategies offered by SLM.

Regardless of the many benefits of the SLM process, Król & Tański (2016) suggested that inadequate surface quality can be considered as its major drawback which is dependent on several factors such as the SLM process parameters and the orientation of the component in the building chamber. The surface finish of AM metals and alloys is considerably rougher than what is found on standard machined surfaces due to the presence of particular surface features formed during the powder-bed laser fusion. Moreover, semi-welded particles on the interior surface of flow conducts could detach and cause contamination of the fluid system. These semi-welded particles belong to the heat affected zone surrounding the melt pool created by a laser beam scanning along the part contour. The temperature in this zone is high enough to provoke sintering of loose powder particles immediately surrounding the melt pool. The higher the energy density, the larger the quantity of such semi-welded particles. Also, the following surface features can affect the fluid flow characteristics. The first is the surface connected porosity which remains even after hot isostatic pressing and likely expanded, as investigated by Tammas-Williams et al.

(2016) for titanium parts fabricated by AM. Yasa et al. (2016) suggested a second feature related to the stair stepping effect resulting from the stepped approximation of inclined and curved surface edges in the layer-by-layer building process which causes a low surface quality.

As explained by Witkin et al. (2016), to increase the attractiveness of AM technology for aerospace applications, particularly for the fabrication of gas turbine engine parts, two important issues must be addressed. The first issue consists of the capability to manufacture geometrically complex components containing internal cavities and channels. The second issue consists in the adequate and economically efficient surface finishing of these internal surfaces which are in contact with fluid flow.

Thakur & Gangopadhyay (2016) showed that for relatively simple part geometries, inadequate surface features may be removed by machining of near net shape parts of nickel-based superalloys to the final dimensions. This strategy has been successfully used by Rawal et al. (2013) to improve the surface finish of Ti-6Al-4V spacecraft components produced using electron beam melting. For highly complex components, and more specifically for those with internal design features, hard polishing tools cannot be used to reduce surface roughness in inaccessible areas; one of the following concurrent processes should be used instead:

- i. Abrasive flow machining. Rhoades (1991) showed that this technology is limited to the polishing of relatively large channels because of its high viscosity putty-like matrix.
- ii. Chemical polishing. To the best of the authors' knowledge, no effective chemical polishing solutions have yet been found for Ni-Cr-Mo alloys, and more specifically for the IN-625 alloy. The latter can be explained by the exceptionally high resistance of these alloys to both oxidizing and reducing environments due to the presence of chromium and molybdenum in their composition as described by Crook (2005).
- iii. Electrochemical polishing. Urlea & Brailovski (2017) demonstrated that this technique is efficient but requires the use of conformal electrodes, which complicates the finishing of narrow channels and cavities.

An economic approach for the polishing of AM components would consist in using a combination of abrasive and chemical polishing techniques. For example, chemical mechanical polishing (CMP), a combination of mechanical grinding and wet etching processes, has been

used by Lee et al. (2016) successfully for polishing of Ti-6Al-4V alloy. In this process, the polishing surface was subjected to the action of corrosive chemical slurry with abrasive colloidal particles under a downforce pressure applied by a pad. In respect to the need to apply a mechanical force, this technique is irrelevant for polishing inaccessible areas. Ramesh et al. (2014) suggested another approach consisting of a combination of chemical and abrasive jet-flow action, which has been used in slurry erosion wear test for IN718 coatings on copper. The surface was subjected to the wear test in a chemical solution with erodent particles to study the erosion wear behavior of the coatings. In the present work, the use of a combination of chemical and abrasive flows for surface polishing has been investigated via a comparative study of three polishing techniques: a) flow of abrasive particles suspended in water, b) flow of a chemical polishing solution without abrasive, and c) flow of abrasive particles suspended in a chemical solution.

## **4.3 Methodology**

### **4.3.1 Experimental setup**

A laboratory polishing setup combining chemical and abrasive flow polishing features was designed for this work. This setup works by pumping a fluid of acid-based chemicals and abrasive particles through the interior part of a hollow cylindrical specimen. Shown in Figure 4.1(a), the setup consists of eight main parts and allows the controlled flow polishing of internal surfaces of tubular components.

The centrifugal pump tank mixer (1) (PTM-1, Levitronix, max. flow rate of 17 lit./min.) is selected for simultaneous pumping and mixing of chemicals and abrasives. The impeller of the PTM is driven by a magnetic field, and helps keep abrasive particles in suspension in the chemical fluid inside the feeding tank (2). The directional control valve (3) is used to direct the fluid flow from the PTM through either the specimen tank (4) or depletion tank (5). The ultrasonic flow sensor (6) (LFS-20, Levitronix) is used to provide a flow range measurement of 0-20 lit./min. The specimen tank (4) contains the cylindrical specimen (7), whose interior surface is being polished by the fluid flow. A chemically-resistant thermocouple (8) (K4FEP-006-6MC, Pyromation Inc.) is used to measure the temperature of the fluid inside the feeding tank (2).

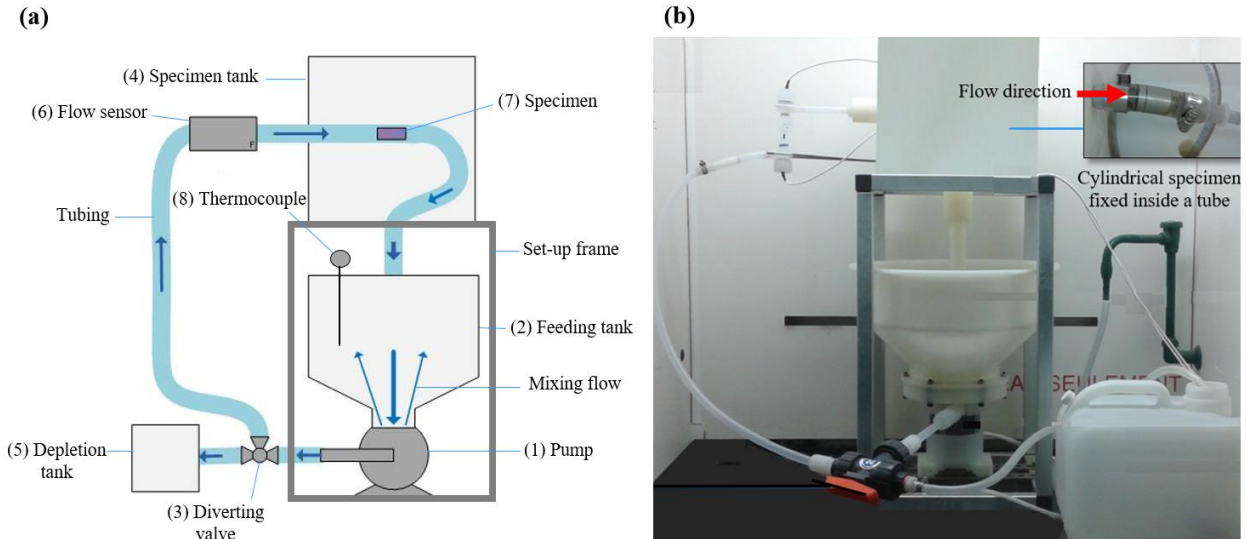


Figure 4.1: (a) Schematic and (b) real illustration of the chemical abrasive polishing setup

In polishing experiments, chemical abrasive fluid is mixed in the PTM (1), and then pumped through the manually operated directional control valve (3) to be directed to the flow sensor (6). The flow rate is measured by the sensor and controlled electronically by regulating the speed of the pump impeller. After that, the fluid is pushed through the specimen tank (4) to polish the surface of the specimen (7). Finally, the fluid is returned to the feeding tank (2) to complete one polishing cycle. When the process is completed, the fluid is purged into the depletion tank (5) using the directional control valve (3). The fluid and abrasive particles are reusable for the next polishing cycle.

### 4.3.2 Experimental conditions

#### *SPECIMENS*

In this study, IN625 specimens were fabricated using an EOSINT M290 (EOS GmbH, Munich Germany) laser powder bed fusion system equipped with a 400 W ytterbium fiber laser and the EOS IN625 Surface 1.0 Parameter Set. The IN625 specimens consisted of two main parts as shown in Figure 4.2(a):

- 1) The specimen holder, which consists of two components: the cylindrical sleeve with a circular outside (OD = 27 mm) and square inside ( $23 \times 23 \text{ mm}^2$ ) and the locking ring with two pins.

2) The edge-shaped specimen containing two surfaces with two different build orientations ( $15^\circ$  and  $135^\circ$ , see explanation below); this specimen is positioned at an angle of  $30^\circ$  with respect to the central axis of the specimen holder (Figure 4.2 (b)).

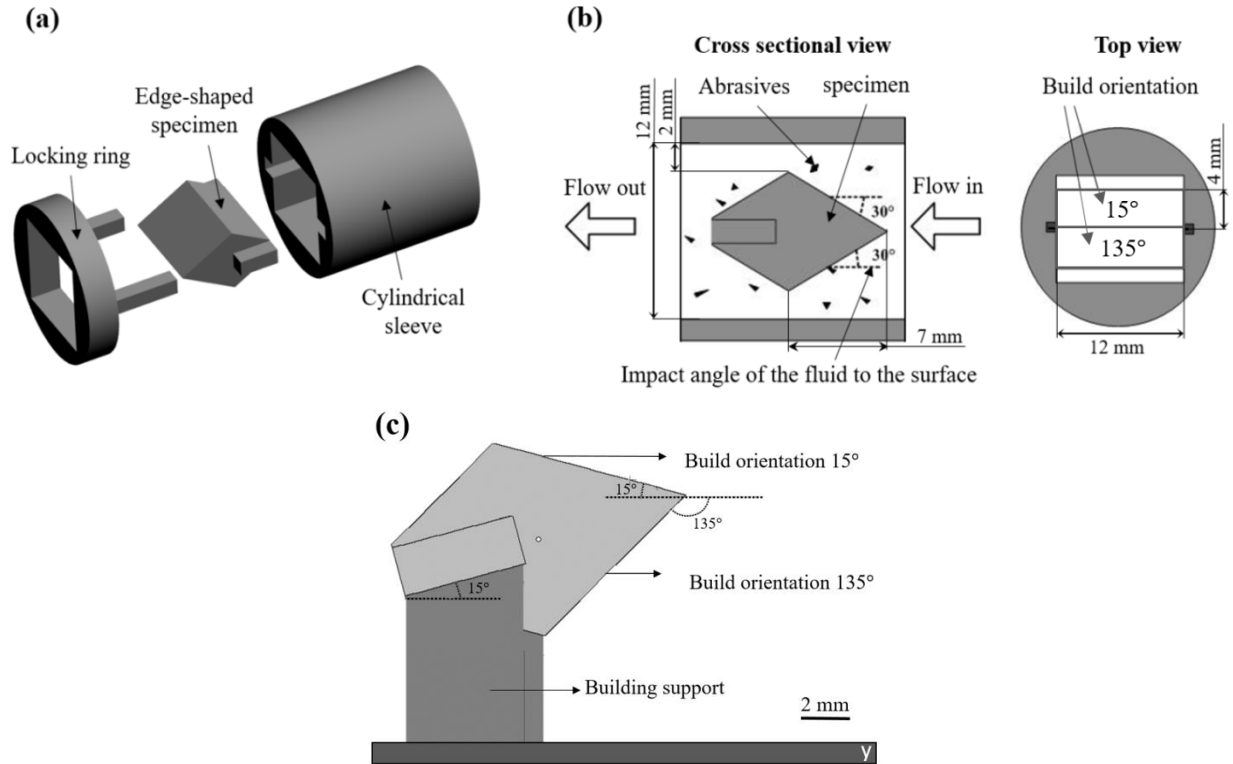


Figure 4.2: (a) Polishing specimen assembly, (b) chemical abrasive fluid flow inside the polished specimen, (c) edge shape specimen on the SLM building platform

Two factors were considered when designing the edge-shaped specimen. Firstly, the previously published results on the build orientation roughness dependence of LPBF-built IN625 parts (Urlea and Brailovski (2017) showed that for the surface build orientations ranging from  $20^\circ$  and  $110^\circ$ , the surface roughness is almost independent of surface orientation, as illustrated in Figure 4.3. To characterize the polishing efficiency over a wide spectrum of surface roughnesses encountered in complex components, two build orientations were tested:  $15^\circ$  (low roughness) and  $135^\circ$  (high roughness) as shown in Figure 4.2(c). Secondly, the  $30^\circ$  orientation of the polished surfaces to the central axis of the specimen holder, and therefore to the fluid flow (Figure 4.2 (b)), had to maximize the processing performance. Kosa & Göksenli (2015) have recently shown that for ductile materials, an impact angle of nearly  $30^\circ$  of abrasive particles to the eroded surface corresponds to the maximum erosion wear rate.

The specimen holder was inserted into a plastic tube, which allowed the polishing fluid, consisting of chemicals and abrasive particles, to flow along the 15° and 135° build orientation surfaces, and then recirculate. The flow direction is shown in Figure 4.2(b).

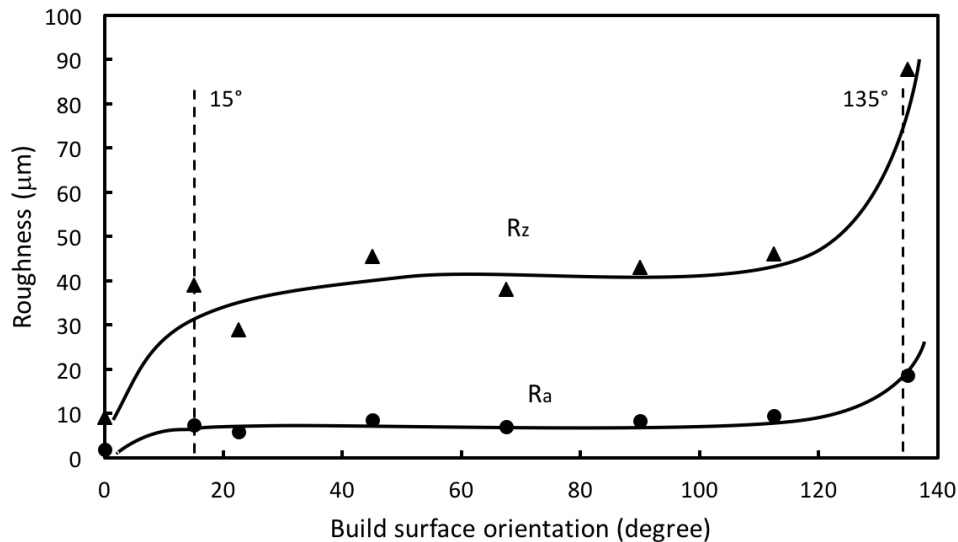


Figure 4.3: Surface roughness as a function of the surface orientation, as measured on as-built IN625 specimens (adapted from Urlea and Brailovski, 2017)

### *CHEMICAL SOLUTION AND ABRASIVE AGENT; POLISHING CONDITIONS*

To select an adequate chemical polishing solution for IN-625 specimens, static chemical polishing experiments were performed first. In these tests, the specimens were immersed into the chemical solution without any dynamic action. Four chemical polishing solution listed in ASM-Vol.9 (2004) were compared : (1) 30%  $\text{HNO}_3$  + 10%  $\text{H}_2\text{SO}_4$  + 10%  $\text{H}_3\text{PO}_4$  + 50% acetic acid, generally recommended for pure nickel; (2) 64.5% acetic acid (ice cooled) + 35%  $\text{HNO}_3$  + 0.5%  $\text{HCl}$ , used for pure nickel and Ni-Co alloys; (3) 30%  $\text{HF}$  + 70%  $\text{HNO}_3$  and (4) 50%  $\text{HF}$  + 50%  $\text{HNO}_3$ , both used for titanium alloys. The proportions presented are in volume percent, and the polishing tests were performed for 8 hours at room temperature.

As shown in Figure 4.4, solution number 4 (50%  $\text{HF}$  + 50%  $\text{HNO}_3$ ) gave the lowest roughness value after static chemical polishing, and was thus selected for the following chemical flow and chemical-abrasive flow polishing. Due to the limitation in corrosion resistance at room temperature of soft tubing and depletion tank of the set-up made of polyvinyl chloride (PVC), the

selected chemical solution was diluted by water to 40 vol.% of concentrated hydrofluoric acid (HF), 40 vol.% of concentrated nitric acid (HNO<sub>3</sub>) and 20 vol.% of distilled water.

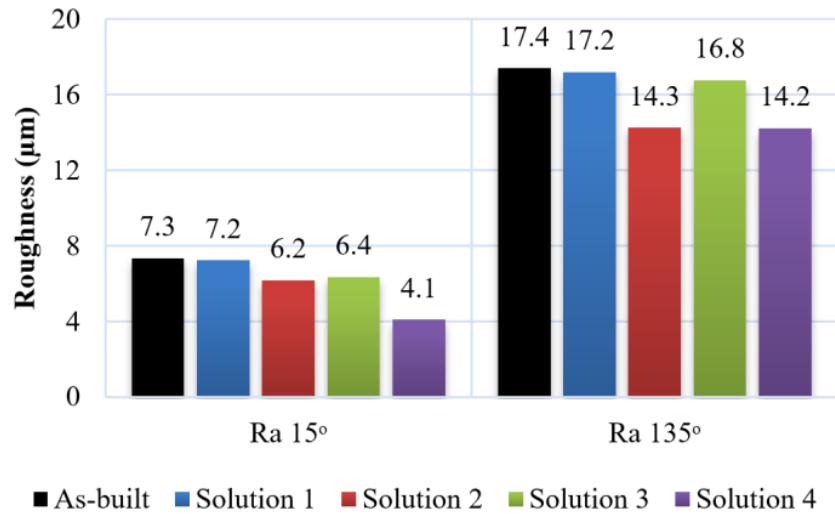


Figure 4.4: Roughness results of static chemical polishing for the four chemical solutions. The tests were performed for 8 hours at room temperature

The selection of abrasive particles was made by considering the most common abrasives on the market. Typically, larger size of abrasive is preferred because the particles could deflect more easily from the direction of the fluid flow and impinge the surface to polish. On the one hand, aluminum oxide is available in a wide variety of size distributions, and it is advantageously more abrasive than silica sand, which is characterized by rounder particles. On the other hand, alumina is less acute and then slightly less abrasive than silicon carbide. However, we wanted to avoid silicon carbide because if some hard particles remain embedded on the surface of nickel superalloys, they could react in the typical gas combustion chamber, leading to accelerated degradation of metallic components. Aluminum oxide grit from Kramer Industries with an average particle size of  $d_{45} = 420 \mu\text{m}$  and specific gravity of 3.94 was used as an abrasive agent. Yin et al. (2004) used aluminum oxide grit of  $17.5 \mu\text{m}$  with the concentration of 3.44 vol.% in the abrasive flow polishing of micro bores. In addition, Ramesh et al. (2014) used abrasive sands with particles size of  $425 \mu\text{m}$  and slurry concentration of 100 gm/liter for studying slurry erosion wear behavior of Inconel-718 coatings on copper. In the present study, the concentration of abrasive particles in the fluid was limited to 6 wt.%, the volume of polishing media was 5 liters,



and the flow rate was kept constant at 10 lit./min. with a pumping pressure of about 32.2 psi. The specimens were polished for 1, 2 and 3 hours.

### 4.3.3 Surface characterization before and after polishing

The two surfaces of the edge-shaped specimens ( $15^\circ$  and  $135^\circ$  build orientations) were characterized using profilometry and confocal microscope to study the effect of polishing on the removal of semi-welded particles and on the surface roughness and topography.

For both build orientations, the surface roughness measurements were conducted along the build direction (Figure 4.5) using a surface roughness tester (SJ-410, Mitutoyo). The arithmetic average values ( $R_a$ ) and the average maximum peak to valley of five points ( $R_z$ ) were measured, and a 0.8 mm sampling length (cut-off) Gaussian filter was used. Each measurement was repeated three times and the mean values and the standard deviations were calculated.

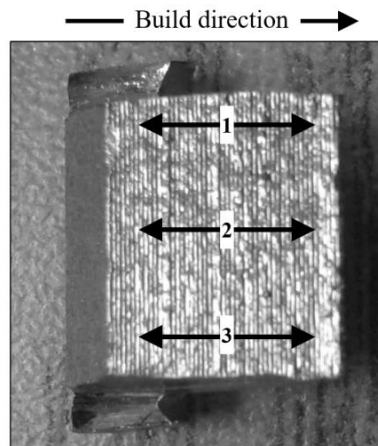


Figure 4.5: Roughness measurement direction of the stylus profilometer for the edge-shaped specimen. Non-polished surface with build orientation of  $15^\circ$

The surface texture and three-dimensional topography of two polished surfaces with build orientations of  $15^\circ$  and  $135^\circ$  were observed using a confocal microscope (OLS 4100, OLYMPUS).

The flow velocity on the edge-shaped specimens (Figure 4.6) is defined by:

$$v = \frac{Q}{A} \quad (4.1)$$

where  $v$  is the fluid velocity,  $Q$  is the flow rate and  $A$  is the cross-sectional area through which the flow passes. Using the approximate dimensions of the cross-sectional area, the velocity of the fluid as a function of the flow rate ( $Q$ ) and its distance on the x-axis ( $x$ ) is obtained by:

$$v = \frac{25 Q}{12(18 - \sqrt{3}x)} \quad (4.2)$$

with the proper units for  $v$  (m/s),  $Q$  (lit./min.) and  $x$  (mm).

As illustrated schematically in Figure 4.2(b), as the slurry flows from the tip of the specimen to its base, the cross-section around the specimen is reduced, and the fluid velocity increases accordingly. Therefore, for a flow rate of 10 lit./min., the minimum (at the tip) and maximum (at the base) fluid velocity were 1.16 and 3.45 m/s, respectively, for an average velocity of 2.31 m/s along the two inclined specimen surfaces to be polished.

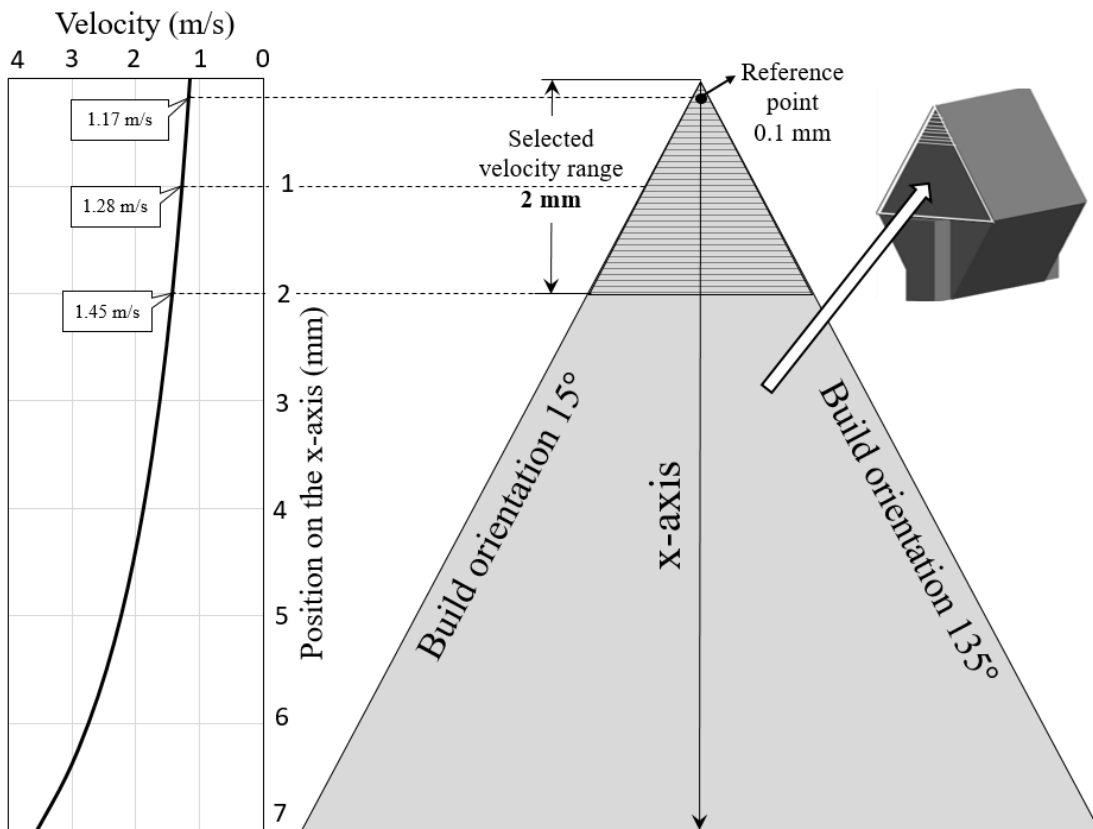


Figure 4.6: Planar view of the edge-shaped specimen captured by a confocal microscope for polishing depth measurements as a function of velocity

To calculate the depth of polishing as a function of flow velocity, the planar images of the edge-shaped specimen were used for a 2-mm distance from the tip of the specimen. A reference point was determined on the as-built specimen with a 0.1 mm distance from the tip along a vertical reference line named the  $x$ -axis, and the tip of the specimen was set at  $x = \text{zero}$ . Then, the polishing depth ( $d$ ) was calculated for each 0.2 mm down from the reference point, measuring the specimen thickness from the reference line to the specimen surface.

## 4.4 Results

### 4.4.1 Static versus flow chemical polishing

The surface roughness values  $R_a$  and  $R_z$  of the as-built and polished SLM-built IN-625 specimens are presented in Figure 4.7. Both chemical polishing processes were carried out for 1 hour. The results clearly indicate that for both build orientations ( $15^\circ$  and  $135^\circ$ ), chemical flow polishing results in a greater surface roughness reduction as compared to static chemical polishing. When chemical polishing was performed dynamically, the  $R_a$  value decreased from 7.0 to 5.6  $\mu\text{m}$ , or by 20%, for a build orientation of  $15^\circ$ , and from 37.8 to 29.4  $\mu\text{m}$ , or by 22%, for 5-point average values of  $R_z$ . The same trend was observed for a build orientation of  $135^\circ$ . Indeed, the  $R_a$  value decreased from 17.4 to 16.7  $\mu\text{m}$ , or by 4%, and the  $R_z$  values from 81.7 to 76.6  $\mu\text{m}$ , or by 6%, when chemical flow polishing was carried out instead of static chemical polishing.

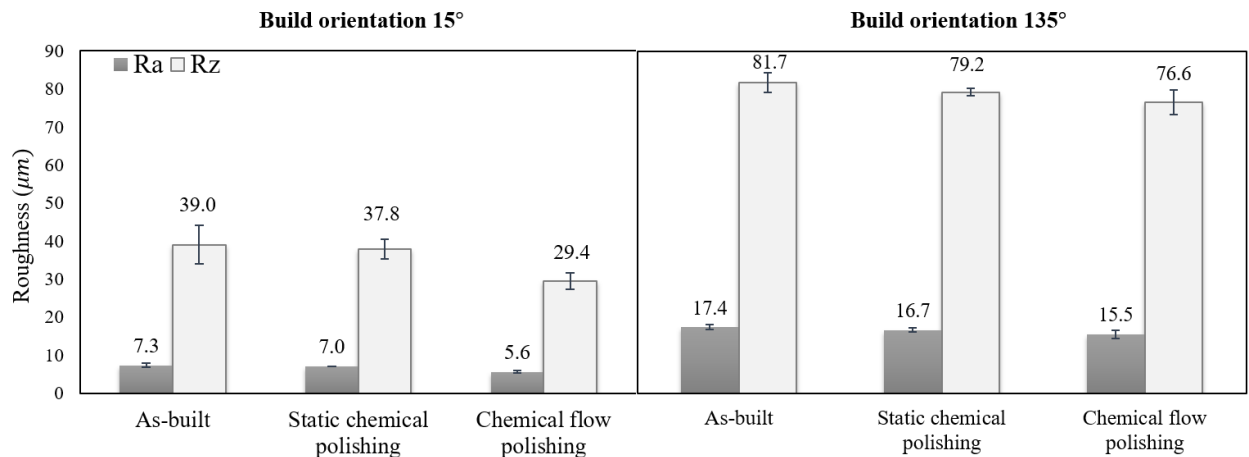


Figure 4.7: Roughness improvement for static chemical polishing and chemical flow polishing processes at build orientations of  $15^\circ$  and  $135^\circ$ . Polishing time for the two processes was 1 hour

The three-dimensional images in Figure 4.8 illustrate the surface topography of the SLM-built IN-625 alloy specimens fabricated at build orientations of  $15^\circ$  and  $135^\circ$ . As shown in the micrographs for the as-built surfaces, the build orientation of the surface seems to significantly influence the concentration of semi-welded particles: their concentration is higher for the  $135^\circ$ -oriented surface than for its  $15^\circ$ -oriented counterpart. After static chemical polishing, the semi-attached particles are removed for both build orientations, but only partially. After chemical flow polishing, most of the semi-welded particles are removed for both build orientations. Consequently, the surface became smoother after chemical flow polishing than after static chemical polishing.

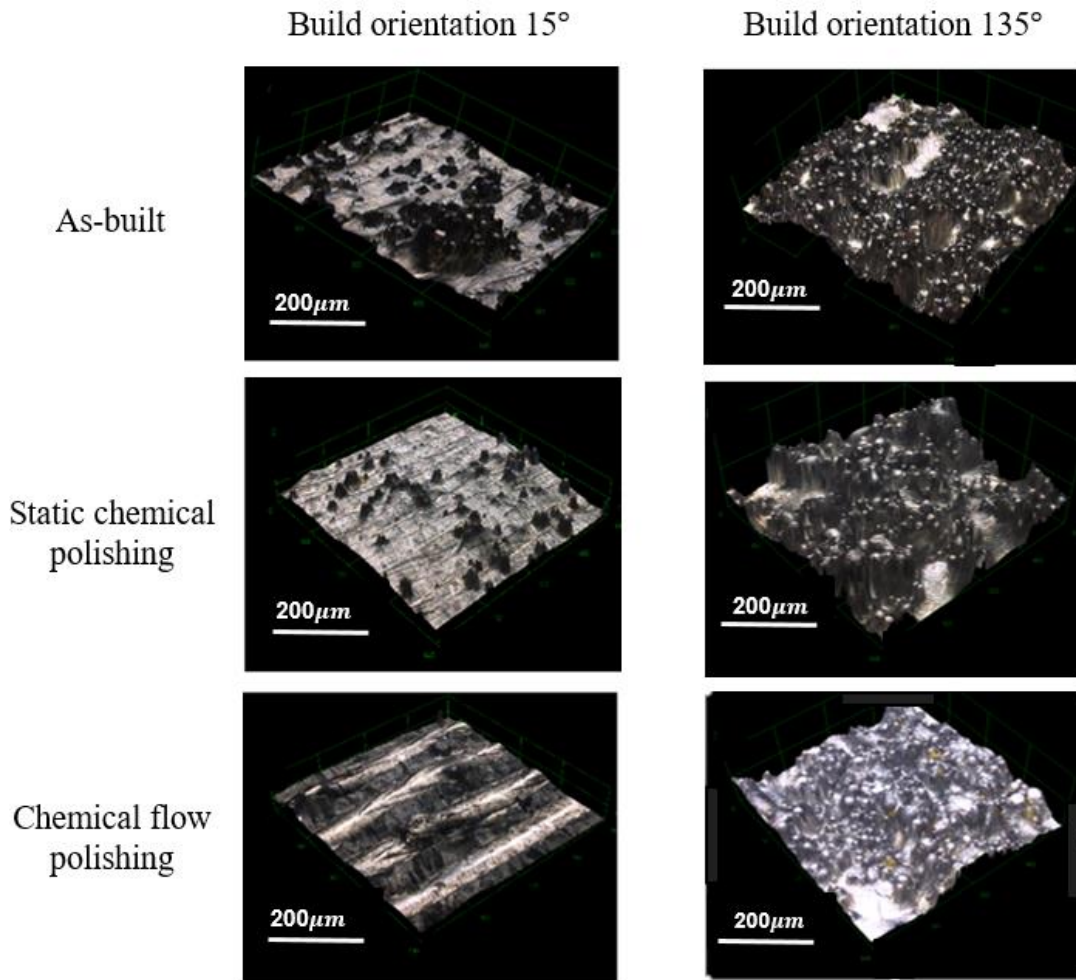


Figure 4.8: 3D topography confocal microscope surface images at two build orientations of  $15^\circ$  and  $135^\circ$  for the as-built, static chemical polished and chemical flow polished surfaces. Polishing time for the two processes was 1 hour

#### 4.4.2 Comparison of chemical, abrasive and chemical-abrasive flow polishing processes

As presented in Figure 4.9, surface roughness reduction was studied for three polishing techniques: a) chemical flow polishing, b) abrasive flow polishing, and c) chemical-abrasive flow polishing. The polishing time was 1 hour for the three processes. More roughness reduction was observed for the chemical-abrasive flow polishing for both build orientations ( $15^\circ$  and  $135^\circ$ ). The results prove the synergy effect of applying combined chemical and abrasive flows. Further, chemical flow polishing seems to be more effective in terms of roughness reduction as compared to abrasive flow polishing. For instance, there was a 6% greater reduction in the  $R_a$  value at a build orientation of  $135^\circ$  after polishing by chemical flow as compared to polishing by abrasive flow.

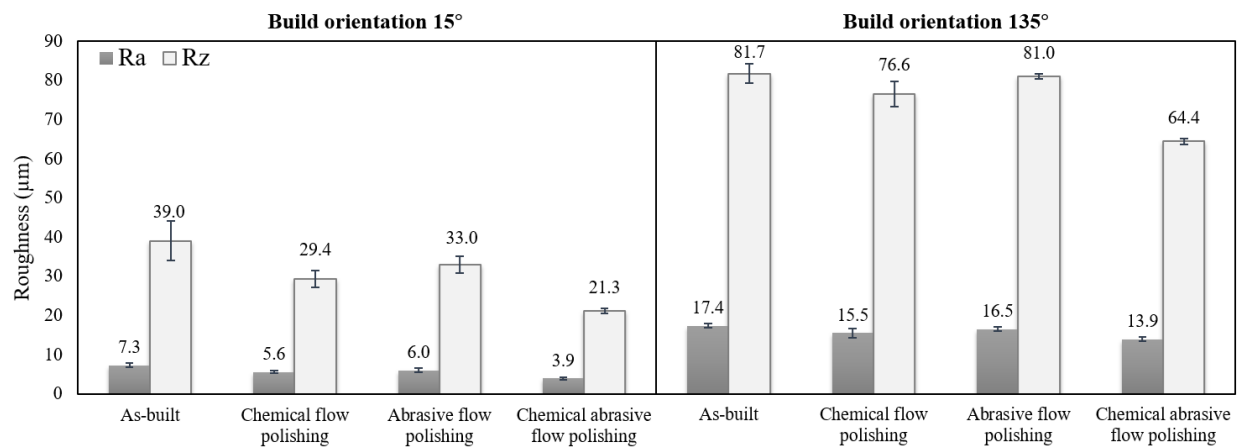


Figure 4.9: Roughness improvement using the three polishing processes at build orientations of  $15^\circ$  and  $135^\circ$ . Polishing time for the three processes was 1 hour

Figure 4.10 compares the time of polishing required to decrease the surface roughness from the as-built value of  $R_a = 17.4 \mu\text{m}$  to  $R_a = 14.2 \pm 0.3 \mu\text{m}$ , using all the studied polishing techniques. To reach this result, we need 8h of static chemical polishing, 3h of either chemical or abrasive flow polishing, and only 1h of chemical-abrasive flow polishing. That means that the polishing time was reduced by a factor of 2.5 by moving from static to chemical flow action. Further, the polishing time was reduced by a factor of 3 when the combination of chemical and abrasive polishing was used as a replacement of chemical or abrasive flow polishing techniques, considered separately.

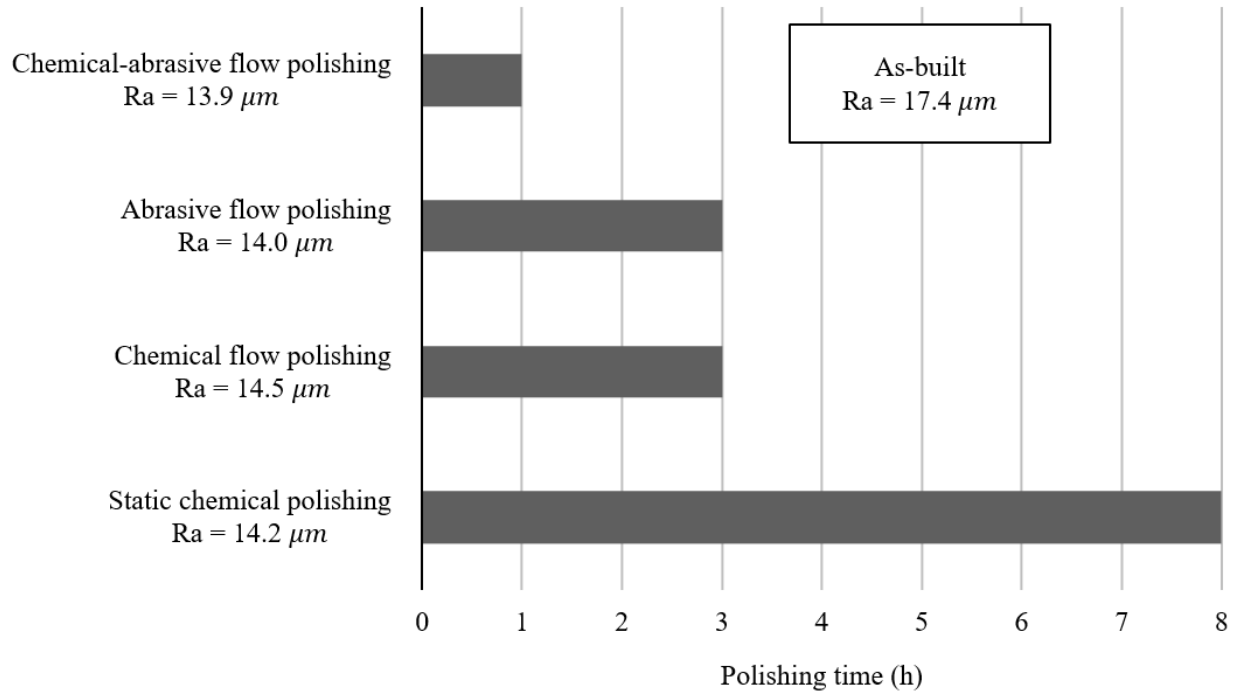


Figure 4.10: Required polishing time for the  $135^\circ$  build orientation surface using different polishing techniques to achieve similar surface roughness

The surface roughness evolution as a function of polishing time is compared in Figure 4.11 for three polishing processes. In Figure 4.11(a-b) and Figure 4.11(c-d),  $R_a$  and  $R_z$  values are plotted for build orientations of  $15^\circ$  and  $135^\circ$ , respectively. If the behavior of chemical flow polishing and abrasive flow polishing, taken separately, is not significantly different, there is no doubt that their combined use results in a significantly greater roughness reduction as compared to the other two techniques.

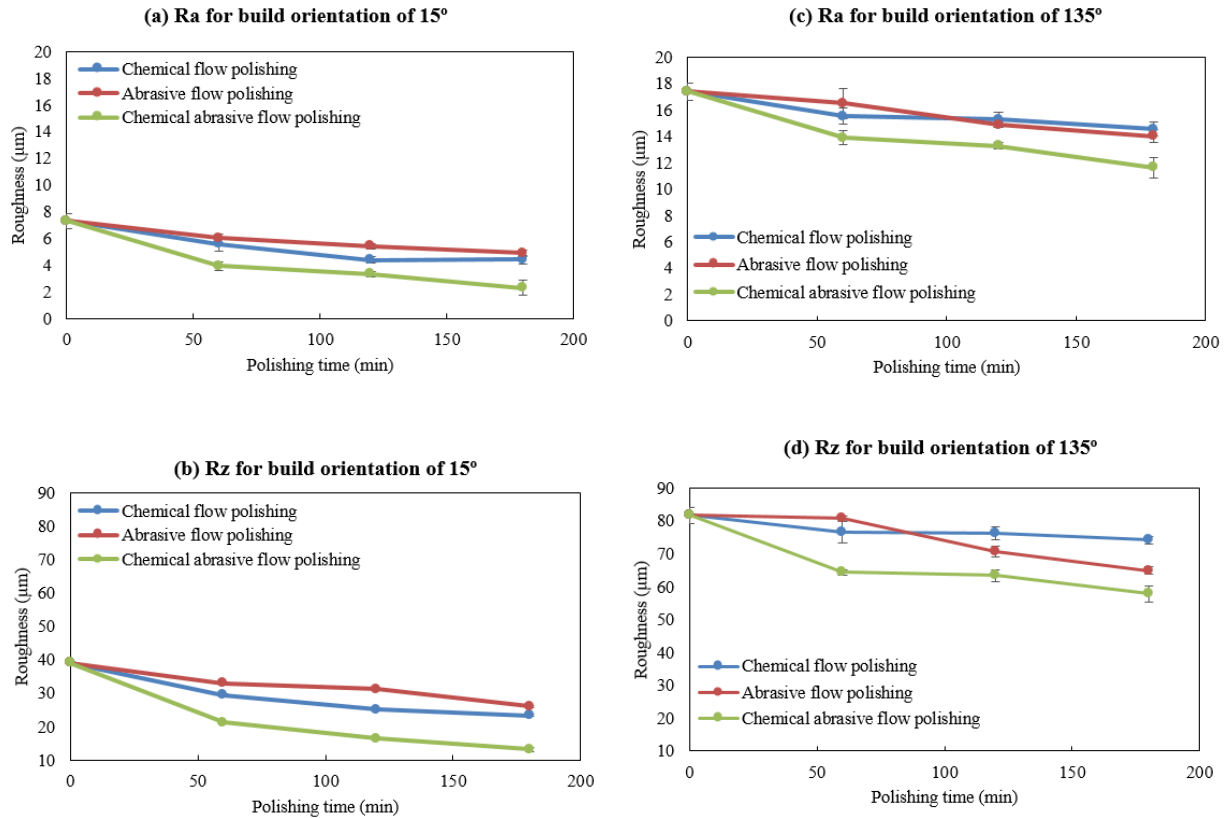


Figure 4.11:  $R_a$  and  $R_z$  roughness versus polishing time through the three polishing techniques for the two build orientations of (a, b)  $15^\circ$  and (c, d)  $135^\circ$

Figure 4.12 presents a 3D roughness profilometry of the  $15^\circ$  build orientation surface for the as-built state and using three polishing techniques for 1, 2 and 3 hours. All the height profiles are in the same range as the as-built profilometry (0-80  $\mu\text{m}$ ). After a 3-hour chemical-abrasive flow polishing, the surface height is even, which is indicated by a larger-distributed green color field on the surface. In other words, the surface roughness is lower after polishing with the combined technique for any time of polishing. Figure 4.13 presents the same information for a build orientation of  $135^\circ$ .

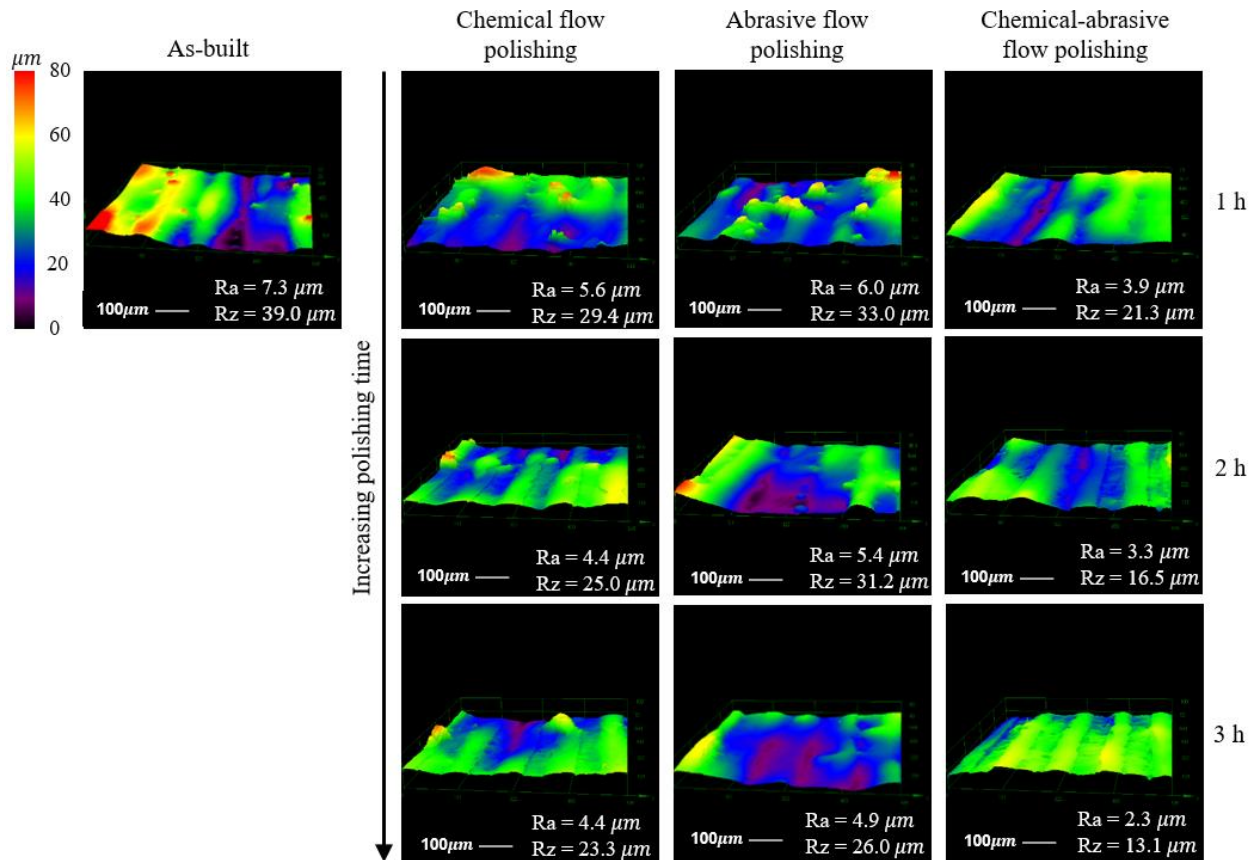


Figure 4.12: 3D surface roughness profilometry for 15° build orientation before and after polishing using three different polishing techniques for each increment of polishing time



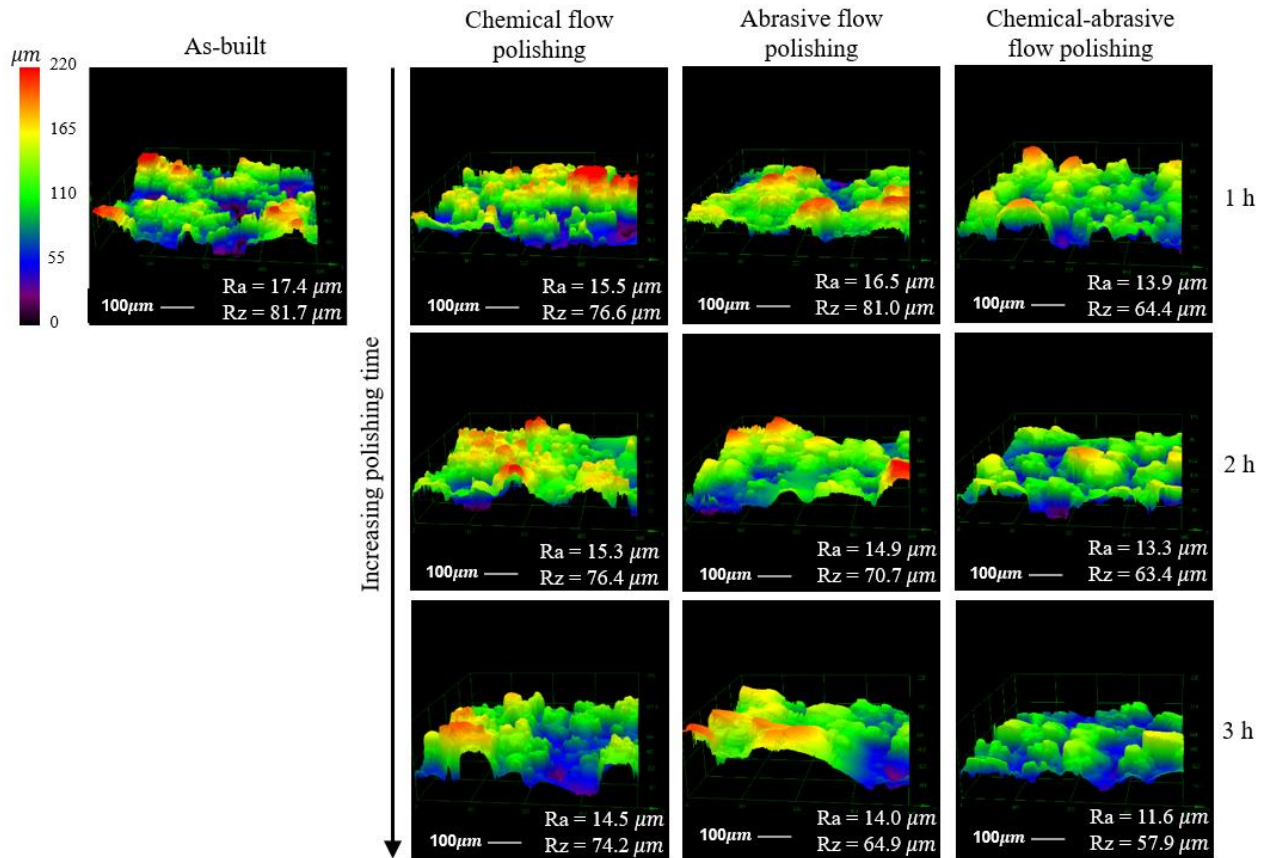


Figure 4.13: 3D surface roughness profilometry for 135° build orientation before and after polishing using three different polishing techniques for each polishing time increment

The polishing depth as a function of fluid velocity on the edge-shaped specimen is shown in Figures 4.14(a), 4.14(b) and 4.14(c) for three polishing techniques (polishing time 1 hour, build orientation 135°). Higher polishing depths were observed for chemical-abrasive flow polishing as compared to either chemical or abrasive flow polishing techniques, taken separately. Figure 4.14(d) presents the material removal pattern on the inclined surfaces with 15° and 135° build orientations. More material removal was obtained by moving from the tip to the base of the edge-shaped specimens due to an increased fluid velocity. The velocities on the inclined surfaces were calculated using Equation 4.2.

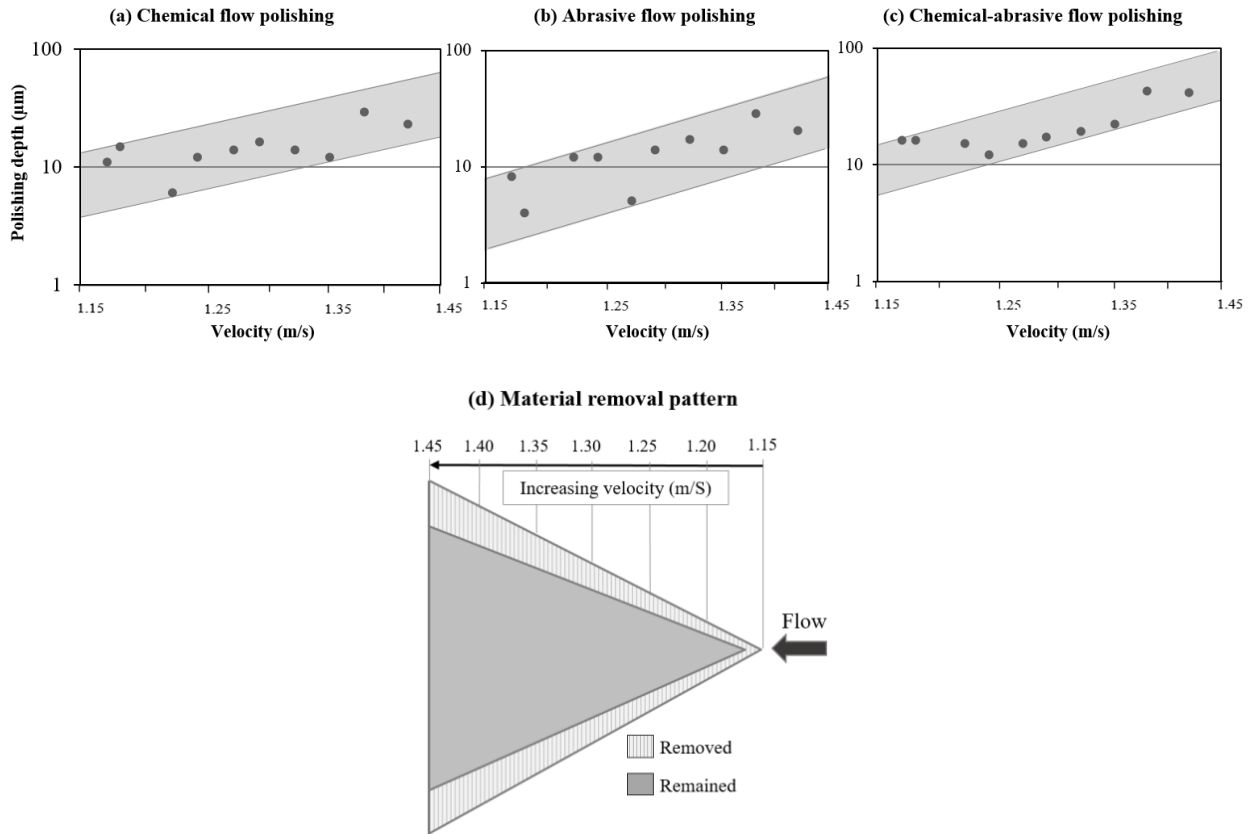


Figure 4.14: The logarithmic graphs show the polishing depth versus fluid velocity of the edge-shaped specimen using (a) chemical flow polishing, (b) abrasive flow polishing and (c) chemical-abrasive flow polishing (polishing time 1 hour, build orientation  $135^\circ$ ). The scheme (d) represents the material removal pattern on the inclined surfaces of the edge-shaped specimen for the selected velocity range

Figures 4.15-(a, b) show the relationship between the polishing depth and the fluid velocity during chemical-abrasive polishing for 1, 2 and 3 hours and for build orientations of (a)  $15^\circ$  and (b)  $135^\circ$ . It can be observed that the longer the polishing time, the less intense is the material removal rate: for 1h  $\rightarrow$  10  $\mu\text{m}/\text{h}$ , for 2h  $\rightarrow$  5  $\mu\text{m}/\text{h}$  and for 3h  $\rightarrow$  2  $\mu\text{m}/\text{h}$ .

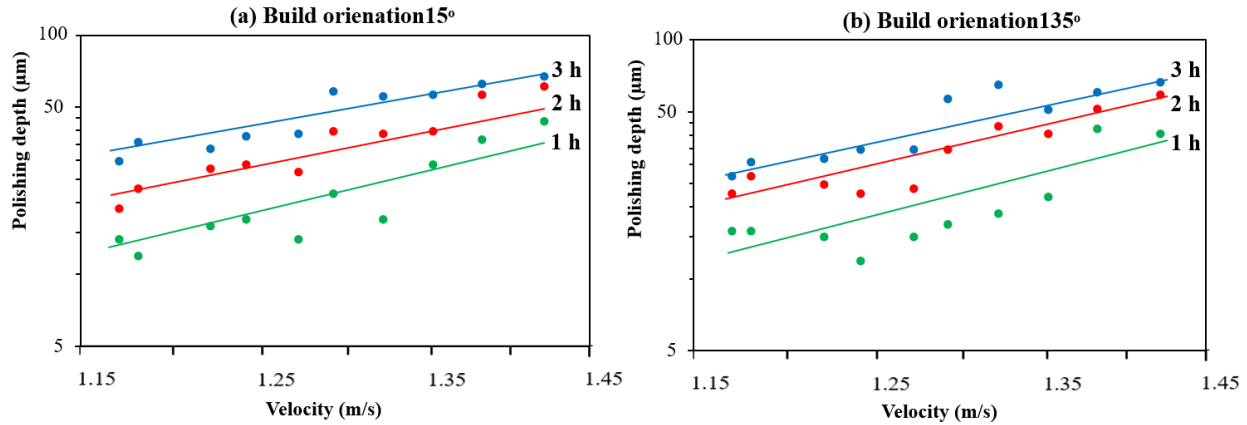


Figure 4.15: Logarithmic graphs of (a) and (b) present the polishing depth versus the velocity for build orientations of  $15^\circ$  and  $135^\circ$ , respectively. The results were obtained after applying chemical-abrasive flow polishing for 1, 2 and 3 hours

## 4.5 Discussion

The results of a combined chemical and abrasive flow polishing of the interior surface of AM-IN-625 tubular components reveal that this technology can notably improve the surface finish. Semi-welded particles were completely removed, and the surface roughness was reduced, providing at least a 45% improvement in  $R_a$  value for a build orientation of  $15^\circ$  and a 20% improvement for a build orientation of  $135^\circ$ .

### 4.5.1 Chemical flow polishing

As explained in ASM-Vol.9 (2004), the chemical polishing mechanism consists in material removal by dissolution. The relation between the passive layer formation rate and its chemical dissolution controls the quality of the polished surface. The surface becomes chemically polished when the rates of layer formation and its dissolution are equal. Metal oxidation happens at a higher layer formation rate and metal etching occurs for the opposite condition. Tuck (1975) explained that the basic chemical reaction, which is responsible for chemical polishing is oxidation. The oxidizing agent in the polishing solution of IN-625 is  $\text{HNO}_3$ . Since the oxidized materials are not soluble, a complexing agent is needed. In our case, HF is used in the solution to produce a soluble complex, and water is added as a diluent.

As presented in the roughness results of Figure 4.7 and confocal images of Figure 4.8, the surface quality of the chemical polished specimens was increased by introducing flow to the process.

Tuck (1975) stated that the dissolution process can be a) diffusion-controlled, b) reaction-controlled, or c) autocatalytic. The reaction-controlled and autocatalytic dissolution phenomena cannot explain the observed advantage of the chemical flow polishing as compared to the static chemical polishing. A reaction-controlled dissolution mainly depends on the concentration of the undissolved species on the polished surface, which is not really affected by flow of the polishing medium as described by Dokoumetzidis et al. (2008). The polishing rate of the autocatalytic reaction can even be reduced by the presence of flow, since this flow may remove the catalyst products from the surface, thus slowing down the reaction.

Opposing to the reaction-controlled and autocatalytic dissolution mechanisms, the diffusion-controlled dissolution is limited by the diffusion of active species to the reacting surface, and the concentration of these species decreases when approaching the surface. Assuming a reactant-depleted layer neighboring the surface with the thickness of  $\delta$ , the rate of reaching species to the surface, or dissolution rate ( $dn/dt$ ), can be defined by Fick's law.

$$\frac{dn}{dt} = DS \frac{c}{\delta} \quad (4.3)$$

where  $S$  is the surface area of the specimen,  $D$  is the diffusion coefficient of the reacting species in the solution, and  $c$  is the concentration of the species in the bulk of the solution. In chemical flow polishing therefore, the dissolution rate increases with the increased flow velocity due to the thickness reduction of the reactant-depleted layer neighboring the surface.

### 4.5.2 Abrasive flow polishing

In abrasive flow polishing, the interior surface is polished by pumping water-abrasive fluid through the specimen. In this operation, erosion is the main mechanism of material removal. Yin et al. (2004) compared abrasive flow polishing action with a lapping operation as the abrasive slurry smoothens the inner surfaces. Thus, the abrasive fluid flowing through the inside of the tubular specimen acts similarly as in the lapping process, leading to a smoother surface as shown in Figure 4.11 and the confocal image analyses in Figures 4.12 and 4.13. A part of the force generated by abrasive slurry is applied to hone semi-welded particles from the specimen surface.

The graphs presenting the polishing depth versus fluid velocity in Figure 4.14(b) show that the higher the fluid velocity, the more material is removed. In fact, by increasing the velocity of the carrying fluid, the impact energy is larger, leading to deeper cutting and greater material removal. The impact angle of the fluid flow on the edge-shaped specimen was designed to be close to  $30^\circ$ , which corresponds to the maximum erosion angle for ductile materials as discussed previously. It is expected that changing the impact angle will affect the results of the polishing process.

### 4.5.3 Combined chemical-abrasive flow polishing

Both the chemical and abrasive flow polishing techniques seem to be applicable for removing semi-welded particles from the surface and, consequently, reducing the surface roughness of AM-IN-625 specimens. The disadvantage with these two methods is their low rate of material removal, which can be seen in the results appearing in Figure 4.14(a), 4.14(b) and 4.14(c). In chemical polishing, this might be due to the high thickness of the passive layer, which is formed on the surface of the specimen. Abrasive flow polishing, on the other hand, needs to provide a higher fluid velocity to efficiently polish the surface. The study by Yin et al. (2004) carried out in this regard showed that a velocity of as high as  $\sim 20$  m/s was required to reach a high quality surface finish in steels, which is five-times greater than maximum 3.5 m/s of our study.

The use of a combination of the two techniques advantageously increases the material removal rate and gives a better surface finish quality. In the combined polishing process, a passive layer formed because of chemical reactions between the chemical agent and the solid surface is continuously removed by abrasive agent of the fluid. This synergy effect of the chemical and abrasive agents enhances the polishing process efficiency, and results in a higher surface finish quality.

According to the polishing depth ( $d$ ) versus fluid velocity ( $v$ ) graphs in Figure 4.15(a) and 4.14(b), the polishing depth increases by increasing the fluid velocity for all the techniques. The material removal pattern on different points of the edge-shaped specimen (different velocities) is shown schematically in Figure 4.14(d). Increasing the velocity from the tip to the base of the specimen caused more material removal from the surface. For chemical flow polishing, this can be explained by a decrease of the reaction area thickness ( $\delta$ ) with an increasing fluid velocity. In abrasive flow polishing, material removal increases as a function of water-abrasive flow velocity, due to a higher quantity of abrasive particles impinging the surface. Furthermore, the abrasive

particles have more energy at higher velocities, and as such, they can remove more materials from the surface. When the combined chemical-abrasive polishing technique is used, the higher the flow velocity, the greater the effect of synergy between the chemical reactions and the surface abrasion.

It is worth noticing that the polishing depth data in the graphs of Figure 4.14 and Figure 4.15 are highly scattered. This might be explained by the fact that the fluid velocity and polishing times of all concurrent polishing techniques were limited, which resulted in mainly semi-welded particle removal during polishing. This notwithstanding, the linear relations fitting the data points indicate that a specific equation can be defined for the polishing depth as a function of velocity and time for chemical-abrasive flow polishing. Using the Taylor's power law, the polishing depth ( $d$ ) is obtained as a function of fluid velocity ( $v$ ) and polishing time ( $t$ ) according to

$$d = K v^n t^m \quad (4.4)$$

where  $K$  and  $n$  and  $m$  are empirical constants. From the logarithmic graphs of Figure 4.15, the constants of Equation 4.3 were calculated for both build orientations of  $15^\circ$  and  $135^\circ$ :  $n = 2.5$ ,  $m = 0.6$ ,  $K = 10 \text{ s}^{1.9} \text{ m}^{-1.5}$ , for  $1.15 \text{ m/s} \leq v \leq 1.45 \text{ m/s}$  and  $1 \text{ h} \leq t \leq 3 \text{ h}$ ).

These results show that in chemical-abrasive polishing, increasing the velocity of the fluid lead to an increase in the polishing depth, with the same exponent of 2.5 for both build orientations. In fact, the similar behavior for the two build orientations might once again be explained by the removal of only semi-welded particles during chemical-abrasive flow polishing, and so that the thickness of removed materials corresponds to the size of semi-welded particles on the surface.

Further studies are required to investigate the effect of fluid impact angle on the surface finish of the SLM-built IN-625. In addition, higher velocities could be applied to increase the polishing rate and quality for the presented chemical-abrasive flow polishing technique.

## 4.6 Conclusions

The main results of this study is summarized as follows:

1. Chemical-abrasive flow polishing appears to be a feasible technology for the polishing of SLM-built IN-625 with internal cavities/channels.

2. Chemical-abrasive flow polishing can remove semi-welded particles from the surface of SLM-built IN-625 components and reduce the  $R_a$  value by about 45% for a build orientation of  $15^\circ$  and by 20% for a build orientation of  $135^\circ$
3. The surface roughness reduction results show a two-fold increase when combining chemical and abrasive polishing as compared to either chemical or abrasive flow polishing taken individually. By switching from chemical flow polishing or abrasive flow polishing to a combined chemical-abrasive flow action, the polishing time is reduced from 3h to 1h for a given  $R_a$  improvement, from  $17.4 \mu\text{m}$  (as-built) to  $14.2 \mu\text{m}$ .
4. The higher the fluid velocity, the greater the polishing depth, irrespective of the polishing technique used. This behavior is independent of the surface build orientation for chemical-abrasive flow polishing. The polishing depth increases by increasing the fluid velocity with an exponent of 2.5 and polishing time with the exponent of 0.6.

## 4.7 Acknowledgements

This work was supported by the Consortium de Recherche et d'Innovation en Aérospatiale au Québec (CRIAQ).

## CHAPTER 5 GENERAL DISCUSSION

### 5.1 Introduction

This chapter goes into discussing the thesis by verifying the scientific hypothesis of the study through the experimental works. Furthermore, it includes some arguments about interesting topics related to the presented work that are recommended to be carried out in the future studies. The chapter is arranged as follows: at first, the general discussion reviews the research problem of the studied work, continues by defining the research question, general and specific objectives, the original scientific hypothesis of the student's contribution, and the important results of the experiments. Then, it is followed by exploring some methodological aspects and results, which were not fully discussed in Chapter 4. At the end, some topic ideas for scaling up the chemical-abrasive polishing setup in continuation of this study are proposed to be carried out. These research ideas are explained in detail.

### 5.2 Original scientific hypothesis

Inconel 625, a nickel-based alloy, is used as engine parts material in aerospace industry. Fully functional parts of IN-625 with complex geometries and high densities are being produced by one of the promising Additive Manufacturing (AM) techniques named Selective Laser Melting (SLM), showing advantages in shorter time to market, lower buy-to-fly ratio and better parts performance. However, due to the limited control over the roughness of the AM components, post-AM surface treatments such as chemical-mechanical polishing could be used. This technique cannot be used for finishing of internal surfaces of engine components which are in contact with hot-corrosive fluids.

Regarding the described research problem, the research question of this work can be specified as follows: could a combination of chemical and abrasive flows technique advantageously be applied for efficient improvement of internal surface finish of AM IN-625 components?

Accordingly, the general objective of this study is to design, manufacture and validate an innovative finishing method combining chemical and abrasive polishing of internal surfaces of IN-625 alloy parts. In addition, the scientific objectives can be listed as:



- 1) Design and manufacture a polishing set-up consisting of wet materials with chemical-abrasive resistance to polishing agents.
- 2) Develop static tests to select an appropriate chemical polishing solution and chemical additives to obtain optimum material removal and improve polishing uniformity.
- 3) Investigate the synergetic effect stemmed from the combined use of abrasive and chemical action by studying three polishing techniques: flow of abrasive particles suspended in water, flow of chemical solution without abrasive, and flow of abrasive particles suspended in chemical solution.

Thereby, the original scientific hypotheses of the student's contribution can be verified: by employing the newly developed chemical-abrasive polishing set-up, the interior surface of IN-625 components will obtain the required surface roughness. The justification of the originality would be that the new chemical-mechanical polishing technique is the first of its kind carrying out pumping acidic chemicals as chemical polishing agent and abrasives as mechanical polishing agent through the interior surfaces of objects that appears viable. In addition, the hypothesis would be rejected if applying experimental set-up of chemical abrasive polishing does not achieve the desirable interior surface roughness of IN-625 alloy.

A three steps procedure was devised, following the three objectives of this work that are developed alongside of the literature review. The three polishing techniques of chemical, abrasive and combined chemical-abrasive polishing were compared to examine the research hypothesis for existence of a synergy effect in combined use of chemical and abrasive flow actions in surface quality improvement. The static and flow chemical polishing were performed to define the influence of dynamic action in surface finish quality of chemical polished specimens. The surface quality improvement in this study referred to removal of semi-welded particles produced during SLM process and the surface roughness reduction after polishing.

Based on the experimental results, the chemical-abrasive flow polishing did remove semi-welded particles from the interior surface of AM IN-625 tubular specimens and did smoothen the surface by improving the  $R_a$  roughness value by 45% for the build orientation of  $15^\circ$  and by 20% for the build orientation of  $135^\circ$ .

### 5.3 Discussion on some methodological aspects and results

It is worth to look over some points of discussion related to the obtained results that are not completely explained in Chapter 4. These valuable subjects are discussed in this section.

#### *The sources of variations in the experimental results*

As explained in Section 4.3.3, the linear roughness average ( $R_a$ ) and the maximum height of the profile ( $R_z$ ) of the edge-shaped specimens were obtained using surface roughness tester (SJ-410, Mitutoyo). The ISO 1997 standard was applied for calculating the roughness results ( $\lambda_c = 0.8$  mm and  $\lambda_s = 2.5$   $\mu$ m). The measurements were performed in direction of the build orientation to cover the surface texture resulting from the stair stepping effect. The measurements were repeated three times in three parallel lines on the surface (Figure 4.5). The mean values and the standard deviations (error bars) of the measurements were calculated and presented in Figures 4.7 and 4.9.

The error bars on the graphs of the roughness as a function of each polishing technique (Figure 4.7 and Figure 4.9), and the graphs of roughness versus polishing time (Figure 4.11) are representation of variation in obtained roughness values. The contributions to these error bars might be from the striped texture of the surface. The amplitude of the stripes varies through the surface of the specimens. This surface feature is formed due to the stair stepping effect during SLM fabrication process. The striped features remain even after polishing with lesser intensity comparing to the as-built surface, which is the result of low level of polishing depth for the three techniques. The chemical-abrasive flow polished surface in Figure 5.1 clearly manifests the striped texture that persists after 1 hour of polishing for the build orientation of  $15^\circ$ . Consequently, the error bars still appear on the graphs for the polished samples. The striped texture cannot be distinguished on the surface with build orientation of  $135^\circ$  due to the high concentration of semi-welded particles that are attached to the specimen surface.

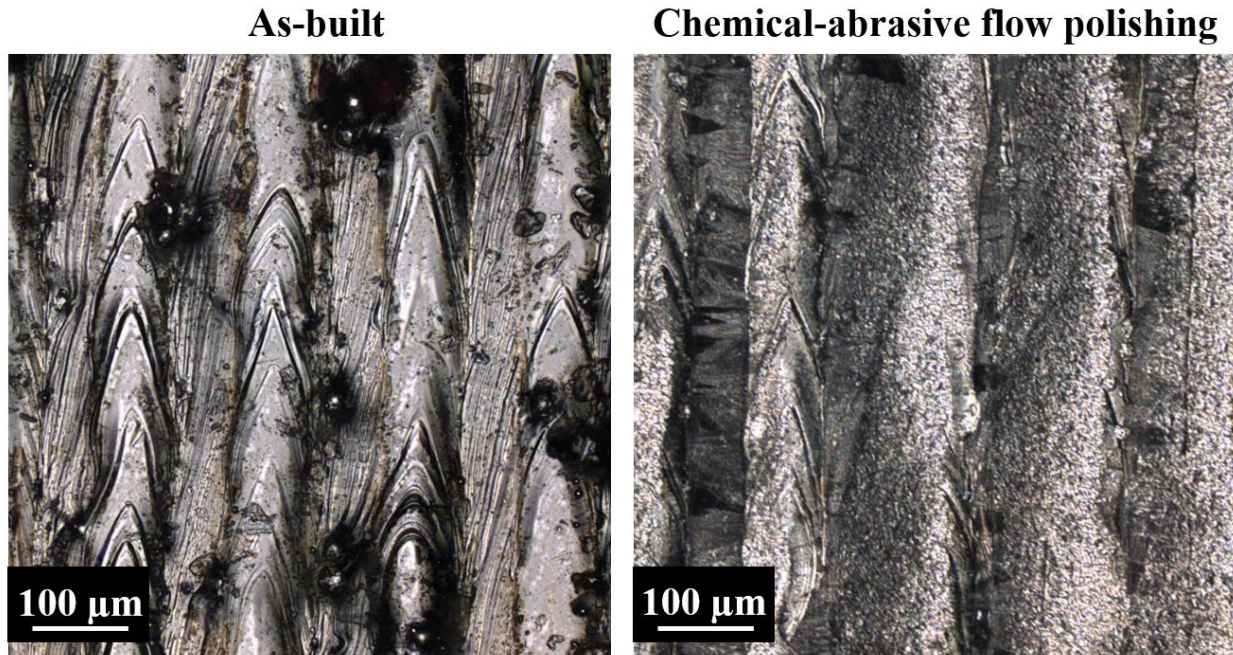


Figure 5.1: Striped texture exists on the as built surface and persists after chemical-abrasive flow polishing for 1 hour on the build orientation of  $15^\circ$ , although the semi-welded particles are completely removed after chemical-abrasive flow polishing

#### *Difficulties for the internal surface polishing of more complex geometries*

An edge-shaped specimen with two inclined surfaces of  $15^\circ$  and  $135^\circ$  build orientations was used for the experimental tests of this work. The specimen was fixed inside a cylindrical sleeve and locked with a ring, giving an angle of  $30^\circ$  with respect to the central axis of the cylinder and likewise the fluid flow (Figure 4.2). According to the discussion in Section 4.3.2, the particle impact angle of  $30^\circ$  to the target surfaces maximizes the erosion wear rate of IN-625 specimen as a ductile material. The designed specimen is not applicable for studying the influence of different impact angles on the erosion wear rate and therefore the surface finish quality.

Indeed, one of the specifications of the SLM-built components is their complex geometries. The tube shape engine parts particularly used in aerospace industry could possess bending angles that are complicated to be polished with most of the finishing techniques such as electrochemical and mechanical techniques. For this reason, it is critical to study the influence of particle impact angle on the surface finish quality using tubular specimens containing bending angles.

For this purpose, it is recommended to design specimens that include different inclined surfaces in the range between 0 to 90° to fully capture the particle impact angle effect. It is predicted to obtain different results for the surface roughness reduction and the polishing depth as function of particle impact angle for chemical-abrasive polishing of SLM-built IN-625. The hypothesis can be verified by the results of a study performed by Kosa & Göksenli (2015) on the effect of impact angle on erosive abrasive wear of non-heat treated steel St 37. They reported that by rising the impact angle from 0°, the wear rate increased until reaching the maximum value at 30°, and then decreased until reaching the minimum value at 75°. It is worth noticing that the speed of wear rate increment until 30° was faster than its decrement after reaching this angle.

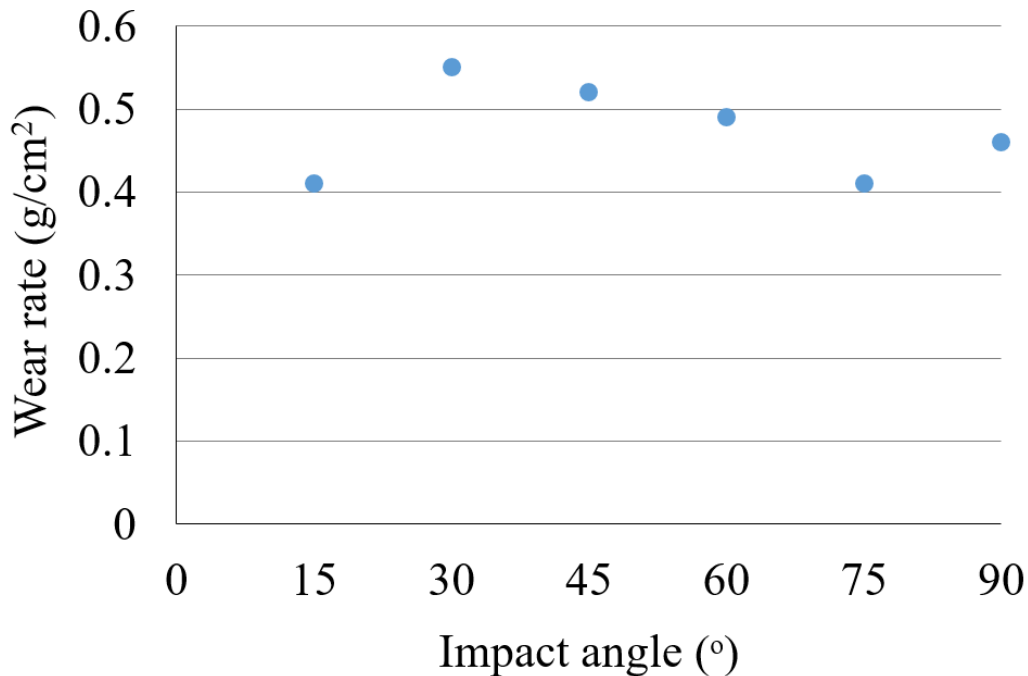


Figure 5.2: Influence of particle impact angle on wear rate of non-heat treated St 37 (ductile material steel) (Kosa & Göksenli, 2015)

The information obtained from performing the proposed experiment to obtain graphs of surface roughness reduction and polishing depth as a function of particle impact angle might be helpful to predict the surface finish quality of 90° bend tube or a T-tube. The challenge facing to the chemical-abrasive flow polishing of a 90° bend tube might be the fact that the polishing (material removal) depth through the internal surface will not be uniform. The reason of this behavior would be variable impact angle and speed of abrasives with respect to the surface. It is predicted

that the whole surface of the specimen will obtain the same polishing depth and therefore surface roughness reduction except the 90° corner of the tube. The bending corner would be polished more intensively because of 90° impact angle of the abrasive particle to the surface. However, the other parts of the tube would be exposed to the abrasive particles impingement with an angle of 0°, since the abrasive particle tend to follow the flow of fluid medium. It is expected that the polishing depth and roughness reduction within the 90° bend tube would be in accordance with the results of the graphs of already proposed experiment for examining different impact angles. For the complex tubular parts of the engines, the effect of variation in impact angle and fluid velocity must be considered ensemble, which will make it complicated to estimate of the final dimensions of the parts after chemical-abrasive polishing process. In addition, this information would be useful to design the part thicker where the material removal due to more aggressive impact angle is more important.

### *Exploring the use of other polishing medium materials to speed up the polishing process*

One of the weaknesses of chemical-abrasive polishing process is its long polishing time considering the resulted polishing depth and the reduced roughness. Furthermore, the material removal rate decreases for longer polishing times. As noted in Section 4.4.2, the hourly polishing depth obtained: for 1h → 10 μm/h, for 2h → 5 μm/h and for 3h → 2 μm/h. These results can be improved further by examining other chemical and abrasive alternatives and additives in the polishing medium. In the following, some important criteria for selection of chemical and abrasive agents are listed to be considered. In addition, the limitations concerning the use of these alternatives for chemical-abrasive flow polishing process are explained.

**CHEMICAL AGENT:** Several chemical solutions for polishing the IN-625 surface were tested in this work. The selected chemical solution of 50% HF + 50% HNO<sub>3</sub> is an effective solution, providing a uniform polished surface. However, the polishing speed was considerably low. The  $R_a$  roughness for the build orientation of 15° reduced from initial value of 7.3 μm to the final of 4.1 μm after polishing time of 8 hours. It is recommended to look for chemical solutions with higher polishing rate to speed up the chemical polishing and consequently the chemical-abrasive

polishing. Considering the conditions of chemical-abrasive polishing process, some criteria for selecting the chemical solution and additives are presented:

- The chemical solution should dissolve the surface material at a controlled rate. The solution of 50% HF + 50% HNO<sub>3</sub> polishes the surface of titanium in less than 10 s (ASM-Vol.9, 2004). Moreover, the polishing action is violent, producing bubbles, gases and change in its color. Therefore, chemical-abrasive flow polishing is not applicable for the titanium and titanium alloys using this solution.
- Some chemical solutions are toxic and dangerous to use, such as hydrofluoric acid (ASM-Vol.9, 2004). Protective clothing and chemical hood are necessary to be used when contacting any of the hazardous solutions and their vapors. Using alternative solutions are preferable as non-toxic solutions, especially when it is carried out on industrial scale.
- Due to the large volume of required chemical solution in the current process and the environmental considerations, the selected chemical solution must be reusable. Some solutions must be prepared fresh and they cannot be stores as stock solutions. Chathapuram et al. (2003) studied chemical mechanical polishing of titanium and titanium nitride, using hydrogen peroxide (H<sub>2</sub>O<sub>2</sub>) as an additive in chemical solution. They found that the polishing rate increases because of oxidizing action of H<sub>2</sub>O<sub>2</sub>. However, the chemicals containing H<sub>2</sub>O<sub>2</sub> must be used fresh because the H<sub>2</sub>O<sub>2</sub> degenerates naturally (Lee, 2010). Also, it is dangerous to store H<sub>2</sub>O<sub>2</sub> or chemicals containing this strong oxidizer with other chemicals, due to its potential to make explosion when it is exposed to incompatible chemicals (UC Center for Laboratory Safety, 2012).
- There is no universal solution applicable for polishing of metals and alloys; chemical solution are limited to polish specific alloys. New experiments are required to obtain the appropriate solution for new alloys (ASM-Vol.9, 2004). Therefore, applicability of the selected solution for chemical polishing of IN-625 must be examined for other family of alloys.

There is no specific instruction for preparing chemical polishing solutions; usually the proper solution is found after testing many different proportions and chemical compositions.

**ABRASIVE AGENT:** As described in Section 4.3.2, aluminum oxide grits with a particle size of  $z_{45} = 420 \mu\text{m}$  was used for this study. The abrasive concentration in the polishing medium was limited to 6 wt.%, the volume of polishing media was 5 liters, and the flow rate was kept constant at 10 lit./min. These limitations were due to the capacity of polishing fluid handling of the utilized centrifugal pump in the setup. The pump stopped working because of deposition of abrasive particles at high concentrations of abrasives in the polishing medium. As a result, the polishing rate becomes considerably low after performing abrasive flow polishing for a certain time due to the reduction of abrasive concentration in the circulating fluid. The  $R_a$  roughness for the build orientation of  $15^\circ$  reduced from  $7.3 \mu\text{m}$  for as-built surface to  $4.89 \mu\text{m}$  after 3 hour polishing. The polishing speed can definitely increase by optimizing the abrasive agent characteristics. This includes examining other abrasive materials with more angled-shaped and hardness, using higher concentrations of abrasives and larger particles by replacing more powerful centrifugal pumps in terms of fluid handling.

It is important to consider the abrasive particle hardness and shape when selecting the appropriate abrasive agent, as discussed in Section 2.3.3. Furthermore, the possible reactions between the abrasive particles and the target surface should be analyzed. Jiang et al. (1998) investigated chemical mechanical polishing of Silicon nitride ( $\text{Si}_3\text{N}_4$ ) with various abrasives. They reported that abrasive particles such as  $\text{CeO}_2$ ,  $\text{ZrO}_2$ ,  $\text{Fe}_2\text{O}_3$  and  $\text{Cr}_2\text{O}_3$  interact with the  $\text{Si}_3\text{N}_4$  surface to form  $\text{SiO}_2$  layer. The hardness of  $\text{CeO}_2$ ,  $\text{ZrO}_2$  and  $\text{Fe}_2\text{O}_3$  abrasives are close to that of  $\text{SiO}_2$ , whereas the hardness of  $\text{Si}_3\text{N}_4$  surface is comparatively higher. Therefore, the produced layer of  $\text{SiO}_2$  is easily and smoothly removed by mechanical action of abrasive particles without damaging the substrate surface.

For the chemical-abrasive flow polishing, it is recommended to examine the possibility of reaction between the candidate abrasive particles with the surface in chemical environment of the medium. This can be investigated through thermodynamic analysis. Evidently, it will not be a satisfactory result if this interaction would lead to the formation of harder layer comparing to the surface material and the abrasives. In this case, effective polishing will take place by using harder

abrasives that lead to more intensive mechanical abrasion. The material selection criteria would be achieving a uniform and scratch free surface that is obtained in a desired speed of polishing.

## 5.4 Scaling up the chemical-abrasive polishing process

The fluid handling and performance of the chemical-abrasive polishing can be improved by increasing the fluid velocity, using higher concentration of abrasives and reusing chemicals and abrasives of the fluid. These can be achieved by some improvements in the actual polishing setup.

To increase the fluid velocity, it is recommended to replace the centrifugal pump with more powerful models that provide higher flow rates. An increase of the flowrate could also be obtained by designing tubular specimens with smaller cross sectional area. As discussed in Section 4.5.3, it is predicted that a minimal velocity of  $\sim 20$  m/s is required to obtain a high finishing quality for chemical-abrasive polishing. With the current pump and cross section of the specimens, the velocity reaches to the maximum of only 3.5 m/s. Considering the formula of (4.1) for the flow velocity ( $v$ ), the proper flow rate ( $F$ ) and cross sectional area of the fluid ( $A$ ) should be regulated by selecting the appropriate pump and design of the specimen respectively.

The limitation for using high concentrations of abrasives is particle deposition inside the centrifugal pump. In the current setup, the centrifugal pump mixes the fluid and keeps the abrasives suspended in the chemical medium. To reach higher concentrations of abrasives (larger than 6 wt.%), using a propeller with chemical abrasive resistant to the polishing fluid is recommended. Having a propeller in the tank would also help to keep the abrasive particles suspended while they are staying there before being re-pumped to the specimen.

It is essential to be able to reuse the chemical and abrasive of the polishing medium from the environmental and economical point of view. The selected chemical solution for this work is not degradable, and therefore it is reusable. Concerning the  $\text{Al}_2\text{O}_3$  abrasives, it is recommended to characterize the sharpness of particles after polishing. The abrasives might lose their sharpness due to the shear forces applied by the centrifugal pump, thus their mechanical action in polishing could be less effective. This prediction is based on the research done by Lee et al. (2016). They stated that non-spherical particles provide higher material removal rate. To reuse the chemical



solution and abrasive particles (if they keep their sharpness), the two polishing agents must be separated using a chemical resistant filter.

## CHAPTER 6 CONCLUSION AND RECOMMENDATIONS

Experimental work was conducted on (i) static and flow chemical polishing, (ii) abrasive flow polishing, and (iii) chemical-abrasive flow polishing of SLM-built tubular specimens of IN-625. The polishing conditions were selected according to the studies presented in the literature review, recommendations provided by the experimental setup parts suppliers and the laboratory security plan.

Results of this work have led to the following conclusions and recommendations that were thoroughly discussed in previous chapters:

1. The feasibility of utilizing combined chemical-abrasive flow polishing for the interior surface of components with internal cavities or channels was determined by examining the three polishing techniques of (i) chemical, (ii) abrasive and (iii) chemical-abrasive flow polishing techniques.
2. The surface finish quality of the SLM-built IN-625 components after chemical-abrasive flow polishing was improved in terms of removal of semi-welded particle from the surface and roughness reduction. However, the surface roughness reduction was relatively low; there was about 45% reduction in  $R_a$  for the build orientation of  $15^\circ$  (smoother surface) and about 20% reduction for the build orientation of  $135^\circ$  (worst-case roughness). Based on the obtained results and reviewed literature, some arguments were provided to use other polishing medium materials to speed up the polishing process. These ideas are concerning the increment of the fluid velocity, the use of higher abrasive concentrations and the reuse of chemicals and abrasives of the polishing fluid.
3. The advantage of utilizing dynamic action in chemical polishing on surface finish quality improvement was confirmed by comparing the results of static versus dynamic (flow) chemical polishing. The  $R_a$  value decreased by 20% for build orientation of  $15^\circ$  (smoother surface) and by 7% for the build orientation of  $135^\circ$  (rougher surface) after switching from static to dynamic chemical action. The major drawback of chemical polishing of IN-625 specimens was utilizing hydrofluoric acid in the polishing solution, which is a powerful contact poison in both forms of liquid and gas. Therefore, further studies are

needed to find an alternative chemical polishing solution to be more appropriate for industrial use.

4. The synergetic effect stemmed from combined use of chemical and abrasive flow polishing was proved by the satisfactory results of switching from chemical flow or abrasive flow actions to a combined chemical-abrasive flow polishing, showing reduction in surface roughness and polishing time. The results of this combination in polishing technique included a two-fold increase in surface roughness reduction and a time reduction from 3h to 1h for the same  $R_a$  decrement from 17.4  $\mu\text{m}$  (as-built) to 14.2  $\mu\text{m}$ .
5. The material removal rate is raised by increasing the velocity of the fluid for the three polishing techniques. In the polishing depth equation for chemical-abrasive flow, the velocity exponent of 2.5 was calculated and a polishing time exponent of 0.6 was obtained for both build orientations of 15° and 135°. Due to the variation of material removal rate by increment of the velocity from the tip to the edge of the specimen, it is predicted that the surface roughness will be vary through the inclined surfaces as a function of velocity. It is predicted that the surface roughness will be decreased from the tip to the edge of the specimen because of the increasing velocity and polishing depth. The correlation between the velocity and surface roughness is recommended to be studied for the future work.
6. The effect of particle impact angle on surface finish quality was not studied in this work since it remained constant, although this parameter has a strong effect in producing a polished surface with different surface quality. This subject needs to be studied in a wider scope since SLM build parts have often complex geometries.
7. The  $R_a$  roughness is not appropriate parameters to show the surface roughness variation after removal of semi-welded particles. This parameter is the average value of the whole profile; therefore, it is hardly influenced by individual peaks or valleys of the surface. It is recommended to look for a more relevant 3D surface roughness parameter to describe the surface roughness changes after polishing with the three techniques investigated in this work.  $S_{pd}$  (density of the peaks) as a feature parameter is used for the 3D surface roughness analysis. This parameter indicates the number of peaks per unit area of the

surface. A large number represents more contact points with other objects.  $S_{pd}$  can be a better choice of surface roughness parameter to be calculated and analyzed for the objective of this work. The density of semi-welded particles would be reduced after surface polishing, and the value of  $S_{pd}$  roughness would decrease as well.

## BIBLIOGRAPHY

- Arısoy, Y. M., Criales, L. E., Özel, T., Lane, B., Moylan, S., & Donmez, A. (2016). Influence of scan strategy and process parameters on microstructure and its optimization in additively manufactured nickel alloy 625 via laser powder bed fusion. *The International Journal of Advanced Manufacturing Technology* 1-25.
- ASM-Vol.9. (2004). *Chemical and Electrolytic Polishing, Metallography and Microstructures* (Vol. 9): ASM International.
- Benedict, G. F. (1987). *Nontraditional manufacturing processes* (Vol. 19): CRC press.
- Bremerstein, T., Potthoff, A., Michaelis, A., Schmiedel, C., Uhlmann, E., Blug, B., & Amann, T. (2015). Wear of abrasive media and its effect on abrasive flow machining results. *Wear*, 342 44-51.
- Chathapuram, V. S., Du, T., Sundaram, K. B., & Desai, V. (2003). Role of oxidizer in the chemical mechanical planarization of the Ti/TiN barrier layer. *Microelectronic Engineering*, 65(4), 478-488.
- Crook, P. (2005). *ASM Handbook, Corrosion of Nickel and Nickel-Base Alloys, Corrosion: Materials* (Vol. 13B): ASM international.
- Dinda, G., Dasgupta, A., & Mazumder, J. (2009). Laser aided direct metal deposition of Inconel 625 superalloy: microstructural evolution and thermal stability. *Materials Science and Engineering: A*, 509(1), 98-104.
- Dokoumetzidis, A., Papadopoulou, V., Valsami, G., & Macheras, P. (2008). Development of a reaction-limited model of dissolution: Application to official dissolution tests experiments. *International journal of pharmaceuticals*, 355(1), 114-125.
- Donachie, M. J. (2000). *Titanium: A Technical Guide, 2nd Edition*: ASM International.
- Gibson, I., Rosen, D., & Stucker, B. (2015). Applications for Additive Manufacture. In *Additive Manufacturing Technologies: 3D Printing, Rapid Prototyping, and Direct Digital Manufacturing* (pp. 451-474). New York, NY: Springer New York.
- Goldstein, E. M. (1960). The Corrosion and Oxidation of Metals: Scientific Principles and Practical Applications (Evans, Ulick R.). *Journal of Chemical Education*, 37(12), 662.
- Gupta, R., & Chahal, B. (2015). Investigation and Optimization of Process Parameters in Electrochemical Aid Abrasive Flow Machining. *International Journal of Scientific and Engineering Research*, 6(2).

- Hocheng, H., Tsai, H., & Tsai, M. (2000). Effects of kinematic variables on nonuniformity in chemical mechanical planarization. *International Journal of Machine Tools and Manufacture*, 40(11), 1651-1669.
- Jiang, M., Wood, N. O., & Komanduri, R. (1998). On chemo-mechanical polishing (CMP) of silicon nitride (Si<sub>3</sub>N<sub>4</sub>) workmaterial with various abrasives. *Wear*, 220(1), 59-71.
- Johl, B., Litchy, M., & Schoeb, R. (2005). *Effect of a Maglev Centrifugal Pump on Slurry Health and Defect Rates*. Paper presented at the PacRim Int. Conference, Korea.
- Kar, K. K., Ravikumar, N., Tailor, P. B., Ramkumar, J., & Sathiyamoorthy, D. (2009). Performance evaluation and rheological characterization of newly developed butyl rubber based media for abrasive flow machining process. *Journal of materials processing technology*, 209(4), 2212-2221.
- Kosa, E., & Göksenli, A. (2015). Effect of Impact Angle on Erosive Abrasive Wear of Ductile and Brittle Materials. *International Journal of Mechanical and Mechatronics Engineering*, 2(9), 1206.
- Kreitzberg, A., Brailovski, V., Turenne, S. (2017). Effect of heat treatment and hot isostatic pressing on the microstructure and mechanical properties of Inconel 625 processed by laser powder bed fusion. *Materials Science and Engineering: A*, 689, 1-10.
- Król, M., & Tański, T. (2016). Surface quality research for selective laser melting of Ti-6Al-4V alloy. *Archives of Metallurgy and Materials*, 61(3), 1291-1296.
- Kurobe, T., Yamada, Y., & Yamamoto, K. (2002). Application of high speed slurry flow finishing method for finishing of inner wall of fine hole die: Effects of the hardness of die material on the polishing characteristics. *Precision engineering*, 26(2), 155-161.
- Kurobe, T., Yamada, Y., Yamamoto, K., & Miura, T. (1998). High speed slurry flow finishing of inner wall of stainless steel capillary(3 rd Report)- effect of annexed glass beads on finishing characteristics. *SEIMITSU KOGAKU KAISHI*, 64(9), 1325-1329.
- Kutzelnigg, A. (1960). The electrolytic and chemical polishing of metals in research and industry. W. I. Mc. G. Tegart. Pergamon Press Ltd. London, 1959, 2. Aufl. IX. 139 S., 35 Abb. und 35 Tab., Geb. 40 s. *Materials and Corrosion*, 11(9), 595-595.
- Lee, H., Lee, D., & Jeong, H. (2016). Mechanical aspects of the chemical mechanical polishing process: A review. *International Journal of Precision Engineering and Manufacturing*, 17(4), 525-536.

- Litchy, M. R., & Schoeb, R. (2005). *Effect of particle size distribution on filter lifetime in three slurry pump systems*. Paper presented at the MRS Proceedings (Vol. 867, pp. W2. 8).
- Luo, J., & Dornfeld, D. A. (2003). Effects of abrasive size distribution in chemical mechanical planarization: modeling and verification. *IEEE Transactions on Semiconductor Manufacturing*, 16(3), 469-476.
- Łyczkowska, E., Szymczyk, P., Dybała, B., & Chlebus, E. (2014). Chemical polishing of scaffolds made of Ti-6Al-7Nb alloy by additive manufacturing. *Archives of Civil and Mechanical Engineering*, 14(4), 586-594.
- Lynn, R. S., Wong, K. K., & Clark, H. M. (1991). On the particle size effect in slurry erosion. *Wear*, 149(1-2), 55-71.
- Mumtaz, K., & Hopkinson, N. (2009). Top surface and side roughness of Inconel 625 parts processed using selective laser melting. *Rapid Prototyping Journal*, 15(2), 96-103.
- Mumtaz, K., & Hopkinson, N. (2010). Selective laser melting of Inconel 625 using pulse shaping. *Rapid Prototyping Journal*, 16(4), 248-257.
- National Research Council (US). (2011). *Prudent Practices in the Laboratory: Handling and Management of Chemical Hazards: Updated Version*.
- Nicholes, K., Litchy, M., Hood, E., Easter, W., Bhethanabotla, V., Cheema, L., & Grant, D. (2003). *Analysis of wafer defects caused by large particles in CMP slurry using light scattering and SEM measurement techniques*. Paper presented at the 2003 Proceedings of the Eighth International Chemical-Mechanical Planarization for ULSI Multilevel Interconnection Conference (CMP-MIC).
- Ojala, N., Valtonen, K., Kivikytö-Reponen, P., Vuorinen, P., & Kuokkala, V. (2015). High speed slurry-pot erosion wear testing with large abrasive particles. *Finnish Journal for Tribology*, 33 36-44.
- Petrovic, V., Vicente Haro Gonzalez, J., Jordá Ferrando, O., Delgado Gordillo, J., Ramón Blasco Puchades, J., & Portolés Griñan, L. (2011). Additive layered manufacturing: sectors of industrial application shown through case studies. *International Journal of Production Research*, 49(4), 1061-1079.
- Preston, F. W. (1927). The Theory and Design of Plate Glass Polishing Machines. *J. Soc. Glass Tech.*, 11 214. Retrieved from <http://ci.nii.ac.jp/naid/10017414050/en/>

- Pyka, G., Burakowski, A., Kerckhofs, G., Moesen, M., Van Bael, S., Schrooten, J., & Wevers, M. (2012). Surface Modification of Ti6Al4V Open Porous Structures Produced by Additive Manufacturing. *Advanced Engineering Materials*, 14(6), 363-370.
- Pyka, G., Kerckhofs, G., Papantoniou, I., Speirs, M., Schrooten, J., & Wevers, M. (2013). Surface roughness and morphology customization of additive manufactured open porous Ti6Al4V structures. *Materials*, 6(10), 4737-4757.
- Rajेशha, S., Venkatesh, G., Sharma, A., & Kumar, P. (2010). Performance study of a natural polymer based media for abrasive flow machining.
- Ramesh, C., Kumar, R. S., Ramakrishna, S., & Venkatesh, K. K. (2014). *Design of Experiments to Study Slurry Erosive Wear Behavior of Inconel-718 coatings on Copper*. Paper presented at the Advanced Materials Research (Vol. 939, pp. 459-464).
- Ramesh, C., Kumar, S., Devaraj, D., & Keshavamurthy, R. (2011). Slurry erosive wear behavior of plasma sprayed inconel-718 coatings on Al6061 alloy. *Journal of Minerals and Materials Characterization and Engineering*, 10(05), 445.
- Rawal, S., Brantley, J., & Karabudak, N. (2013, 12-14 June 2013). *Additive manufacturing of Ti-6Al-4V alloy components for spacecraft applications*. Paper presented at the 2013 6th International Conference on Recent Advances in Space Technologies (RAST) (pp. 5-11).
- Relekar, M. K. M., Kalase, M. A. B., & Dubal, M. S. P. ABRASIVE WATER JET MACHINING.
- Rhoades, L. (1991). Abrasive flow machining: a case study. *Journal of Materials Processing Technology*, 28(1), 107-116.
- Sankar, M. R., Jain, V., Ramkumar, J., & Joshi, Y. (2011). Rheological characterization of styrene-butadiene based medium and its finishing performance using rotational abrasive flow finishing process. *International Journal of Machine Tools and Manufacture*, 51(12), 947-957.
- Shankar, V., Rao, K. B. S., & Mannan, S. (2001). Microstructure and mechanical properties of Inconel 625 superalloy. *Journal of Nuclear Materials*, 288(2), 222-232.
- Si, L., Guo, D., Luo, J., Lu, X., & Xie, G. (2011). Abrasive rolling effects on material removal and surface finish in chemical mechanical polishing analyzed by molecular dynamics simulation. *Journal of Applied Physics*, 109(8), 084335.



- Silva, F. J., Casais, R., Martinho, R., & Baptista, A. (2011). Role of abrasive material on micro-abrasion wear tests. *Wear*, 271(9), 2632-2639.
- Singh, R., & Johl, B. (2001). *Characterization of a Silica Based STI CMP Slurry in a Vacuum-Pressure Dispense Slurry Delivery System and Pump Loop*. Paper presented at the Proc. VMIC Conference.
- Spur, G., Eichhorn, H., & Bottke, D. (1997). Strömungsschleifen-Eine Verfahrensübersicht. *Industrie Diamanten Rundschau*, 31(1), 84-88.
- T. S. Gonçalves, A.M. Spohr, R. M. de Souza, & L. Macedo de Menezes. (2008). Surface roughness of auto polymerized acrylic resin according to different manipulation and polishing methods: an in situ evaluation. *Angle Orthodontist*, 78 931-934.
- Tammas-Williams, S., Withers, P. J., Todd, I., & Prangnell, P. B. (2016). The Effectiveness of Hot Isostatic Pressing for Closing Porosity in Titanium Parts Manufactured by Selective Electron Beam Melting. *Metallurgical and Materials Transactions A*, 47(5), 1939-1946.
- Thakur, A., & Gangopadhyay, S. (2016). State-of-the-art in surface integrity in machining of nickel-based super alloys. *International Journal of Machine Tools and Manufacture*, 100 25-54.
- Tuck, B. (1975). The chemical polishing of semiconductors. *Journal of Materials Science*, 10(2), 321-339.
- UC Center for Laboratory Safety. (2012). Standard operation procedure: hydrogen peroxide. Retrieved from <http://www.chemengr.ucsb.edu/~ceweb/faculty/scott/Chemical%20SOPs/Hydrogen%20peroxide.pdf>
- Urlea, V., & Brailovski, V. (2017). Electropolishing and electropolishing-related allowances for powder bed selectively laser-melted Ti-6Al-4V alloy components. *Journal of Materials Processing Technology*, 242 1-11.
- Vossen, J. L., & Kern, W. (1978). *Thin film processes*: Academic Press.
- Wang, A., Liu, C., Liang, K., & Pai, S. (2007). Study of the rheological properties and the finishing behavior of abrasive gels in abrasive flow machining. *Journal of mechanical science and technology*, 21(10), 1593-1598.

- Witkin, D., Helvajian, H., Steffeney, L., & Hansen, W. (2016). *Laser post-processing of Inconel 625 made by selective laser melting*. Paper presented at the Proceeding of SPIE San Francisco, California, United States (Vol. 9738, pp. 97380W).
- Wohlers, T. (2016). *Wohlers Report 2016 Published: Additive Manufacturing Industry Surpassed \$5.1 Billion*: Wohlers Associates, Inc.
- Yadav, S. K., Singh, M. K., & Singh, B. R. (2011). Effect of Unconventional Machining on Surface Roughness of Metal: Aluminum and Brass-A Case Study of Abrasive Flow. *SAMRIDDHI-J. Phys. Sci. Eng. Technol.*, 2 53-60.
- Yadroitsev, I., & Smurov, I. (2010). Selective laser melting technology: from the single laser melted track stability to 3D parts of complex shape. *Physics Procedia*, 5 551-560.
- Yasa, E., Poyraz, O., Solakoglu, E. U., Akbulut, G., & Oren, S. (2016). A Study on the Stair Stepping Effect in Direct Metal Laser Sintering of a Nickel-based Superalloy. *Procedia CIRP*, 45 175-178.
- Yasunaga, N. (1994). Recent advances in ultraprecision surface finishing technologies in Japan. *International journal of the Japan Society for Precision Engineering*, 28(3), 191-195.
- Yin, L., Ramesh, K., Wan, S., Liu, X. D., Huang, H., & Liu, Y. C. (2004). Abrasive flow polishing of micro bores. *Materials and Manufacturing Processes*, 19(2), 187-207.
- Yoojin Lee. (2010). Effect of hydrogen peroxide concentration on the rate of reaction. Retrieved from <https://www.slideshare.net/wkkok1957/effect-of-ph-on-catalase>
- Zu, J., Hutchings, I., & Burstein, G. (1990). Design of a slurry erosion test rig. *Wear*, 140(2), 331-344.